

NACA RM SL54H27

# NACA

## RESEARCH MEMORANDUM

CLASSIFICATION CHANGED  
**UNCLASSIFIED**

for the

Declassified by authority of NASA  
Classification Change Notices No. 212  
Dated \*\* 1971

TO U. S. Air Force

By Authority of 10131 Date 12-15-70

INVESTIGATION OF A 1/4-SCALE MODEL OF THE REPUBLIC F-105

AIRPLANE IN THE LANGLEY 19-FOOT-PRESSURE TUNNEL

INFLUENCE OF TRAILING-EDGE FLAP SPAN AND DEFLECTION

ON THE LONGITUDINAL CHARACTERISTICS

By Patrick A. Cancro and H. Neale Kelly

Langley Aeronautical Laboratory  
Langley Field, Va.

X71-71426	(ACCESSION NUMBER)	(THRU)	(CODE)	(CATEGORY)
	(PAGES)			
(NASA CR OR TMX OR AD NUMBER)				
RESTRICTION TO NASA OFFICES AND NASA				
Restriction/Classification Cancelled				
FF No. 602(A)				

ATIONAL ADVISORY COMMITTEE  
FOR AERONAUTICS

WASHINGTON

SEP 2 1970

---

RESEARCH MEMORANDUM

for the

U. S. Air Force

---

INVESTIGATION OF A 1/4-SCALE MODEL OF THE REPUBLIC F-105

AIRPLANE IN THE LANGLEY 19-FOOT PRESSURE TUNNEL

INFLUENCE OF TRAILING-EDGE FLAP SPAN AND DEFLECTION

ON THE LONGITUDINAL CHARACTERISTICS


By Patrick A. Cancro and H. Neale Kelly

SUMMARY

Development tests on a 1/4-scale model of the Republic F-105 airplane are being conducted in the Langley 19-foot pressure tunnel. The second phase, the results of which are presented herein, was made at a Reynolds number of  $9.0 \times 10^6$  and a Mach number of 0.20. Exploratory tests were made at Reynolds numbers of 3, 6, 7, and  $8 \times 10^6$  and corresponding Mach numbers of 0.06, 0.13, 0.16, and 0.18.

The purpose of the present tests was to obtain the longitudinal force and moment characteristics of the model equipped with trailing-edge flaps of various spans and deflections. In addition, an investigation was made to show the effect of Reynolds number and also the effect of a transonic inlet with the original horizontal tail and with a larger span horizontal tail.

In order to expedite the issuance of the data for this airplane, no analysis of the data has been presented.



## INTRODUCTION

The F-105 airplane is a  $45^\circ$  sweptback, midwing, low-tail, supersonic fighter-bomber being developed by the Republic Aviation Corporation for the U. S. Air Force. At the request of the Air Force, development tests on a 1/4-scale model of the F-105 are being conducted in the Langley 19-foot pressure tunnel to determine the low-speed aerodynamic characteristics of the basic design and, if necessary, to develop modifications which will provide the model with satisfactory low-speed stability and control characteristics.

The initial longitudinal stability and control tests of a model of the F-105 airplane (ref. 1) indicated that the model possessed acceptable longitudinal stability characteristics as long as the trailing-edge flaps were neutral. With the trailing-edge flaps deflected, however, it was found that the model did not possess sufficient static margin at the most rearward anticipated center-of-gravity position (38 percent mean aerodynamic chord). Furthermore, because of the nonlinear lift characteristics of the horizontal tail and the associated pitch-up, satisfactory stability could not be obtained at the most forward center-of-gravity position (22 percent mean aerodynamic chord). Although various other modifications were attempted (see ref. 1), satisfactory stability could only be obtained by reducing either the flap span or deflection, or both.

The primary purpose of the tests presented herein was to determine the greatest flap span and deflection that could be used and still retain an adequate static margin up to and including the landing angle of attack. These tests were made at tail incidences required to trim the model at an angle of attack of  $12^\circ$  for the 22-percent and 38-percent center-of-gravity locations. In addition, tests were made at various Reynolds numbers and with a transonic-type elliptical inlet and larger span horizontal tail. The model was tested through an angle-of-attack range of  $-4^\circ$  through the stall.

## COEFFICIENTS AND SYMBOLS

$C_L$	lift coefficient, $Lift/qS$
$C_{L_{max}}$	maximum lift coefficient
$C_D$	drag coefficient, $Drag/qS$
$C_m$	pitching-moment coefficient, $Pitching\ moment/qS\bar{c}$ (an additional subscript denotes location of center of gravity)

- b wing span, ft
- c local streamwise chord, ft
- $\bar{c}$  mean aerodynamic chord,  $\frac{2}{S} \int_0^{b/2} c^2 dy$ , ft
- y spanwise distance from plane of symmetry, ft
- z vertical distance from mean aerodynamic chord extended, ft
- $\alpha$  angle of attack, deg
- $\delta_f$  trailing-edge flap deflection, trailing edge down for positive deflection, deg
- $\delta_n$  drooped leading-edge flap deflection, leading edge down for positive deflection, deg
- $i_t$  tail incidence relative to the wing-chord plane, trailing edge down for positive incidence, deg

## MODEL

## Model Description

The model was primarily of steel-reinforced wood construction; however, the inlets, trailing-edge flaps, and leading-edge flaps were aluminum.

Basic model.- The basic model for the longitudinal stability and control tests was a 1/4-scale model of the F-105 airplane wing, fuselage, and vertical tail. Principal dimensions and design features of the model and a photograph of the model installed in the Langley 19-foot pressure tunnel are presented in table I and figures 1 and 2.

It should be noted here that between the tests reported in reference 1 and the tests presented herein, the model was sent back to Republic Aviation Corporation for the fitting of additional control-setting brackets and a revision to the lateral-control system. In the course of these modifications, the wing contour and flap positioning were rechecked. The flap gap was found to be unsymmetrical and the wing leading-edge radius was not in agreement with the specified airfoil section ordinates. In consequence, the trailing-edge flap positioning was altered slightly

and the forward 10 percent of the wing was reworked to bring it into agreement with the calculated airfoil ordinates to within  $\pm 0.003$  inch.

Horizontal tail.- The horizontal tail was located at a tail height of  $0.123b/2$  below the mean-aerodynamic-chord plane extended, and it was possible to obtain tail-incidence settings of  $7^\circ$ ,  $3.5^\circ$ ,  $0^\circ$ ,  $-3.5^\circ$ ,  $-9.5^\circ$ ,  $-14^\circ$ ,  $-20^\circ$ , and  $-25^\circ$ . A larger span horizontal tail was also tested. Details of the horizontal tails may be seen in figure 1 and table I.

Trailing-edge flaps.- The wing was equipped with a single slotted trailing-edge flap which extended from  $0.133b/2$  to  $0.800b/2$ . The flap was cut so that flaps extending from  $0.133b/2$  to  $0.600b/2$ ,  $0.650b/2$ , and  $0.700b/2$  could also be tested. Hereinafter, the flap span is designated by the outboard end location in percent span. For example, the  $0.133b/2$  to  $0.600b/2$  span flap is identified as a 60-percent-span trailing-edge flap. The flap could be set at angles of  $0^\circ$ ,  $40^\circ$ , and  $46^\circ$  perpendicular to the flap hinge line through the use of interchangeable steel positioning brackets. Details of the measured flap settings and gaps are compared with the design loft data furnished by Republic Aviation Corporation and may be seen in figure 3.

Leading-edge flaps.- An inversely tapered drooped leading-edge flap with interchangeable deflection brackets of  $0^\circ$ ,  $7.5^\circ$ ,  $20^\circ$ , and  $30^\circ$  perpendicular to the hinge line was provided as a stall-control device. Details of the leading-edge flap may be seen in figure 3 and table I.

External stores.- Except for a few tests, external stores representative of 450-gallon pylon-mounted fuel tanks were attached at the  $0.606b/2$  station. Details of the external stores can be found in figure 4 and table I.

Inlets.- The model was equipped with either a supersonic-type or a transonic-type elliptical wing-root inlet. Photographs of these inlets may be seen in figure 5.

#### Model Nomenclature

Listed below are the designations given to the various component parts of the model. The complete model configurations are obtained by combining the appropriate model components with the basic model.

- A basic model (wing plus fuselage)
- E external stores
  - subscript: 0 indicates outboard location ( $0.606b/2$ )
  - suffix: 450 indicates 450-gallon fuel tank

- F single slotted trailing-edge flap  
prefix: flap span (fraction of wing semispan)  
subscript: deflection, trailing edge down for positive deflection, deg
- I wing-root inlet  
subscript: SE indicates supersonic-type elliptical inlet  
TE indicates transonic-type elliptical inlet
- N inversely tapered drooped leading-edge flap  
subscript: deflection, leading edge down for positive deflection, deg
- T horizontal tail  
prefix: vertical position (fraction of wing semispan)  
subscript: incidence, trailing edge down for positive incidence, deg  
superscript: \* indicates increased tail span
- V vertical tail


#### TESTS

All tests reported herein were conducted in the Langley 19-foot pressure tunnel at a tunnel pressure of approximately  $2\frac{1}{3}$  atmospheres. For most of the tests, the Reynolds number, based on the mean aerodynamic chord, was  $9.0 \times 10^6$  and the Mach number was 0.20. However, exploratory tests were made to determine the effect of Reynolds number. These tests were conducted at Reynolds numbers of 3.0, 6.0, 7.0, and  $8.0 \times 10^6$  with corresponding Mach numbers of 0.06, 0.13, 0.16, and 0.18. The model was mounted on the normal three-support system at  $0^\circ$  angle of yaw and was tested through an angle-of-attack range of  $-4^\circ$  through the stall.

Longitudinal characteristics of the model for the various flap span arrangements at a tail incidence required to trim this model at  $\alpha = 12^\circ$  for the 0.22 $\bar{c}$  and 0.38 $\bar{c}$  center-of-gravity positions were obtained. A transonic-type elliptical inlet was tested and data were obtained with the original horizontal tail and with an increased span horizontal tail.

#### CORRECTIONS

Jet-boundary corrections determined by the method of reference 2 have been applied to all force and moment data. Corrections for support





ture and interference effects and for air-flow misalignment have not been applied. Internal drag of the inlets and duct system is included in the drag data presented herein.

#### PRESENTATION OF DATA

The comparison (fig. 6) of the results of tests for the flaps-neutral condition presented herein with tests of a comparable configuration presented in reference 1 shows the two sets of results to be similar except for small differences at the higher angles of attack. This indicates that the reworking of the wing leading edge that occurred between the initial and present tests had little effect on the measured characteristics.

Similar comparisons (fig. 7) with  $\delta_f = 46^\circ$  show noticeable stability changes at a lift coefficient of about 0.8 between the initial tests (ref. 1) and the tests presented herein. The differences in test results shown in figure 7 are attributed to the change in flap positioning that occurred between the initial and present tests. This effect should be kept in mind in comparing the flap-deflected results presented herein with those presented in reference 1.

The longitudinal stability characteristics about the 0.25 $\bar{c}$  are summarized in tables II, III, and IV. The results of the tests about the 0.22 $\bar{c}$  and 0.38 $\bar{c}$  for the various flap configurations are contained in figures 8 to 21. A static-margin summary chart is presented in figure 22. The effect of various trailing-edge flap spans and the effect of various leading-edge flap deflections on the longitudinal stability characteristics may be seen in figures 23 and 24, respectively. Tests were made to determine the effect of Reynolds number on the longitudinal characteristics of the model, and the results are presented in figures 25 and 26. The data obtained with the transonic elliptical inlet can be found in figures 27 to 29. The results of a horizontal-tail span increase with the transonic elliptical inlet are presented in figure 30.

Langley Aeronautical Laboratory,  
National Advisory Committee for Aeronautics,  
Langley Field, Va., August 12, 1954.

*Patrick A. Cancro*  
Patrick A. Cancro  
Mechanical Engineer

Approved:

*Eugene C. Draley*  
Eugene C. Draley  
Chief of Full-Scale Research Division

*H. Neale Kelly*  
H. Neale Kelly  
Aeronautical Research Scientist

eba



  
REFERENCES

1. Kelly, H. Neale, and Cancro, Patrick A.: Investigation of a 1/4-Scale Model of the Republic F-105 Airplane in the Langley 19-Foot Pressure Tunnel - Longitudinal Stability and Control of the Model Equipped With a Supersonic-Type Elliptical Wing-Root Inlet. NACA RM SL54F28, U. S. Air Force, 1954.
2. Sivells, James C., and Salmi, Rachel M.: Jet-Boundary Corrections for Complete and Semispan Swept Wings in Closed Circular Wind Tunnels. NACA TN 2454, 1951.

  
AL



TABLE I.- DESIGN CHARACTERISTICS OF THE REPUBLIC F-105 AIRPLANE AND THE 1/4-SCALE MODEL OF THE F-105 AIRPLANE

	Full-scale	1/4-scale
<u>Wing Assembly</u>		
Basic data:		
Root airfoil, measured parallel to airplane center line at $0.38b/2$	NACA 65A005.5	NACA 65A005.5
Tip airfoil, measured parallel to airplane center line	NACA 65A003.7	NACA 65A003.7
Angle of incidence, deg	0	0
Geometric twist, deg	0	0
Sweep of quarter-chord line (true), deg	45	45
Taper ratio	0.467	0.467
Aspect ratio (excluding inlet area)	3.182	3.182
Dihedral, deg	-3.5	-3.5
Dimensions:		
Root chord (theoretical), parallel to airplane center line, ft	15.000	3.750
Tip chord (theoretical), parallel to airplane center line, ft	7.000	1.750
Mean aerodynamic chord, parallel to airplane center line, ft	11.485	2.871
Location of mean aerodynamic chord, spanwise (projected), ft	7.690	1.923
Span, measured normal to airplane center line, ft	34.934	8.734
Area:		
Wing area (excluding inlet area), sq ft	385.0	24.662
<u>Horizontal-Tail Assembly</u>		
Basic data:		
Root airfoil, streamwise	NACA 65A006	NACA 65A006
Tip airfoil, streamwise	NACA 65A004	NACA 65A004
Taper ratio:		
Basic horizontal tail	0.456	0.456
Modified horizontal tail	0.401	0.401
Aspect ratio:		
Basic horizontal tail	3.06	3.06
Modified horizontal tail	3.49	3.49
Dihedral, deg	0	0
Dimensions:		
Root chord (theoretical), ft	7.50	1.875
Tip chord (theoretical):		
Basic horizontal tail, ft	3.42	0.855
Modified horizontal tail, ft	3.01	0.752
Mean aerodynamic chord (theoretical):		
Basic horizontal tail, ft	5.71	1.428
Modified horizontal tail, ft	5.58	1.395
Span:		
Basic horizontal tail, ft	16.67	4.168
Modified horizontal tail, ft	18.33	4.582
0.25c of wing to 0.25c of horizontal tail (theoretical):		
Basic horizontal tail, ft	20.68	5.232
Modified horizontal tail, ft	20.96	5.302
Vertical location below fuselage center line, in.	-18.00	-4.5

TABLE I.- DESIGN CHARACTERISTICS OF THE REPUBLIC F-105 AIRPLANE AND THE 1/4-SCALE MODEL OF THE F-105 AIRPLANE - CONTINUED

NACA RM SLSH27

Horizontal-Tail Assembly - Concluded

Full-scale                      1/4-scale

Area:

Horizontal-tail area (theoretical):

Basic, sq ft . . . . .	90.97	5.685
Modified, sq ft . . . . .	96.32	6.020
Horizontal-tail area (exposed):		
Basic, sq ft . . . . .	60.77	3.798
Modified, sq ft . . . . .	66.13	4.133

Vertical-Tail Assembly

Basic data:

Root airfoil, measured parallel to airplane center line at 0.167b/2 . . . . .	NACA 65A006	NACA 65A006
Tip airfoil, measured parallel to airplane center line . . . . .	NACA 65A004	NACA 65A004
Sweepback of quarter-chord line, deg . . . . .	45	45
Aspect ratio (theoretical) . . . . .	1.593	1.593
Taper ratio (theoretical) . . . . .	0.365	0.365
Sweepback of rudder hinge line, deg . . . . .	29.358	29.358
Rudder deflections, measured in a plane normal to the hinge line, deg . . . . .	32 to -32	0,12,24,35

Dimensions:

Root chord (theoretical), ft . . . . .	10.03	2.508
Tip chord (theoretical), ft . . . . .	3.67	0.9175
Mean aerodynamic chord (theoretical), ft . . . . .	7.34	1.835
0.25c̄ of wing to 0.25c̄ of vertical tail (theoretical), ft . . . . .	17.40	4.412
Vertical-tail height, measured from fuselage center line, ft . . . . .	10.92	2.729
Rudder chord (average), ft . . . . .	1.86	0.458
Rudder span, measured normal to fuselage center line, ft . . . . .	6.83	1.708

Area:

Vertical-tail area (theoretical), sq ft . . . . .	74.8	4.670
Vertical-tail area (exposed), sq ft . . . . .	48.0	3.000
Rudder area (including overhang), sq ft . . . . .	11.39	0.712

Fuselage

Length, ft . . . . .	62.0	15.049
Maximum width, ft . . . . .	4.375	1.094
Maximum height (excluding canopy), ft . . . . .	6.50	1.625
Volume (including canopy), cu ft . . . . .	1142	17.87
Location of station 0 (measured upstream from nose of airplane), in. . . . .	39.672	9.918
Side area (excluding vertical tail), sq ft . . . . .	346	21.6
Frontal area (including canopy), sq ft . . . . .	24.7	1.542

TABLE I.- DESIGN CHARACTERISTICS OF THE REPUBLIC F-105 AIRPLANE AND THE 1/4-SCALE MODEL OF THE F-105 AIRPLANE - CONCLUDED

	Full-scale	1/4-scale
<u>Trailing-Edge Flaps</u>		
Basic data:		
Type . . . . .	Single slotted	Single slotted
Deflection, measured in a plane normal to 0.82c line, deg . . . . .	0 to 46.2	0,30,35,40,46
Dimensions (maximum span flap):		
Average chord, measured parallel to airplane center line . . . . .	0.25c	0.25c
Span (one flap), measured normal to airplane center line, ft . . . . .	11.7	2.925
Location of outboard edge, measured normal to airplane center line, in. . . . .	168.0	42
Location of inboard edge, measured normal to airplane center line, in. . . . .	27.85	6.963
Area (maximum span flap):		
Area of both trailing-edge flaps, sq ft . . . . .	69.6	4.35
<u>Leading-Edge Flaps</u>		
Basic data:		
Type . . . . .	Drooped nose	Drooped nose
Deflection, measured in a plane normal to hinge line, deg . . . . .	0 to 20	0,7.5,15,20,25,30
Location of inboard edge, measured normal to airplane center line, in. . . . .	82.149	20.537
Location of outboard edge, measured normal to airplane center line, in. . . . .	199.78	49.945
Dimensions:		
Average leading-edge flap chord (streamwise) . . . . .	0.12c	0.12c
Span (one flap), measured normal to airplane center line, ft . . . . .	9.8	2.45
Area:		
Area of both leading-edge flaps, sq ft . . . . .	22.7	1.419
<u>External Tanks (450-gallon capacity)</u>		
Length, in. . . . .	227.55	56.89
Diameter (max.), in. . . . .	29.0	7.25
Angle of incidence, relative to fuselage center line, deg . . . . .	-3.0	-3.0
Spanwise location, measured from fuselage center line, in. . . . .	129.0	31.75
Vertical location of nose of tank, measured below fuselage center line, in. . . . .	-40.04	-10.01
Longitudinal location of nose of tank, measured from fuselage station 0, in. . . . .	391.16	97.79

TABLE II. SUMMARY OF THE LONGITUDINAL STABILITY CHARACTERISTICS OF A 1/4-SCALE MODEL OF THE F-105 AIRPLANE WITH A TAIL ASPECT RATIO OF 3.06 AND A SUPERSONIC ELLIPTICAL INLET

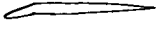
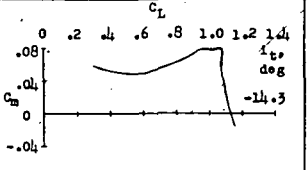
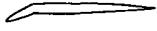
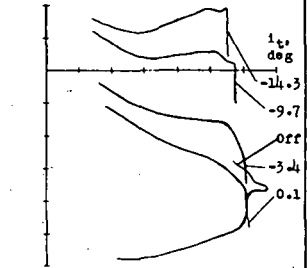
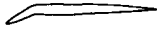
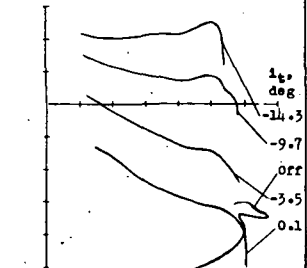
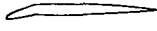
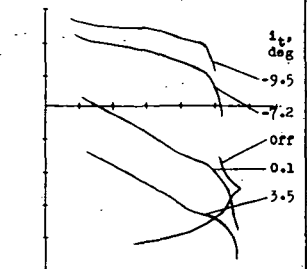
Wing, aspect ratio . . . . .	3.18	Fuselage . . . . .	basic
Tail, aspect ratio . . . . .	3.06	Inlet . . . . .	supersonic-type elliptical

Wing configuration		Speed-brake deflection		Store	Tail configuration			CL at $\alpha=12^\circ$	CL max	$\alpha$ at CL max	$C_m$ characteristics about $0.25^\circ$	Fig.
T.E. device	Stall-control device	Horizontal, deg	Vertical, deg		Height 2x/b	NACA airfoil section	$i_t$ , deg					
None	None	0	0	None	-0.123	65A series	off	0.63	0.95	26.7		6
Single slotted flap 0.135b/2 to 0.600b/2 $\delta = 46^\circ$	 L.E. flap 0.382b/2 to 0.950b/2 $\delta = 20^\circ$	0	0	450 gal	-0.123	65A series	-7.3	0.99	1.20	20.6		8
							-3.5	1.01	1.21	19.4		9
							off	1.07	1.15	18.3		
							3.5	1.06	1.29	19.8		
Single slotted flap 0.135b/2 to 0.650b/2 $\delta = 46^\circ$	 L.E. flap 0.382b/2 to 0.950b/2 $\delta = 20^\circ$	0	0	450 gal	-0.123	65A series	-7.3	1.02	1.22	28.0		10
							-3.5	1.03	1.26	28.6		11
							off	1.11	1.19	19.0		
							3.5	1.10	1.31	20.4		
Single slotted flap 0.135b/2 to 0.700b/2 $\delta = 46^\circ$	 L.E. flap 0.382b/2 to 0.950b/2 $\delta = 20^\circ$	0	0	450 gal	-0.123	65A series	-9.7	1.02	1.22	25.0		12
							-7.3	1.05	1.27	29.0		13
							off	1.23	1.20	18.4		
							0.1	1.10	1.32	21.0		
							3.5	1.15	1.33	19.8		

<sup>o</sup> Highest angle of test.



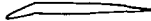
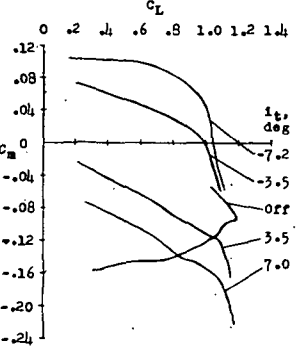
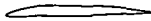
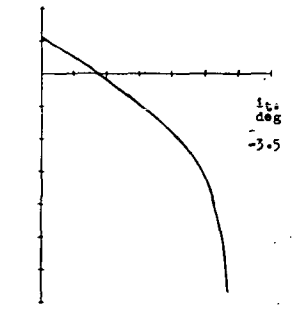
TABLE II.- SUMMARY OF THE LONGITUDINAL STABILITY CHARACTERISTICS OF A 1/8-SCALE MODEL OF THE F-105 AIRPLANE WITH A TAIL ASPECT RATIO OF 3.06 AND A SUPERSONIC ELLIPTICAL INLET - Continued

Wing configuration		Speed-brake deflection		Store	Tail configuration			CL at $\alpha=12^\circ$	CL <sub>max</sub>	$\alpha$ at CL <sub>max</sub>	C <sub>m</sub> characteristics about 0.25c	Fig.
T.E. device	Stall-control device	Horizontal, deg	Vertical, deg		Height, 2x/b	NACA airfoil section	i <sub>t</sub> , deg					
Single slotted flap 0.133b/2 to 0.800b/2 $\delta = 46^\circ$		0	0	450 gal	-0.123	65A series	-14.3	1.05	1.20	24.8*		24
Single slotted flap 0.133b/2 to 0.800b/2 $\delta = 46^\circ$		0	0	450 gal	-0.123	65A series	-14.3	1.16	1.32	21.0		14
							-9.7	1.18	1.32	21.6		
							Off	1.19	1.35	21.0		15
							-3.4	1.14	1.41	21.0		
							0.1	1.16	1.42	21.5		
Single slotted flap 0.133b/2 to 0.800b/2 $\delta = 40^\circ$		0	0	450 gal	-0.123	65A series	-14.3	0.98	1.30	24.0		16
							-9.7	1.03	1.37	23.0		
							Off	1.15	1.34	21.2		17
							-3.5	1.07	1.44	23.4		
							0.1	1.12	1.44	23.0		
Single slotted flap 0.133b/2 to 0.700b/2 $\delta = 40^\circ$		0	0	450 gal	-0.123	65A series	-9.5	0.97	1.22	28.6*		18
							-7.2	1.00	1.23	28.0		
							Off	1.07	1.19	19.0		19
							0.1	1.06	1.30	20.6		
							3.5	1.08	1.35	20.8		

\* Highest angle of test.



TABLE II.- SUMMARY OF THE LONGITUDINAL STABILITY CHARACTERISTICS OF A 1/4-SCALE MODEL OF THE F-105 AIRPLANE WITH A TAIL ASPECT RATIO OF 3.06 AND A SUPERSONIC ELLIPTICAL INLET - Concluded

Wing configuration		Speed-brake deflection		Store	Tail configuration			CL at $\alpha=12^\circ$	CL max	$\alpha$ at CL max	Cm characteristics about 0.25c	Fig.
T.E. device	Stall-control device	Horizontal, deg	Vertical, deg		Height, 2z/b	NACA airfoil section	$i_t$ , deg					
Single slotted flap 0.135b/2 to 0.650b/2 $\delta = 40^\circ$		0	0	450 gal	-0.123	65A series	-7.2	0.96	1.22	29.0*		20
							-3.5	0.99	1.28	21.4		21
							0	1.05	1.19	18.6		21
							3.5	1.07	1.33	21.0		21
							7.0	1.10	1.39	21.0		21
None		0	0	None	-0.123	65A series	-3.5	0.66	1.16	28.6		26

\* Highest angle of test.



TABLE III. SUMMARY OF THE LONGITUDINAL STABILITY CHARACTERISTICS OF A 1/4-SCALE MODEL OF THE F-105 AIRPLANE WITH A TAIL ASPECT RATIO OF 3.06 AND A TRANSONIC ELLIPTICAL INLET

Wing, aspect ratio . . . . .	3.18	Fuselage . . . . .	basic
Tail, aspect ratio . . . . .	3.06	Inlet . . . . .	transonic-type elliptical

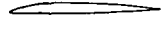
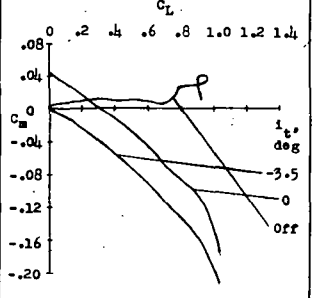
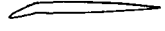
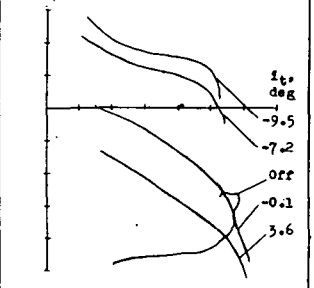
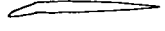
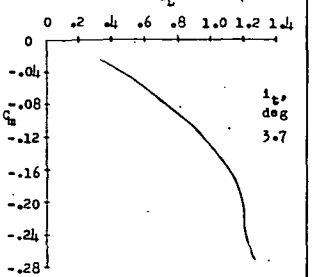
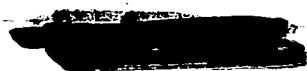
Wing configuration		Speed-brake deflection		Store	Tail configuration			C <sub>L</sub> at α=12°	C <sub>L</sub> max	α at C <sub>L</sub> max	C <sub>m</sub> characteristics about 0.25c	Fig.
T.E. device	Stall-control device	Horizontal, deg	Vertical, deg		Height 2z/b	NACA airfoil section	i <sub>t</sub> , deg					
None	 L.E. flap 0.382b/2 to 0.950b/2 δ = 7.5°	0	0	None	-0.123	65A series	-3.5	0.65	1.12	28.8°		27
Single slotted flap 0.133b/2 to 0.700b/2 δ = 46°	 L.E. flap 0.382b/2 to 0.950b/2 δ = 20°	0	0	450 gal	-0.123	65A series	-9.5	1.02	1.21	28.9°		
							-7.2	1.04	1.23	28.9°		
							off	1.12	1.16	18.0		
							-0.1	1.10	1.22	27.4		
							3.6	1.13	1.31	21.0		

TABLE IV. SUMMARY OF THE LONGITUDINAL STABILITY CHARACTERISTICS OF A 1/4-SCALE MODEL OF THE F-105 AIRPLANE WITH A TAIL ASPECT RATIO OF 3.49 AND A TRANSONIC ELLIPTICAL INLET

Wing, aspect ratio . . . . .	3.18	Fuselage . . . . .	basic
Tail, aspect ratio . . . . .	3.49	Inlet . . . . .	transonic-type elliptical

Wing configuration		Speed-brake deflection		Store	Tail configuration			C <sub>L</sub> at α=12°	C <sub>L</sub> max	α at C <sub>L</sub> max	C <sub>m</sub> characteristics about 0.25c	Fig.
T.E. device	Stall-control device	Horizontal, deg	Vertical, deg		Height 2z/b	NACA airfoil section	i <sub>t</sub> , deg					
Single slotted flap 0.133b/2 to 0.700b/2 δ = 46°	 L.E. flap 0.382b/2 to 0.950b/2 δ = 20°	0	0	450 gal	-0.123	65A series	3.7	1.16	1.32	20.9		30

\*Highest angle of test



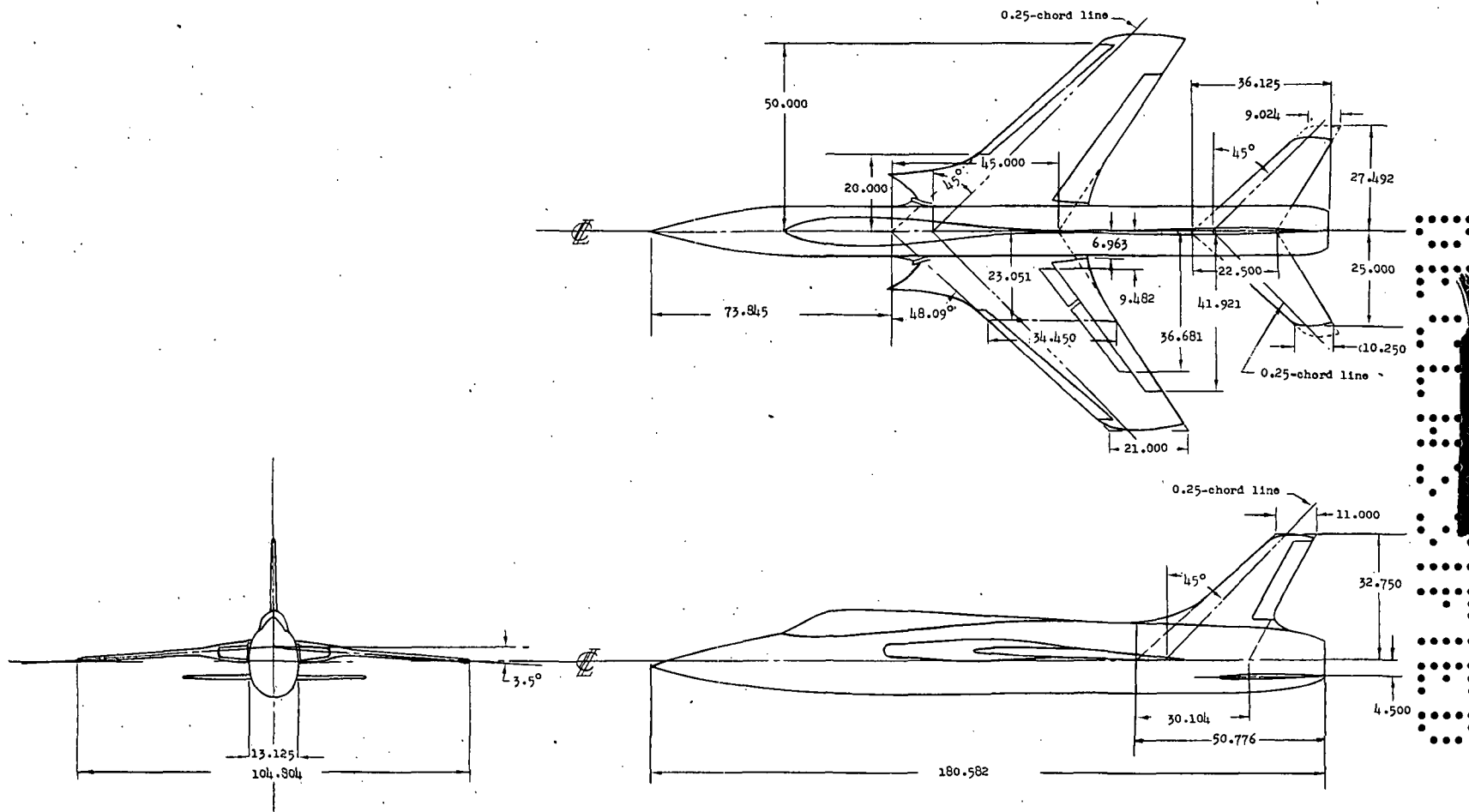


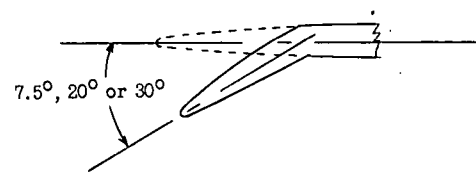
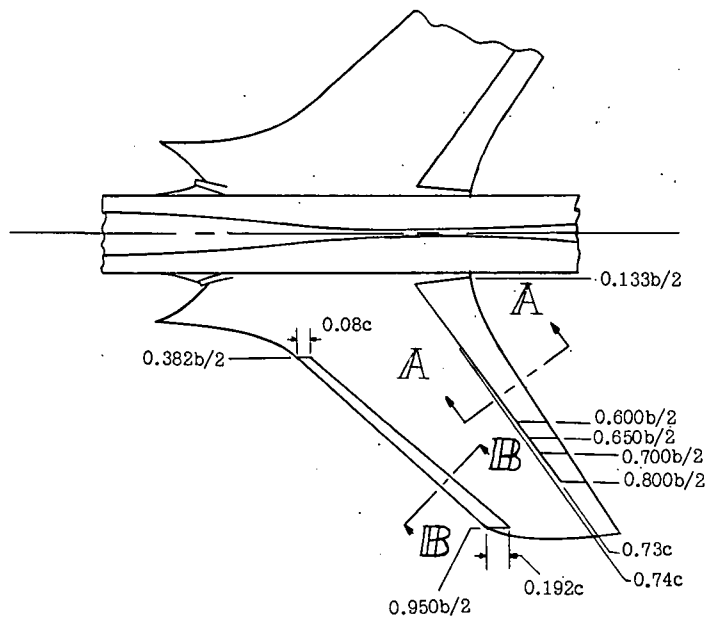
Figure 1.- Three-view drawing of a 1/4-scale model of the F-105 airplane.  
 (Dimensions in inches unless otherwise noted.)





L-84117

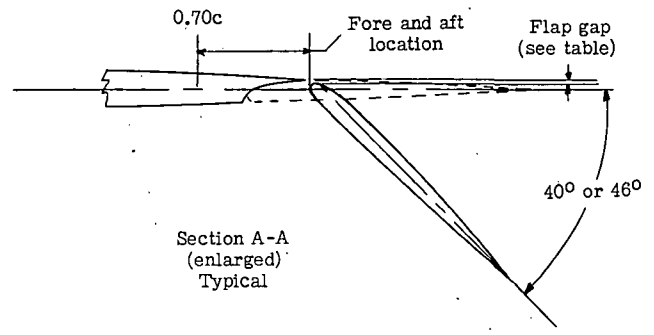
Figure 2.- The 1/4-scale model of the F-105 airplane mounted on the normal three-support system of the Langley 19-foot pressure tunnel.



Section B-B  
(enlarged)  
Typical

Wing Flap Data  
(46° deflection only)

Flap station b/2	Deflection			Flap gap, inches			Fore and aft position, inches		
	Actual		Loft	Actual		Loft	Actual		Loft
	L.H.	R.H.		L.H.	R.H.		L.H.	R.H.	
0.242	46°49'	46°26'	46°13'	0.41	0.40	0.415	2.72	2.73	2.72
.415	46°42'	46°45'	46°13'	.31	.32	.350	2.92	2.91	2.90
.647	46°34'	46°54'	46°13'	--	--	--	--	--	--
.669	--	--	--	.345	.34	.295	2.45	2.47	2.47



Section A-A  
(enlarged)  
Typical

(a) Leading-edge flap.

(b) Trailing-edge flap.

Figure 3.- Details of the leading- and trailing-edge flaps.

037129103

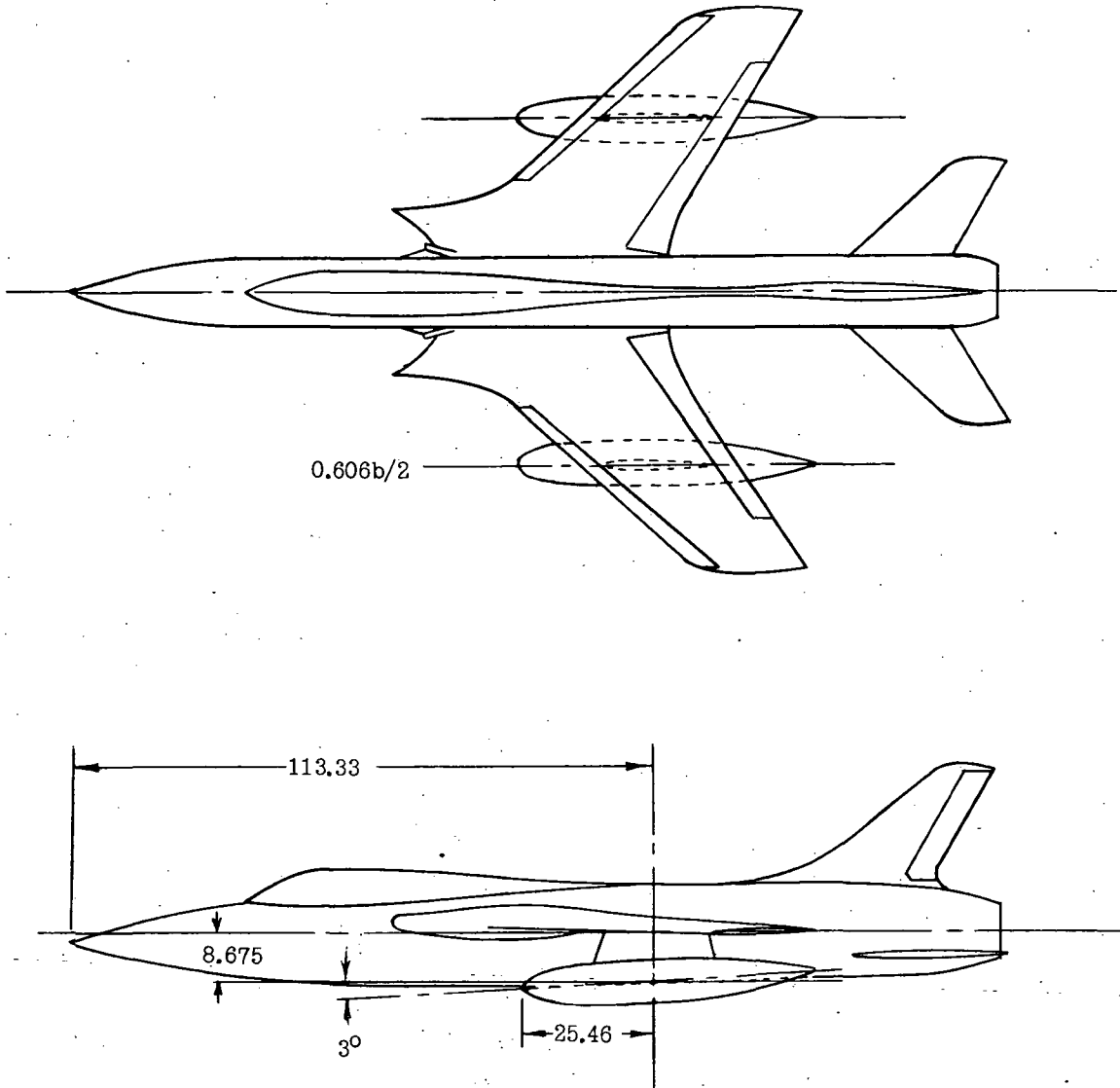
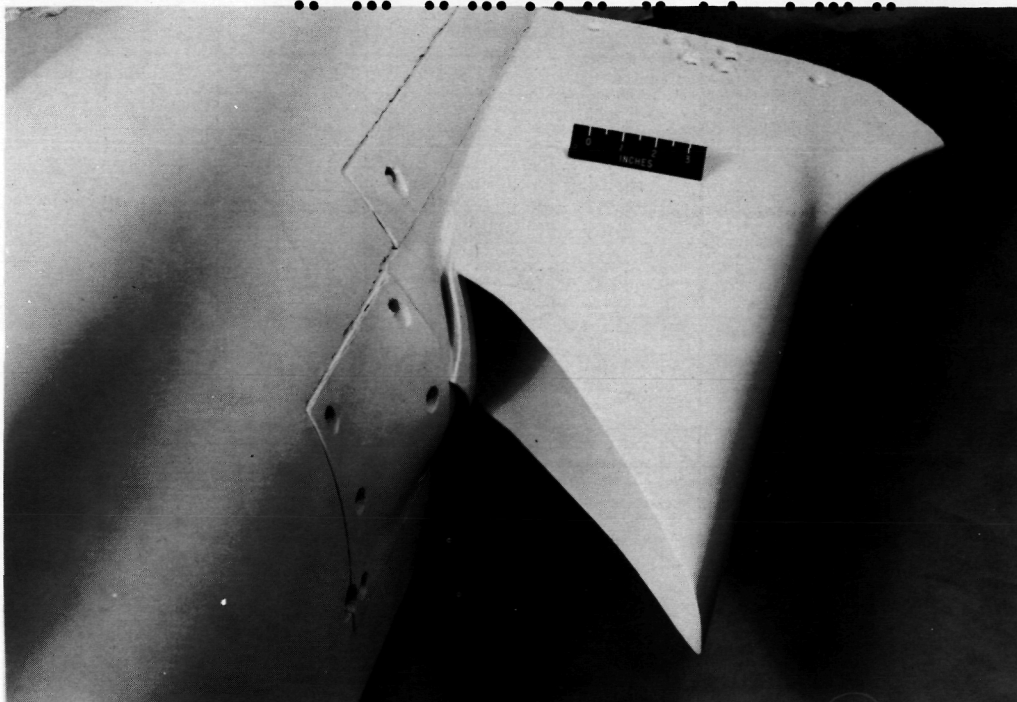
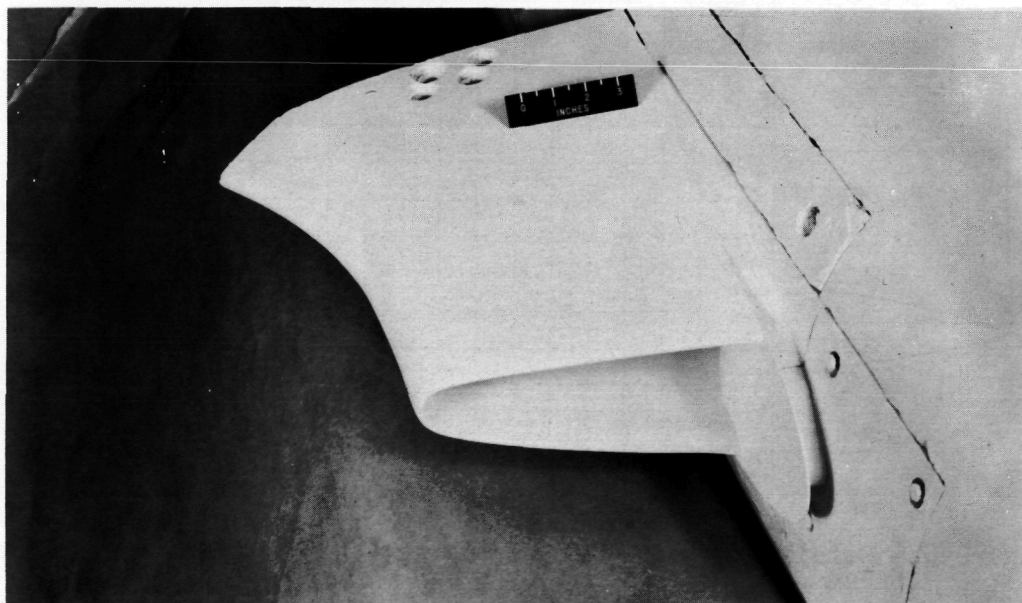


Figure 4.- Details of the external stores. (All dimensions in inches).

~~SECRET~~



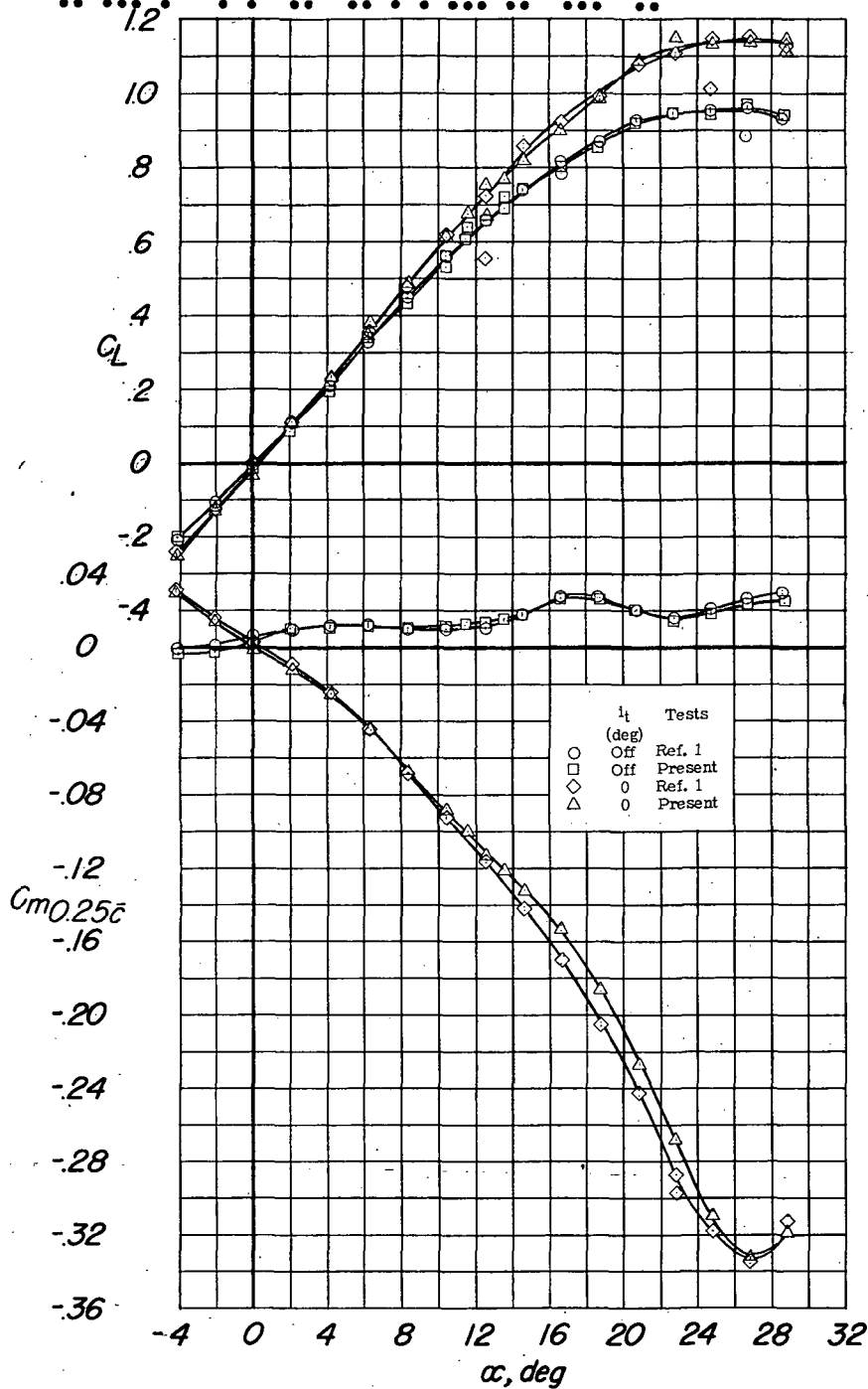
(a) Supersonic-type elliptical inlet. L-85123



(b) Transonic-type elliptical inlet. L-85124

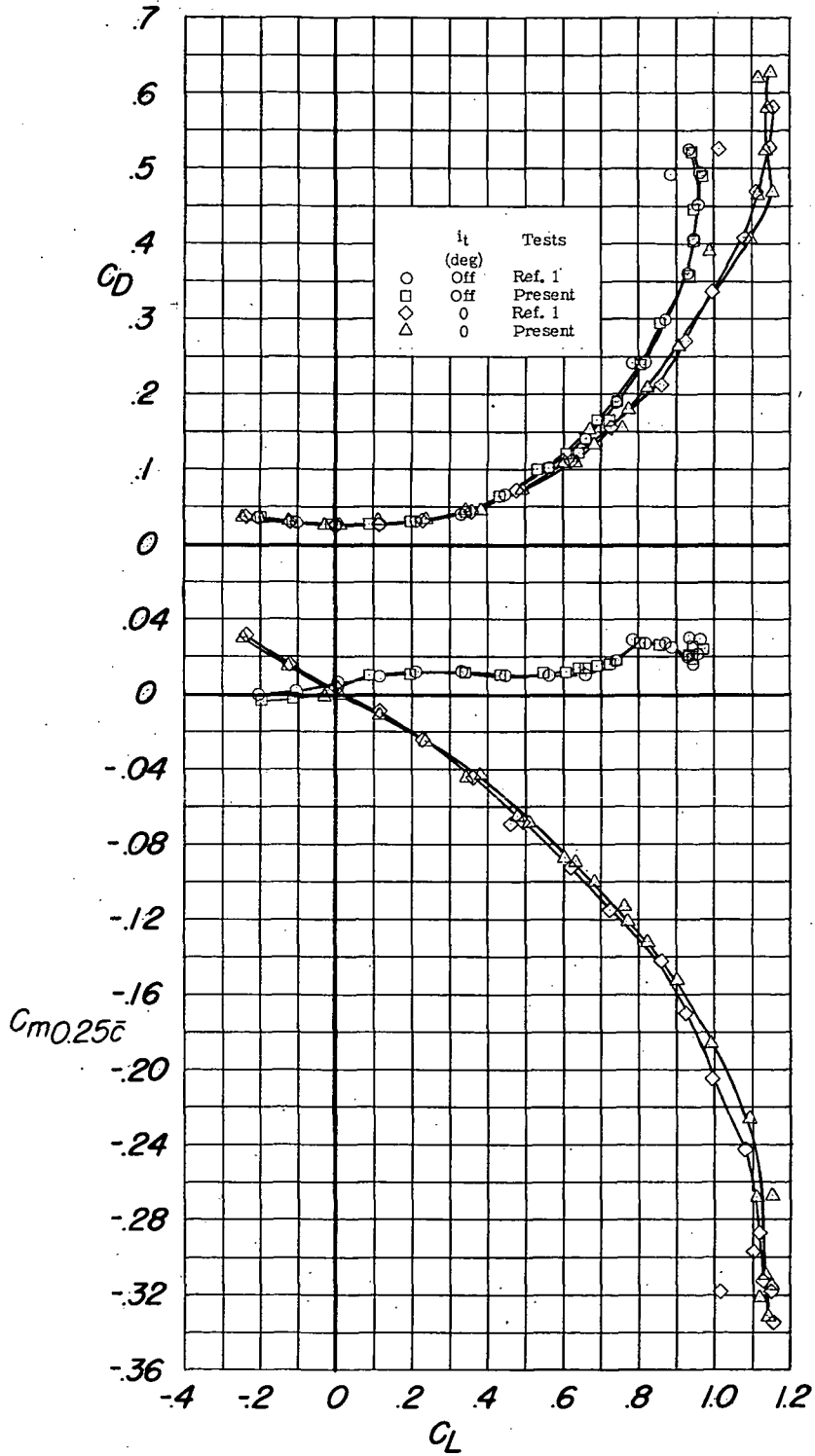
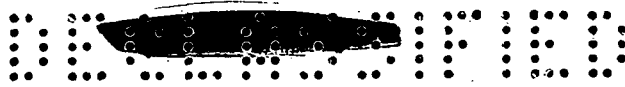
Figure 5.- Wing-root inlets of the 1/4-scale model of the F-105 airplane (without wing).

~~SECRET~~



(a)  $C_L$  and  $C_{m_{0.25c}}$  against  $\alpha$ .

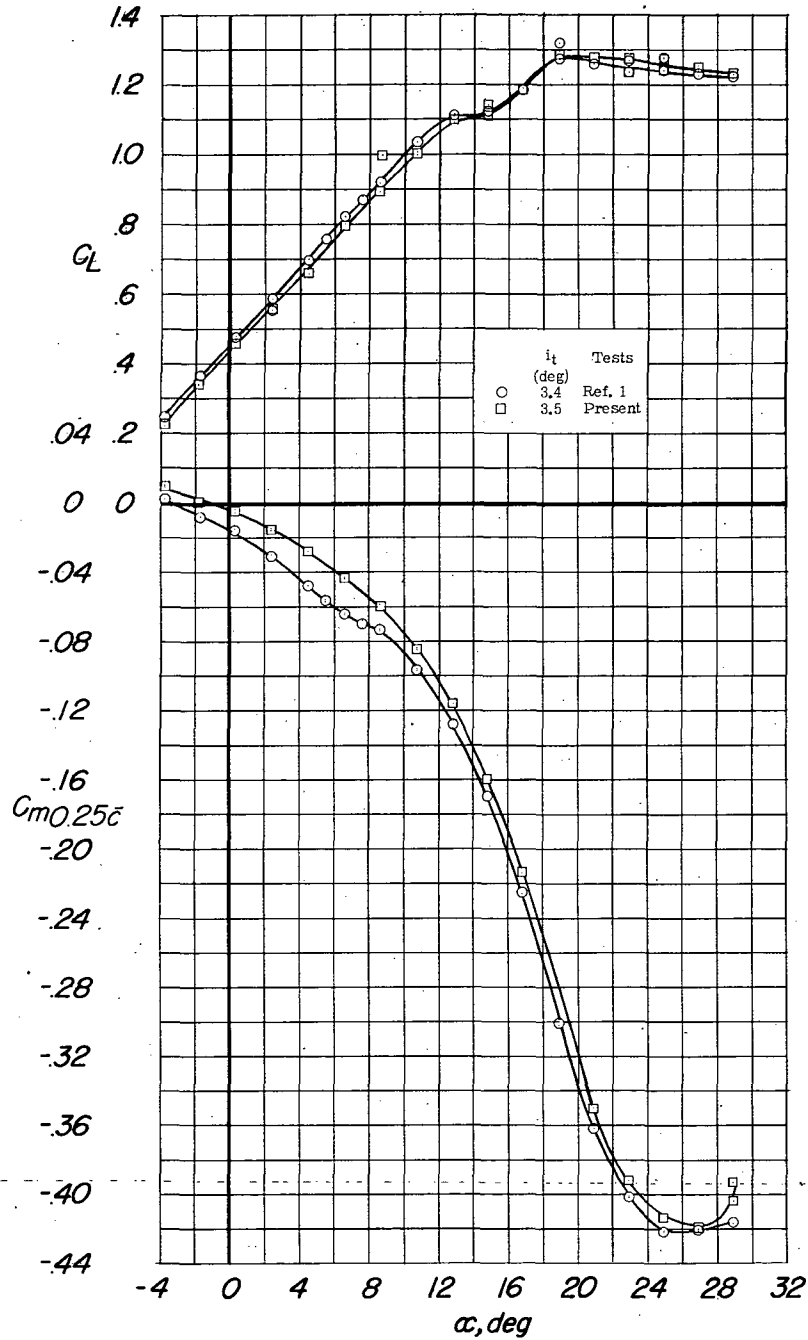
Figure 6.- Longitudinal characteristics of the model obtained during the present tests and the tests of reference 1. Configuration: A + V +  $I_{SE} + (-0.123)T$ ; center-of-gravity location,  $0.25\bar{c}$ .



(b)  $C_D$  and  $C_{m0.25c}$  against  $C_L$ .

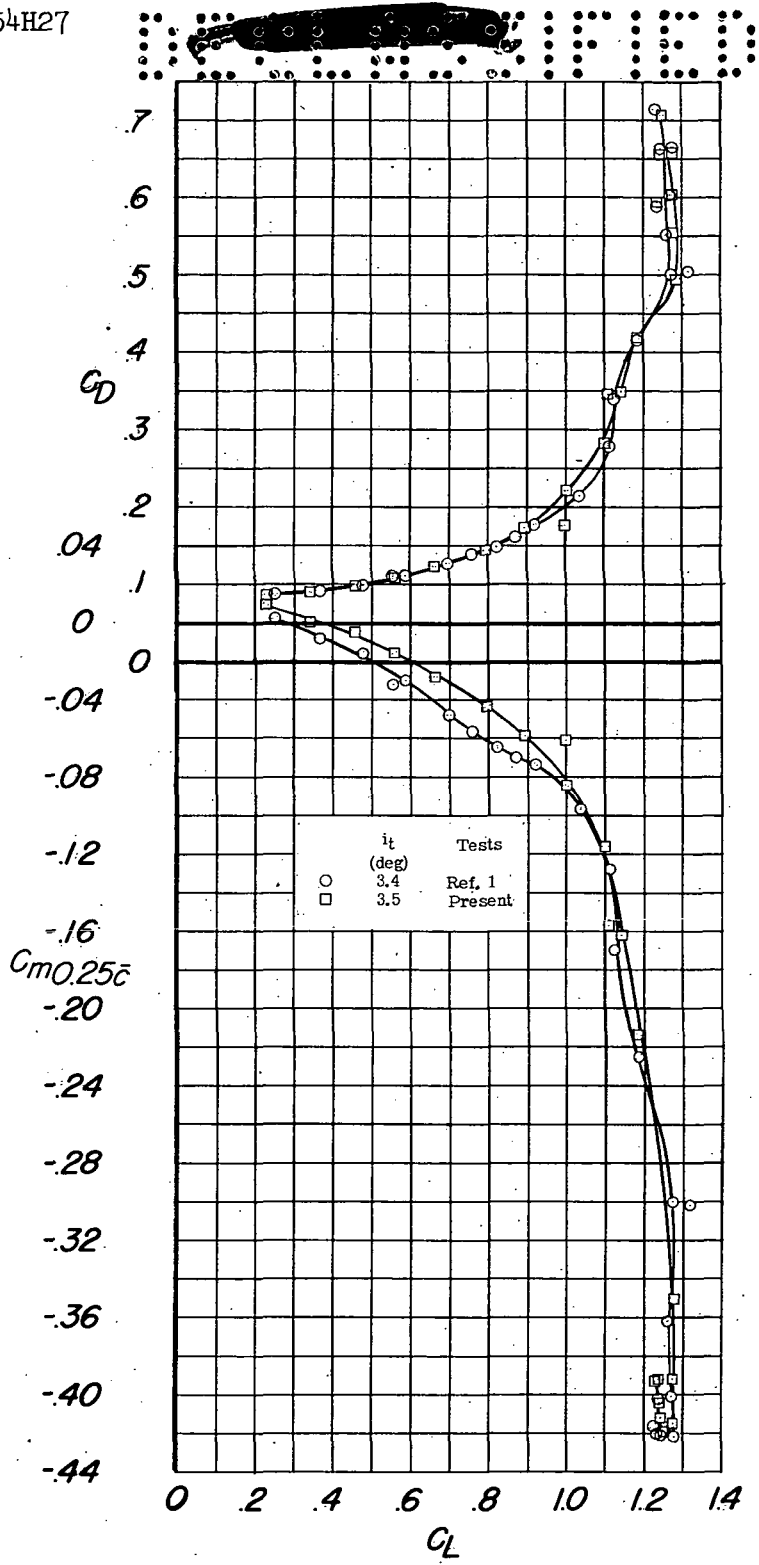
Figure 6.- Concluded.





(a)  $C_L$  and  $C_{m_{0.25c}}$  against  $\alpha$ .

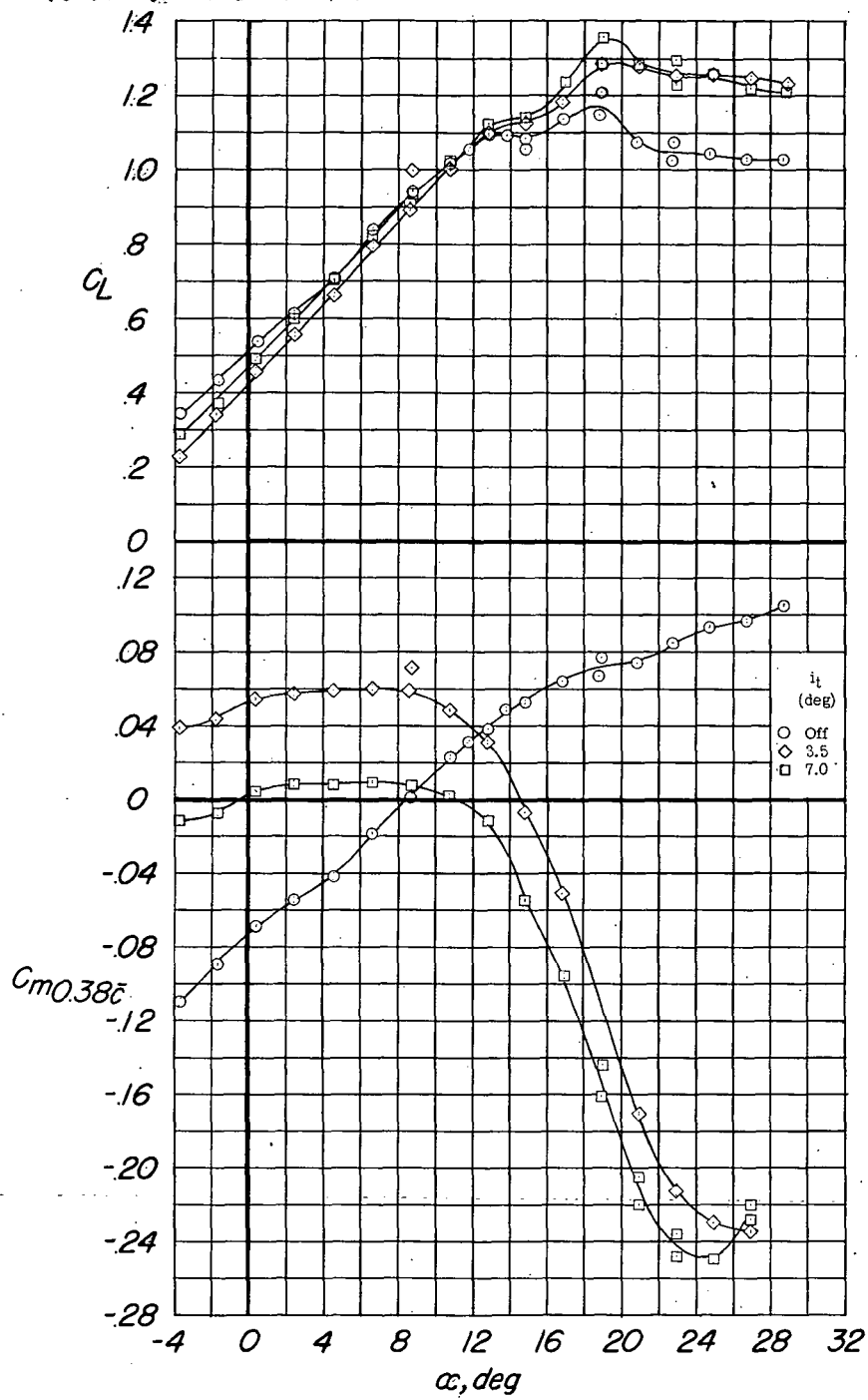
Figure 7.- Longitudinal characteristics of the model with 60-percent-span trailing-edge flaps deflected  $46^\circ$  and the leading-edge flaps drooped  $20^\circ$  obtained during the present tests and the tests of reference 1. Configuration: A + V + I<sub>SE</sub> + (-0.123)T + 0.60F<sub>46</sub> + N<sub>20</sub> + E<sub>0450</sub>; center-of-gravity location, 0.25 $\bar{c}$ .



(b)  $C_D$  and  $C_{m0.25\bar{c}}$  against  $C_L$ .

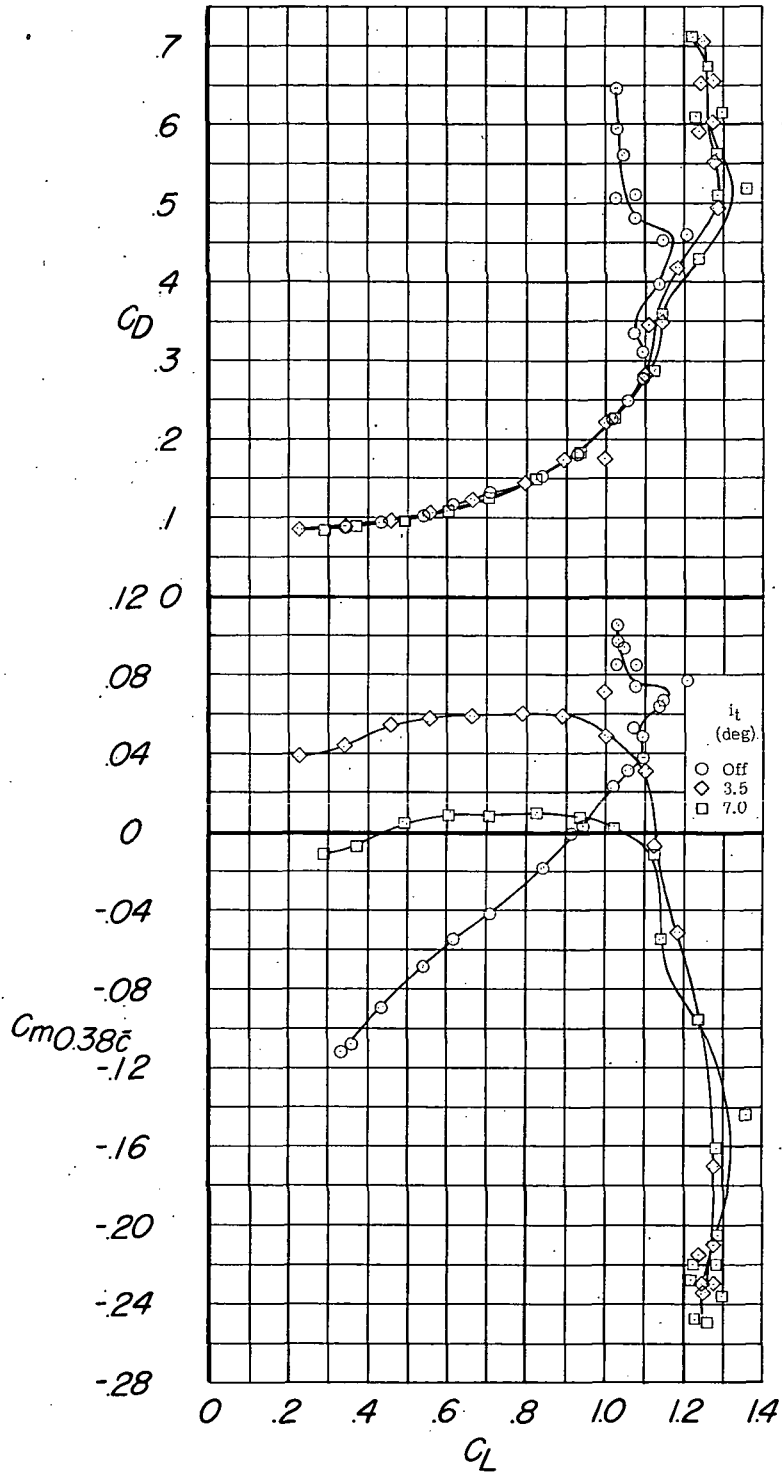
Figure 7.- Concluded.





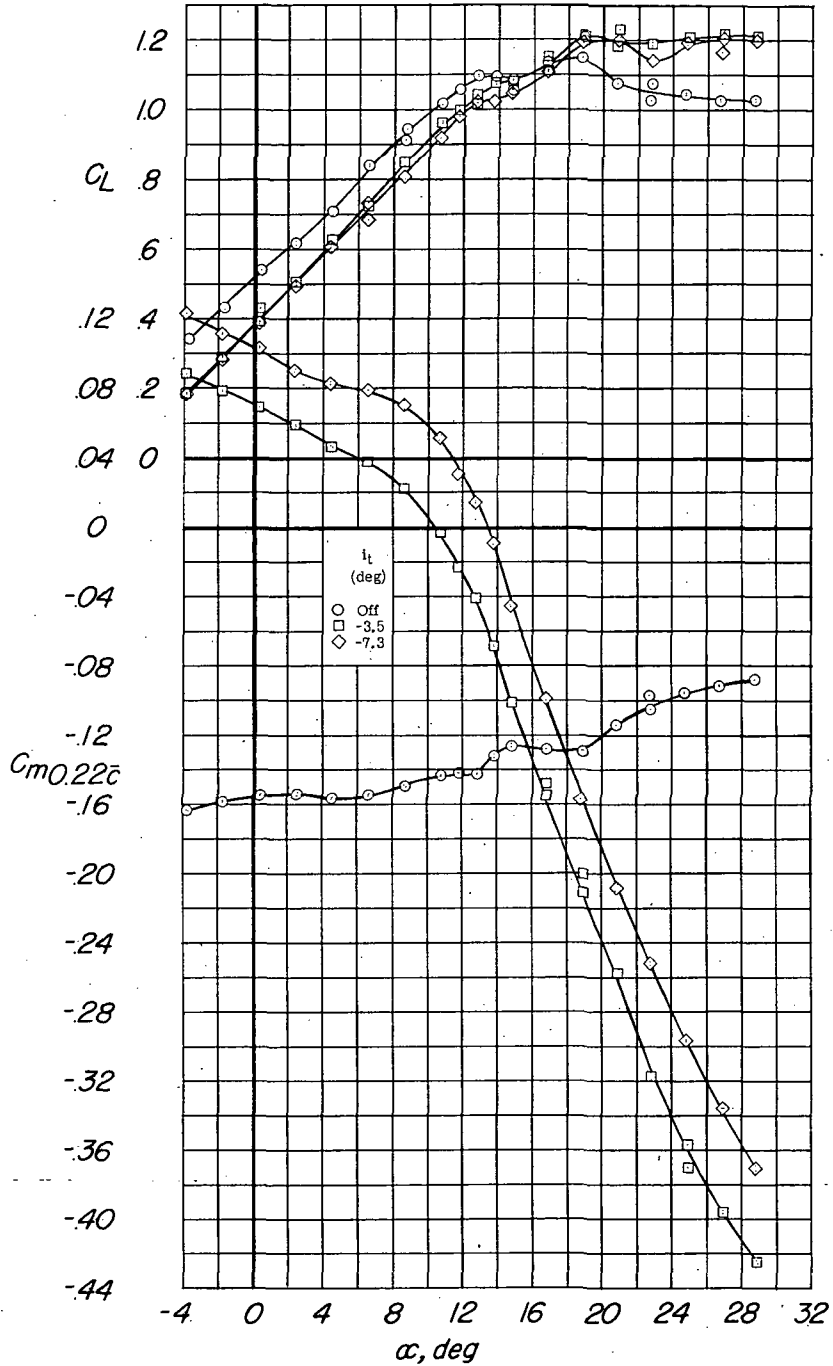
(a)  $C_L$  and  $C_{m0.38\bar{c}}$  against  $\alpha$ .

Figure 8.- Longitudinal characteristics of the model with 60-percent-span trailing-edge flaps deflected  $46^\circ$  and the leading-edge flaps drooped  $20^\circ$ . Configuration: A + V + ISE + (-0.123)T + 0.60F<sub>46</sub> + N<sub>20</sub> + E<sub>0450</sub>; center-of-gravity location, 0.38 $\bar{c}$ .



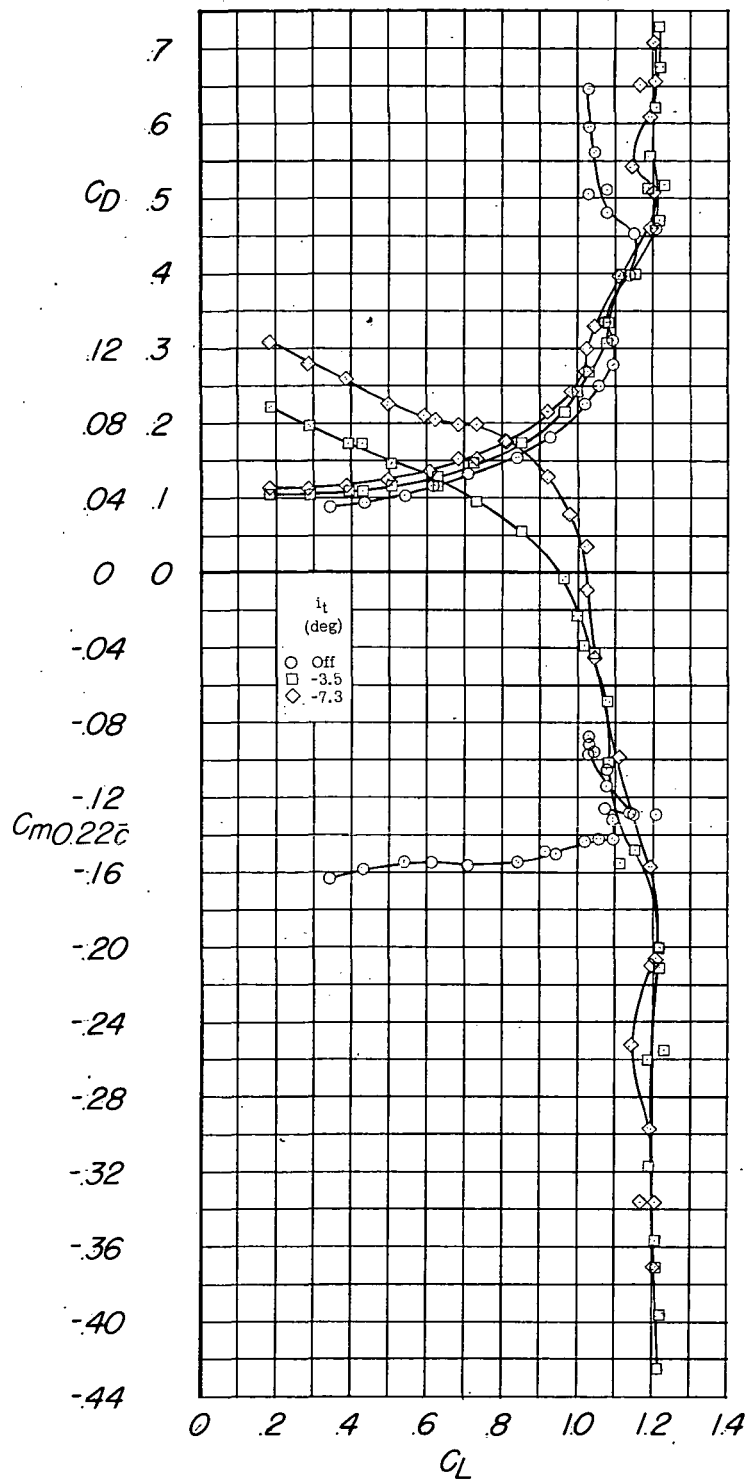
(b)  $C_D$  and  $C_{m_{0.38\bar{c}}}$  against  $C_L$ .

Figure 8.- Concluded.



(a)  $C_L$  and  $C_{m_{0.22\bar{c}}}$  against  $\alpha$ .

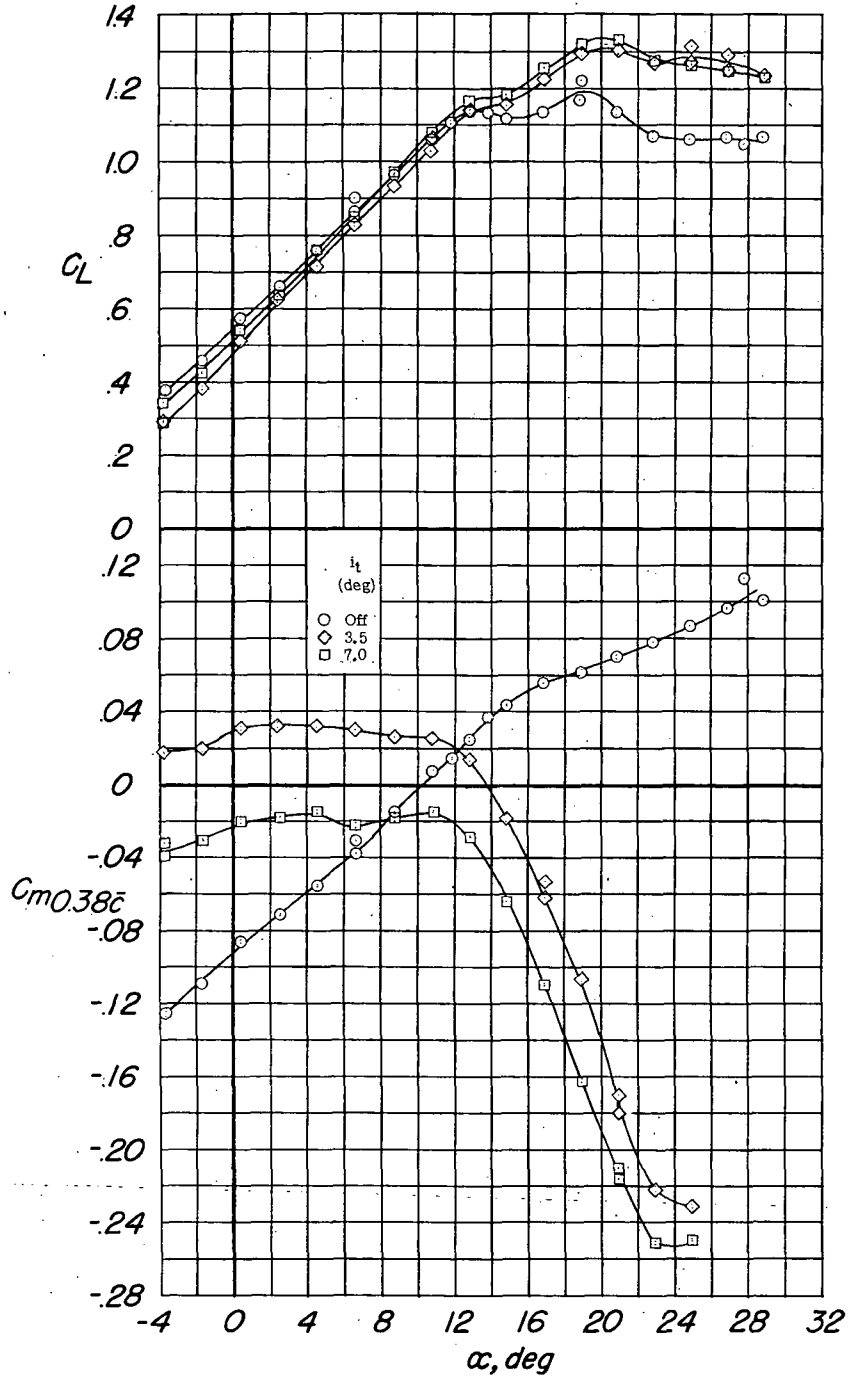
Figure 9.- Longitudinal characteristics of the model with 60-percent-span trailing-edge flaps deflected  $46^\circ$  and the leading-edge flaps drooped  $20^\circ$ . Configuration: A + V + ISE + (-0.123)T + 0.60F<sub>46</sub> + N<sub>20</sub> + E<sub>0450</sub>; center-of-gravity location, 0.22 $\bar{c}$ .



(b)  $C_D$  and  $C_{m_{0.22\bar{c}}}$  against  $C_L$ .

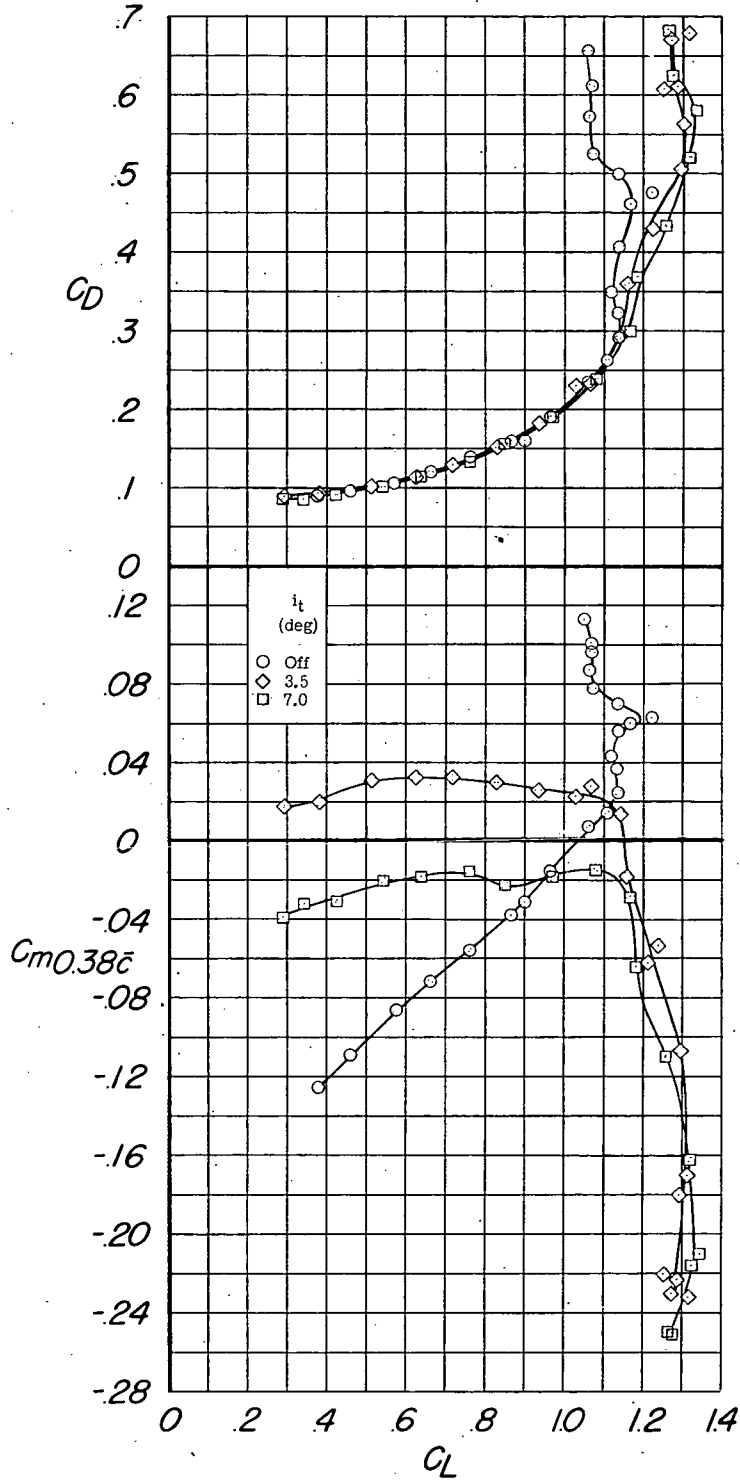
Figure 9.- Concluded.





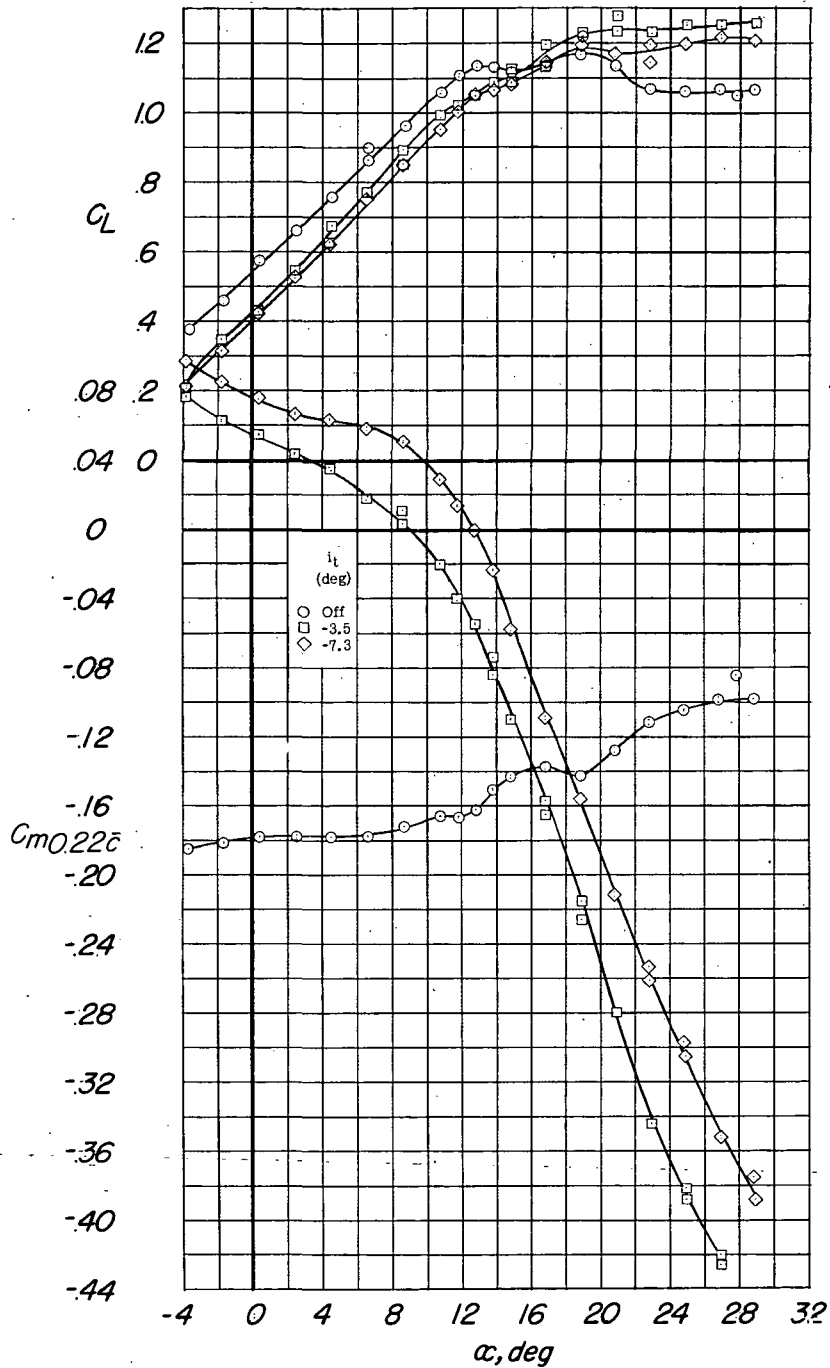
(a)  $C_L$  and  $C_{m0.38\bar{c}}$  against  $\alpha$ .

Figure 10.- Longitudinal characteristics of the model with 65-percent-span trailing-edge flaps deflected  $46^\circ$  and the leading-edge flaps drooped  $20^\circ$ . Configuration: A + V + I<sub>SE</sub> + (-0.123)T + 0.65F<sub>46</sub> + N<sub>20</sub> + E<sub>0450</sub>; center-of-gravity location, 0.38 $\bar{c}$ .



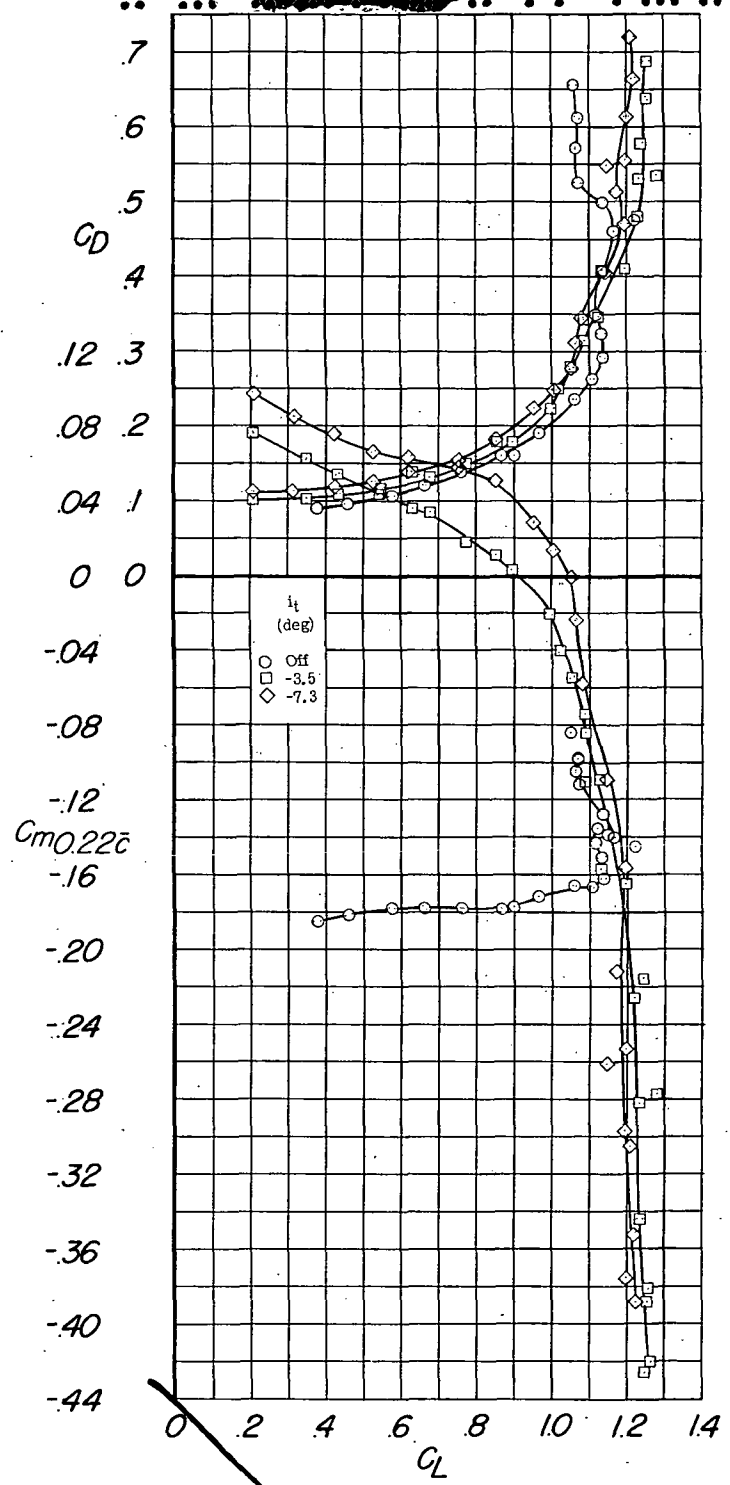
(b)  $C_D$  and  $C_{m0.38\bar{c}}$  against  $C_L$ .

Figure 10.- Concluded.



(a)  $C_L$  and  $C_{m0.22\bar{c}}$  against  $\alpha$ .

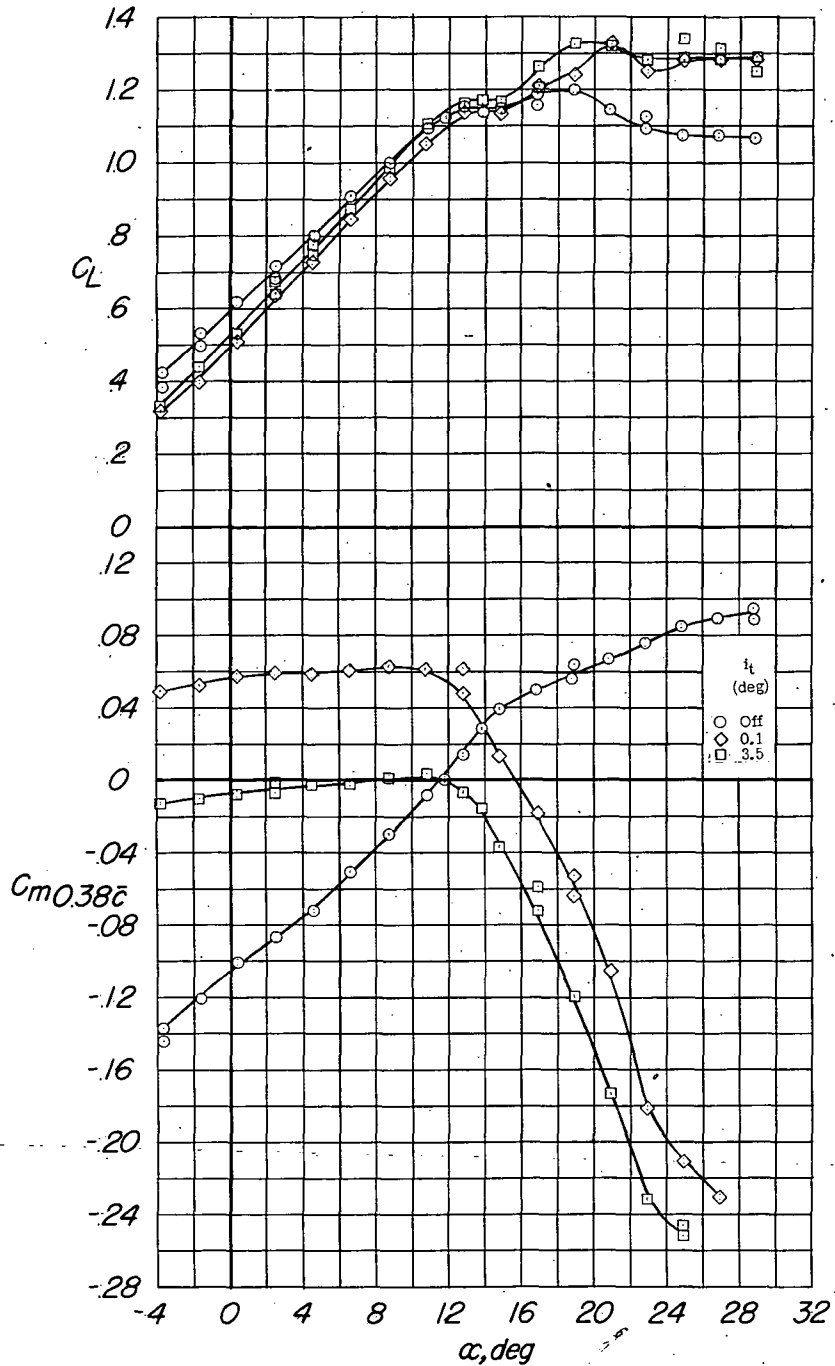
Figure 11.- Longitudinal characteristics of the model with 65-percent-span trailing-edge flaps deflected  $46^\circ$  and the leading-edge flaps drooped  $20^\circ$ . Configuration: A + V + I<sub>SE</sub> + (-0.123)T + 0.65F<sub>46</sub> + N<sub>20</sub> + E<sub>0</sub>450; center-of-gravity location,  $0.22\bar{c}$ .



(b)  $C_D$  and  $C_{m0.22\bar{c}}$  against  $C_L$ .

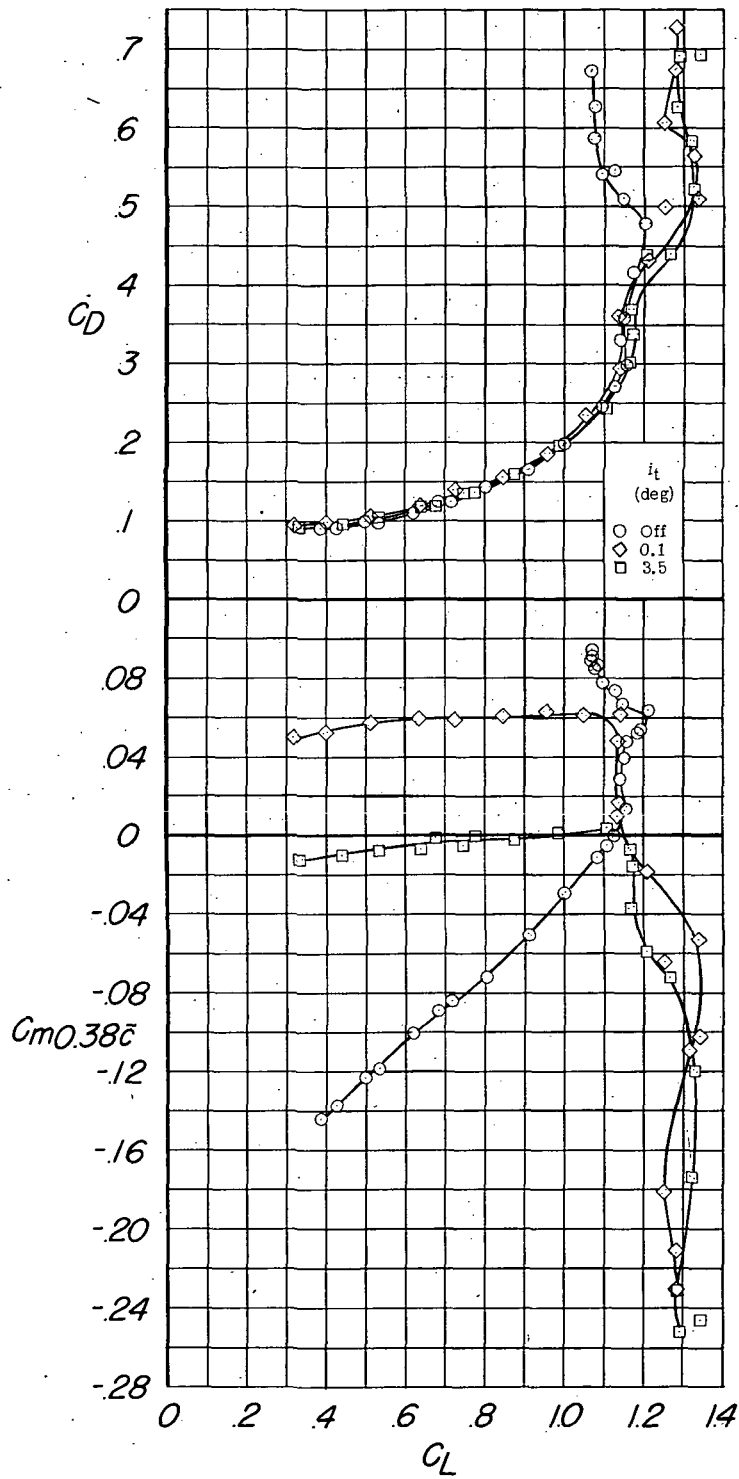
Figure 11.- Concluded.





(a).  $C_L$  and  $C_{m0.38c}$  against  $\alpha$ .

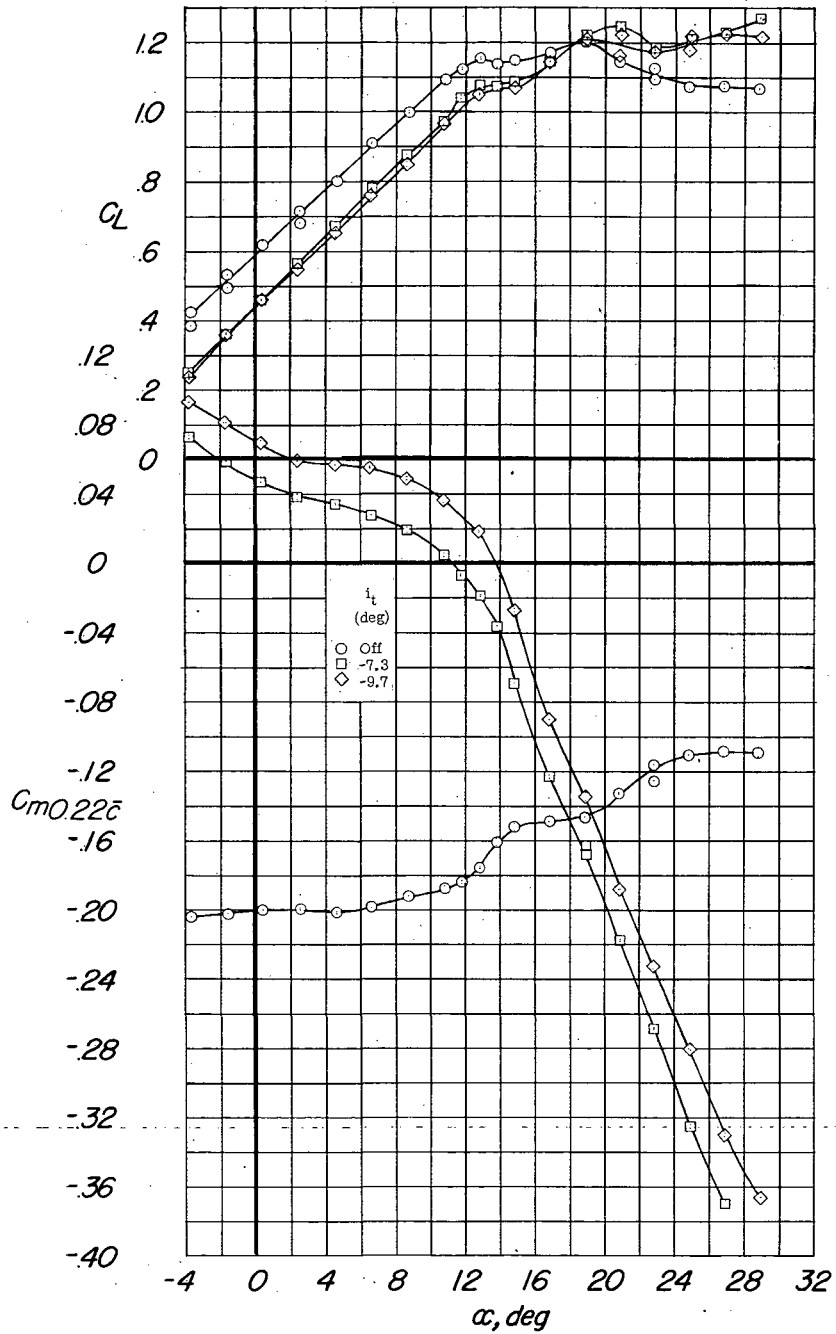
Figure 12.- Longitudinal characteristics of the model with 70-percent-span trailing-edge flaps deflected  $46^\circ$  and the leading-edge flaps drooped  $20^\circ$ . Configuration: A + V +  $I_{SE}$  +  $(-0.123)T$  +  $0.70F_{46}$  +  $N_{20}$  +  $E_{0450}$ ; center-of-gravity location,  $0.38\bar{c}$ .



(b)  $C_D$  and  $C_{m0.38\bar{c}}$  against  $C_L$ .

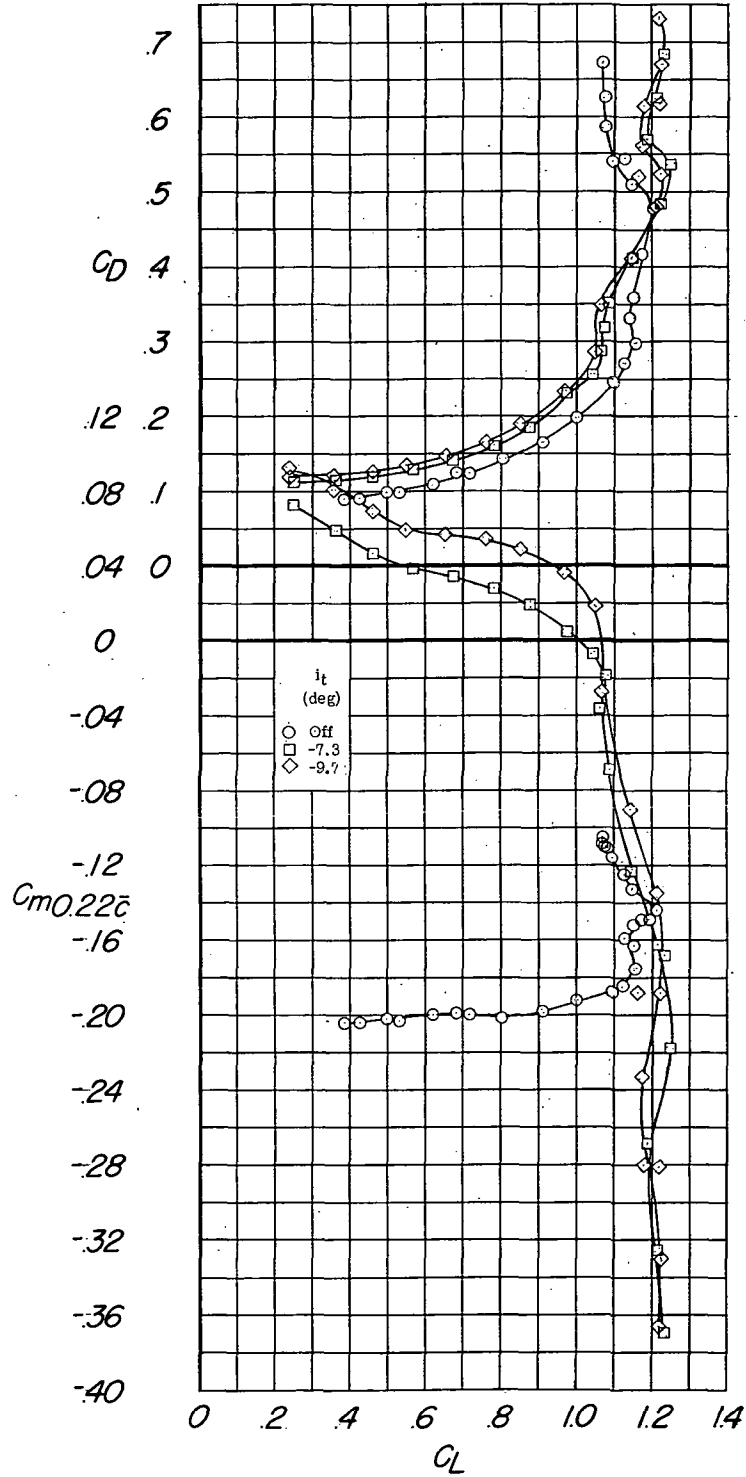
Figure 12.- Concluded.





(a)  $C_L$  and  $C_{m0.22\bar{c}}$  against  $\alpha$ .

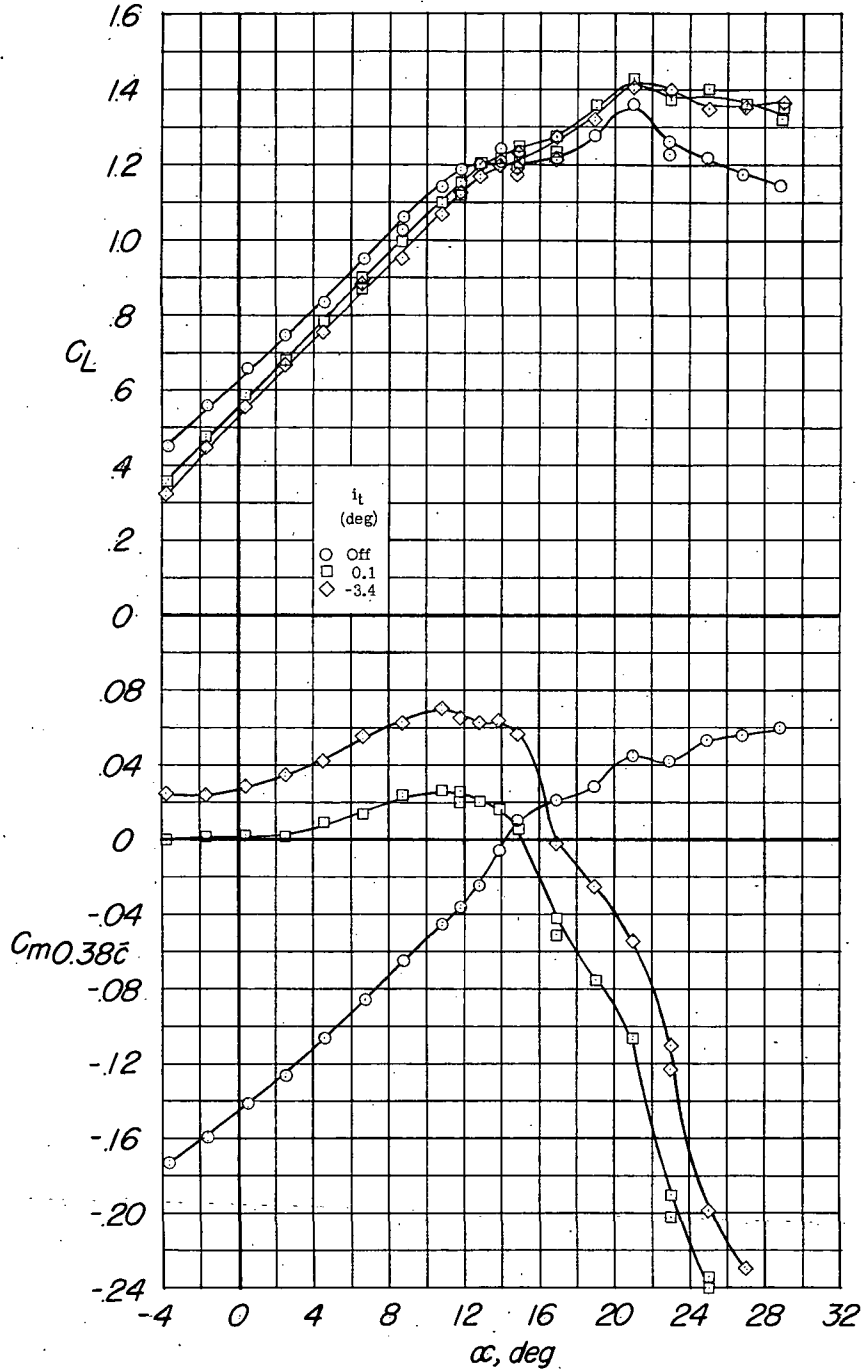
Figure 13.- Longitudinal characteristics of the model with 70-percent-span trailing-edge flaps deflected  $46^\circ$  and the leading-edge flaps drooped  $20^\circ$ . Configuration: A + V + I<sub>SE</sub> + (-0.123)T + 0.70F<sub>46</sub> + N<sub>20</sub> + E<sub>0450</sub>; center-of-gravity location, 0.22 $\bar{c}$ .



(b)  $C_D$  and  $C_{m0.22\bar{c}}$  against  $C_L$ .

Figure 13.- Concluded.

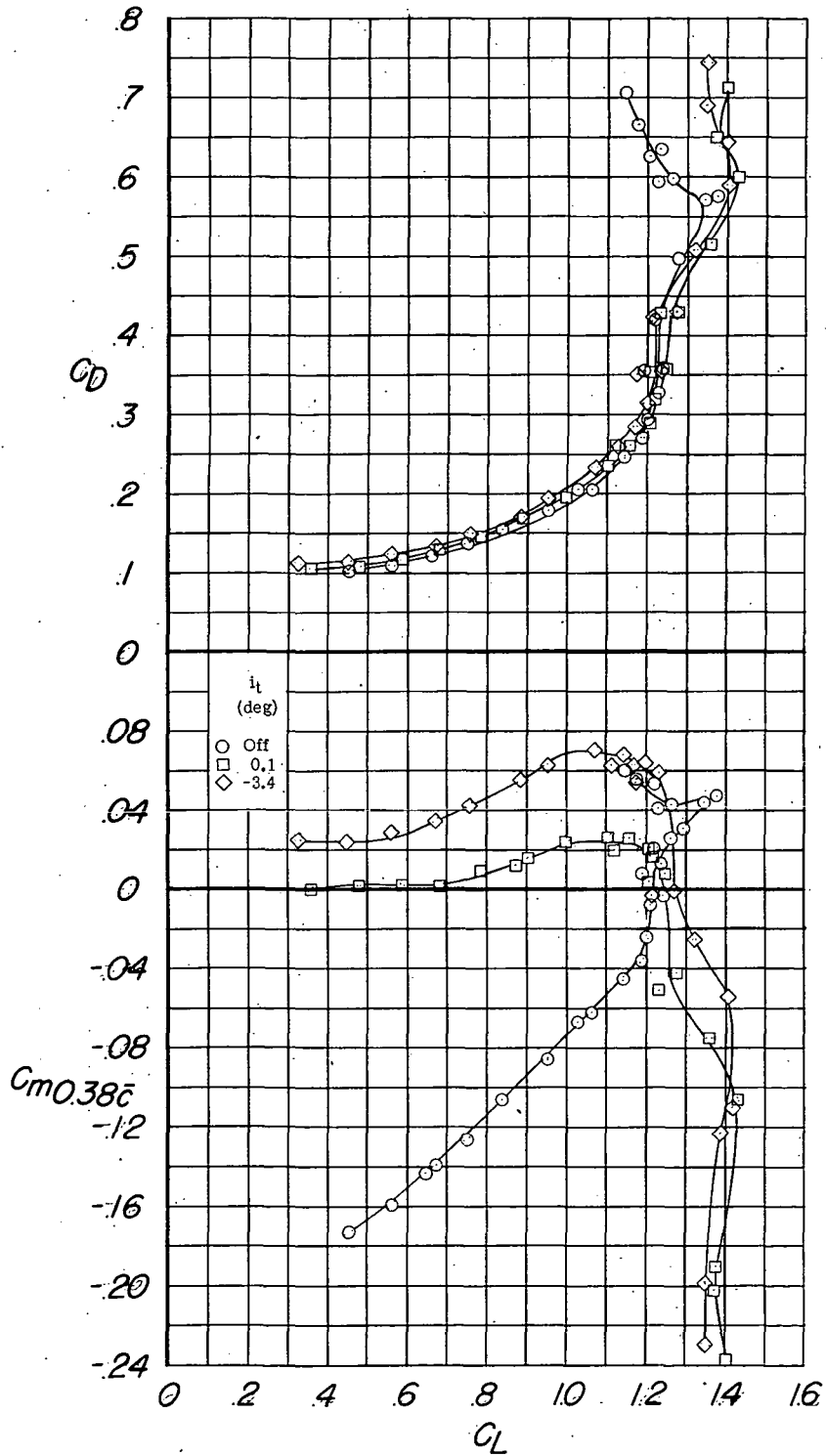




(a)  $C_L$  and  $C_{m0.38\bar{c}}$  against  $\alpha$ .

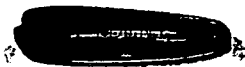
Figure 14.- Longitudinal characteristics of the model with 80-percent-span trailing-edge flaps deflected  $46^\circ$  and the leading-edge flaps drooped  $30^\circ$ . Configuration: A + V + I<sub>SE</sub> + (-0.123)T + 0.80F<sub>46</sub> + N<sub>30</sub> + E<sub>0450</sub>; center-of-gravity location, 0.38 $\bar{c}$ .

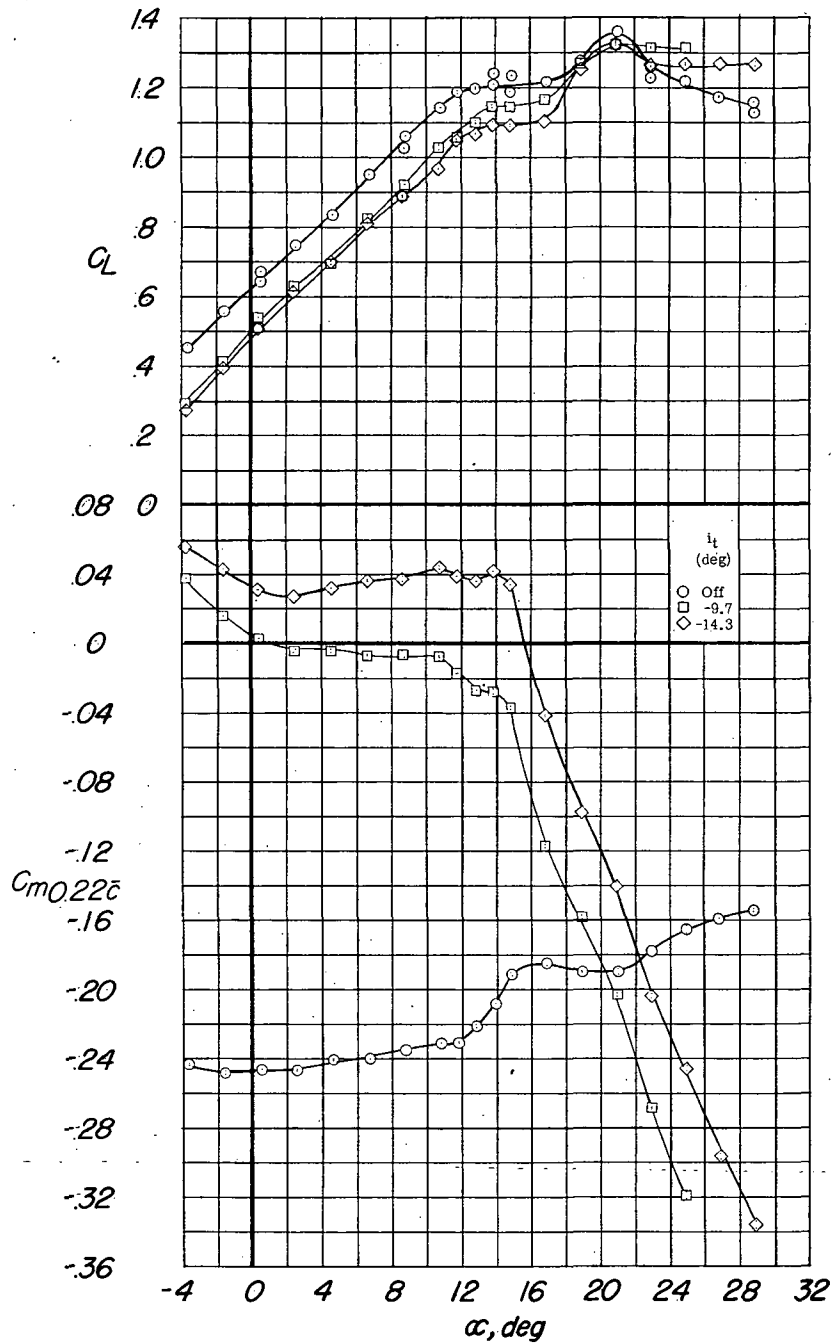




(b)  $C_D$  and  $C_{m0.38c}$  against  $C_L$ .

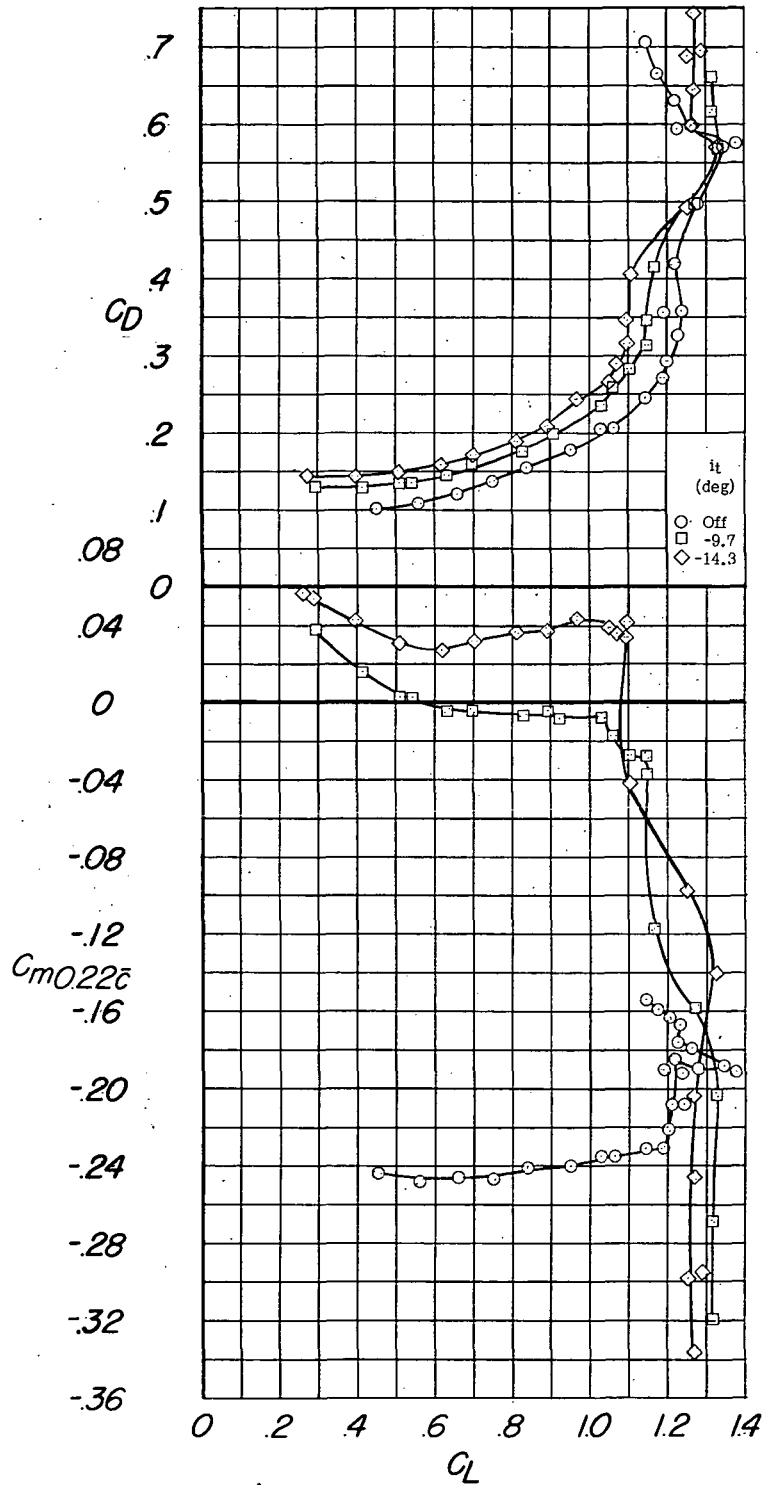
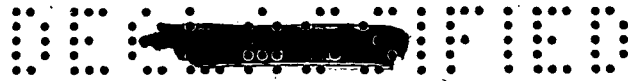
Figure 14.- Concluded.





(a)  $C_L$  and  $C_{m_{0.22\bar{c}}}$  against  $\alpha$ .

Figure 15.- Longitudinal characteristics of the model with 80-percent-span trailing-edge flaps deflected  $46^\circ$  and the leading-edge flaps drooped  $30^\circ$ . Configuration: A + V + I<sub>SE</sub> + (-0.123)T + 0.80F<sub>46</sub> + N<sub>30</sub> + E<sub>0</sub>450; center-of-gravity location, 0.22 $\bar{c}$ .

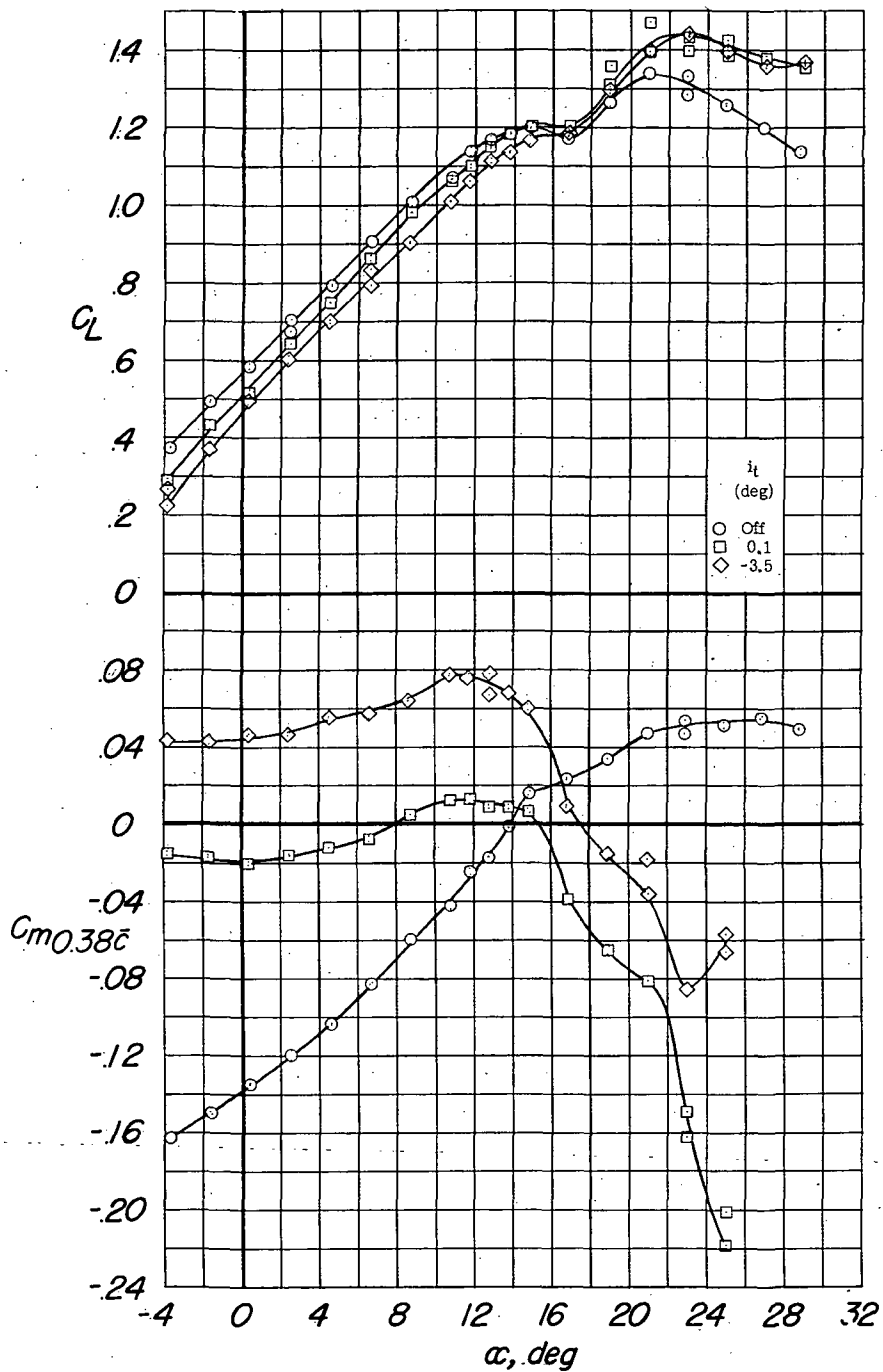


(b)  $C_D$  and  $C_{m0.22c}$  against  $C_L$ .

Figure 15.- Concluded.

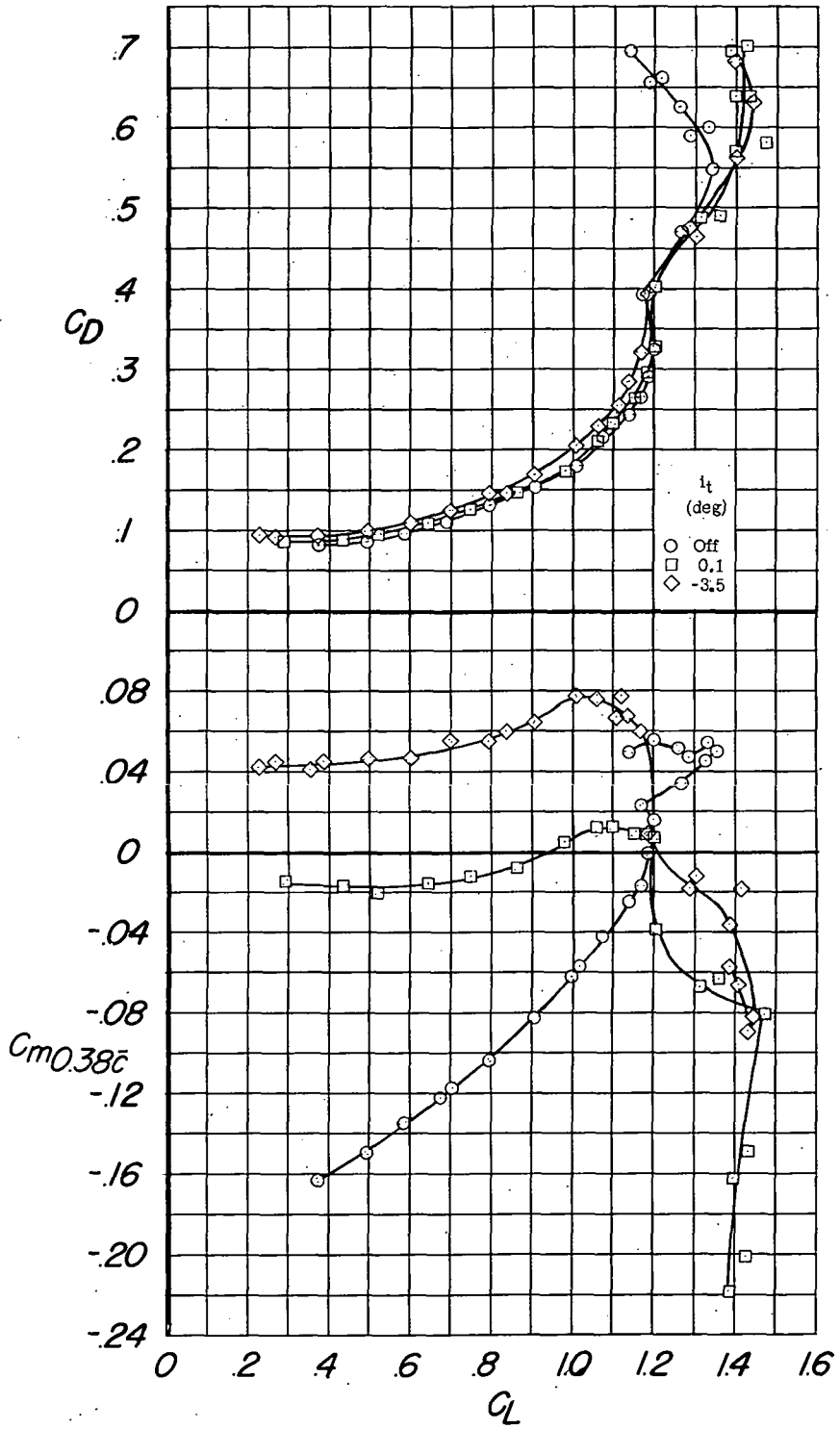






(a)  $C_L$  and  $C_{m0.38\bar{c}}$  against  $\alpha$ .

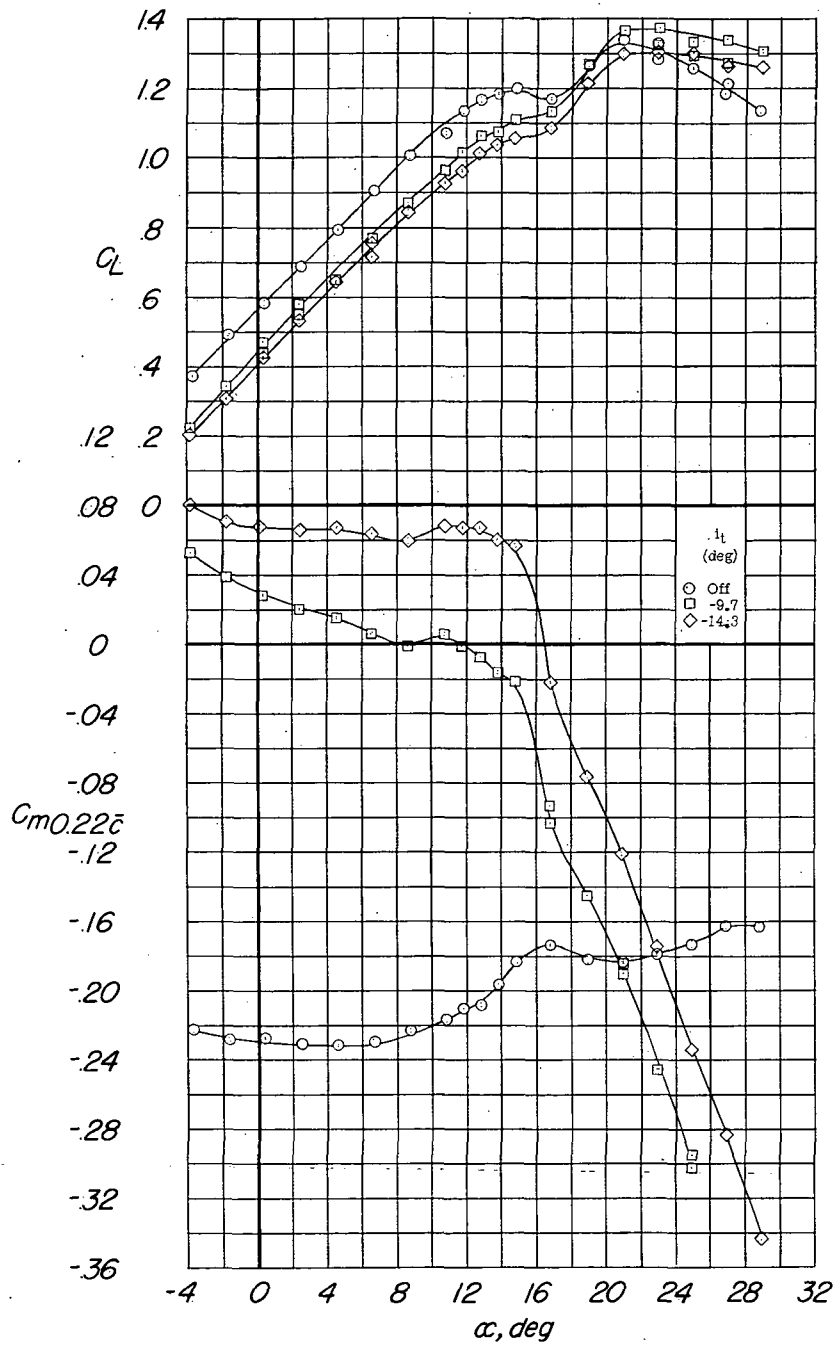
Figure 16.- Longitudinal characteristics of the model with 80-percent-span trailing-edge flaps deflected  $40^\circ$  and the leading-edge flaps drooped  $30^\circ$ . Configuration: A + V + I<sub>SE</sub> + (-0.123)T + 0.80F<sub>40</sub> + N<sub>30</sub> + E<sub>0450</sub>; center-of-gravity location, 0.38 $\bar{c}$ .



(b)  $C_D$  and  $C_{m0.38c}$  against  $C_L$ .

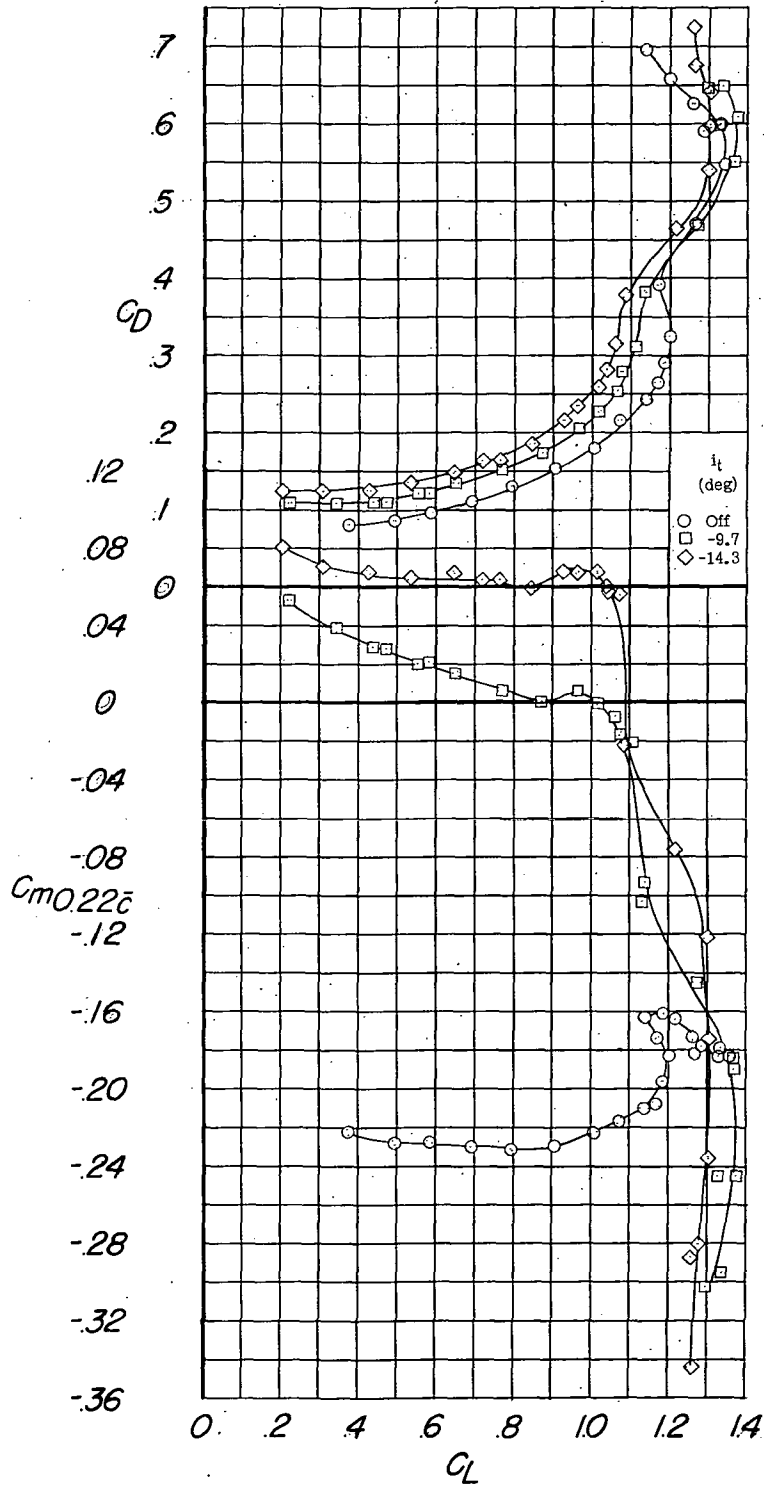
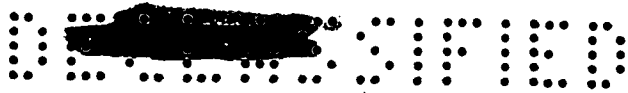
Figure 16.- Concluded.





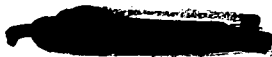
(a)  $C_L$  and  $C_{m0.22\bar{c}}$  against  $\alpha$ .

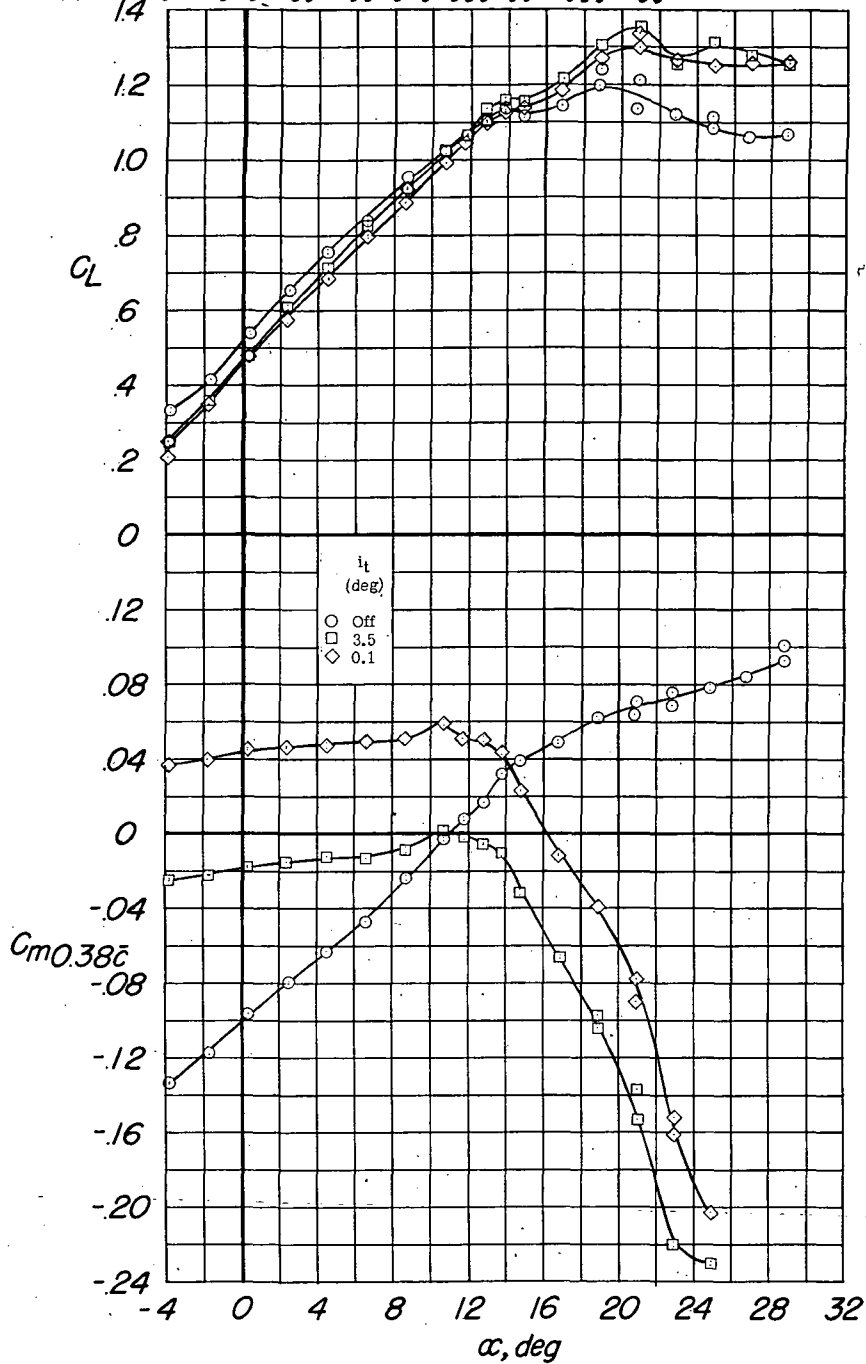
Figure 17.- Longitudinal characteristics of the model with 80-percent-span trailing-edge flaps deflected  $40^\circ$  and the leading-edge flaps drooped  $30^\circ$ . Configuration: A + V + I<sub>SE</sub> + (-0.123)T + 0.80F<sub>40</sub> + N<sub>30</sub> + E<sub>0450</sub>; center-of-gravity location, 0.22 $\bar{c}$ .



(b)  $C_D$  and  $C_{m_{0.22\bar{c}}}$  against  $C_L$ .

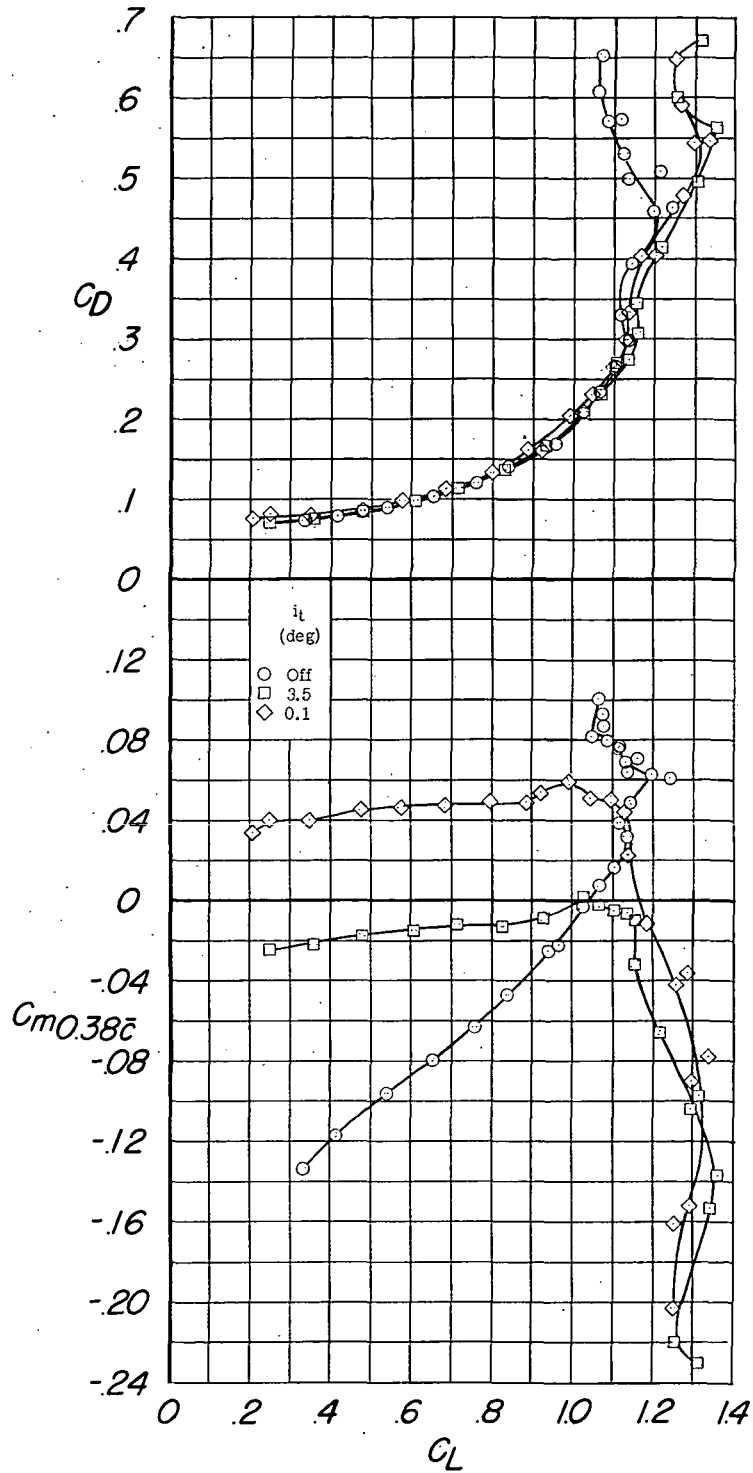
Figure 17.- Concluded.





(a)  $C_L$  and  $C_{m0.38\bar{c}}$  against  $\alpha$ .

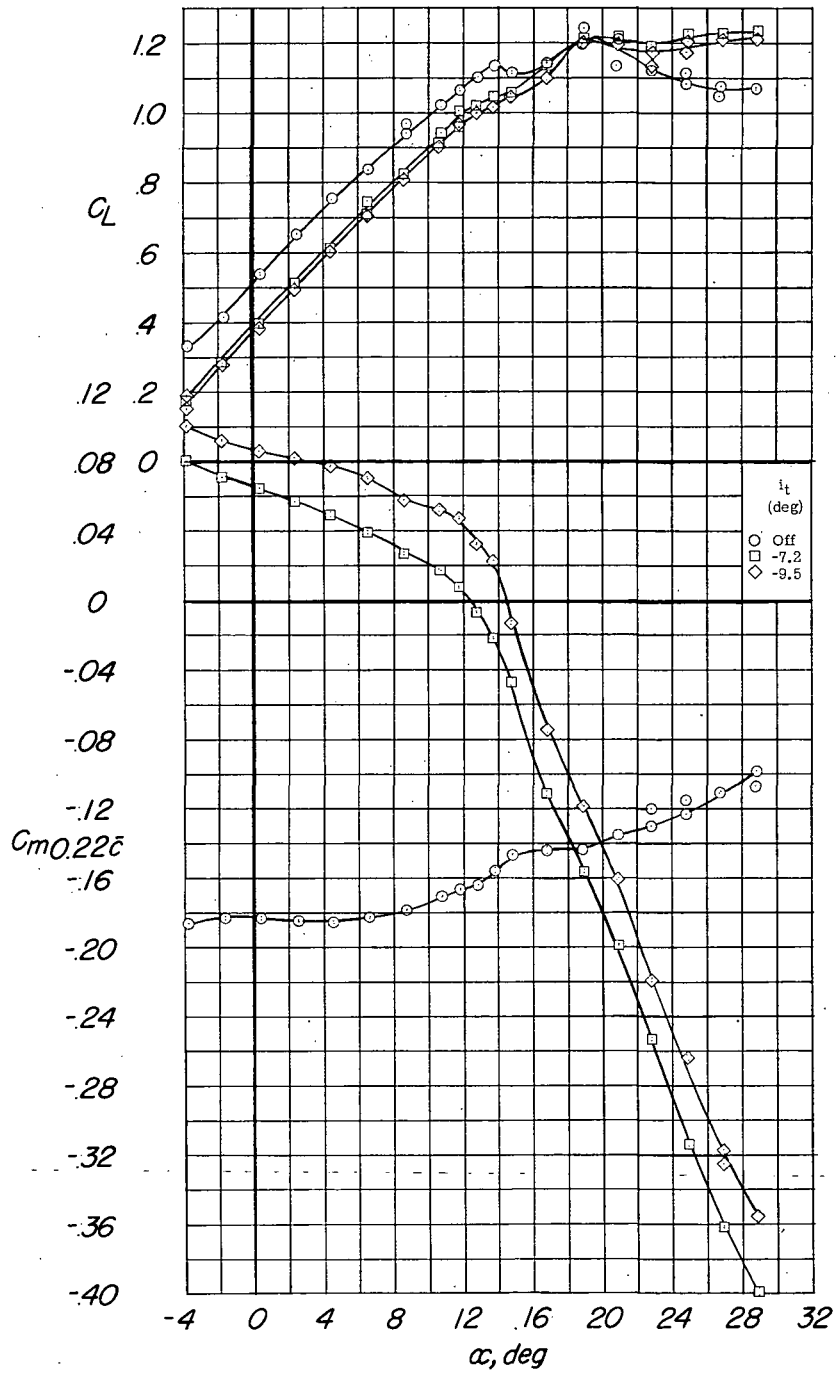
Figure 18.- Longitudinal characteristics of the model with 70-percent-span trailing-edge flaps deflected  $40^\circ$  and the leading-edge flaps drooped  $20^\circ$ . Configuration: A + V +  $I_{SE}$  +  $(-0.123)T$  +  $0.70F_{40}$  +  $N_{20}$  +  $E_{0450}$ ; center-of-gravity location,  $0.38\bar{c}$ .



(b)  $C_D$  and  $C_{m0.38c}$  against  $C_L$ .

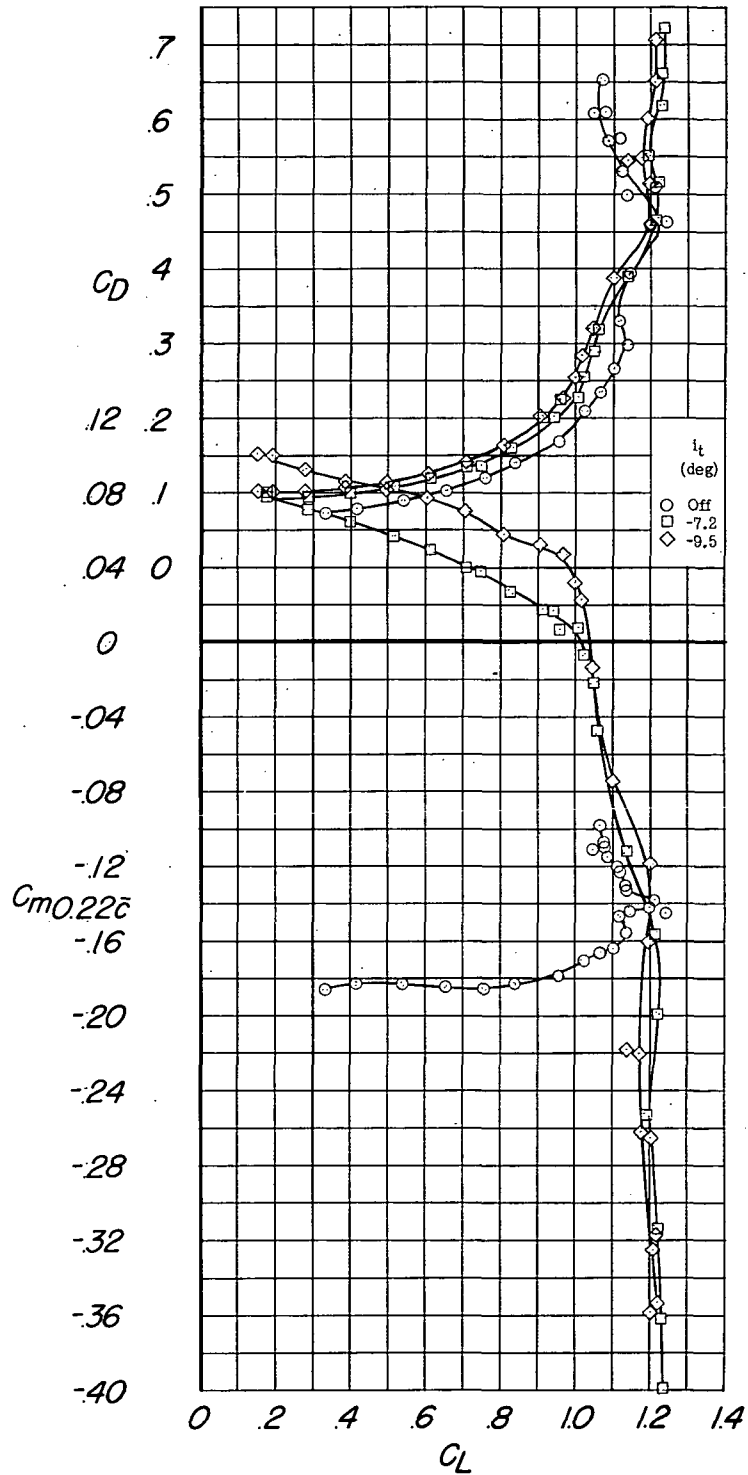
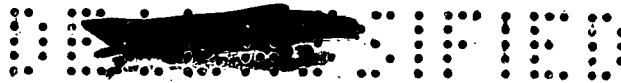
Figure 18.- Concluded.





(a)  $C_L$  and  $C_{m_{0.22\bar{c}}}$  against  $\alpha$ .

Figure 19.- Longitudinal characteristics of the model with 70-percent-span trailing-edge flaps deflected  $40^\circ$  and the leading-edge flaps drooped  $20^\circ$ . Configuration: A + V + I<sub>SE</sub> + (-0.123)T + 0.70F<sub>40</sub> + N<sub>20</sub> + E<sub>0.450</sub>; center-of-gravity location, 0.22 $\bar{c}$ .

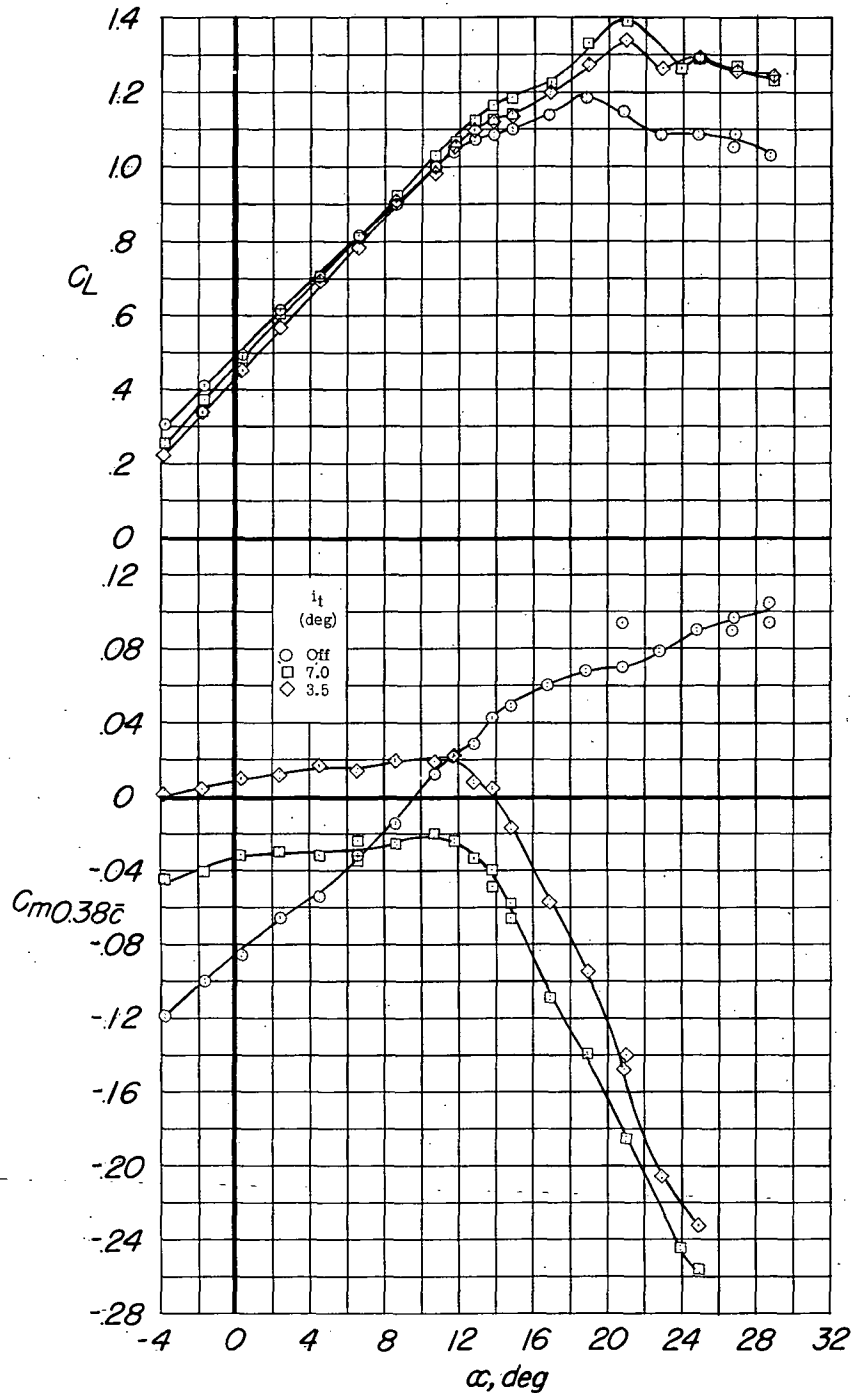


(b)  $C_D$  and  $C_{m0.22\bar{c}}$  against  $C_L$ .

Figure 19.- Concluded.

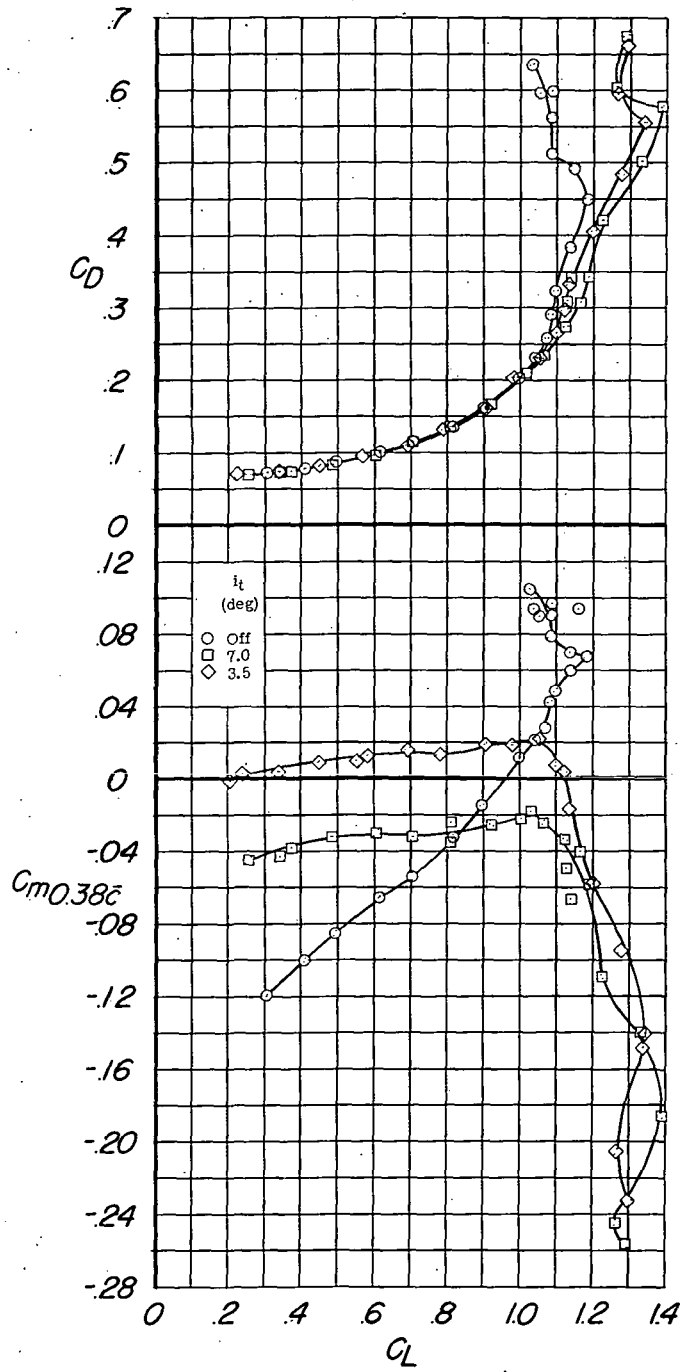
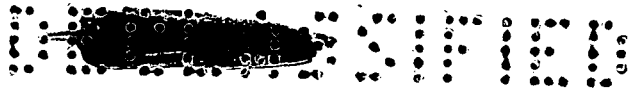






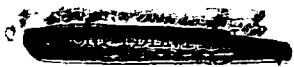
(a)  $C_L$  and  $C_{m_{0.38\bar{c}}}$  against  $\alpha$ .

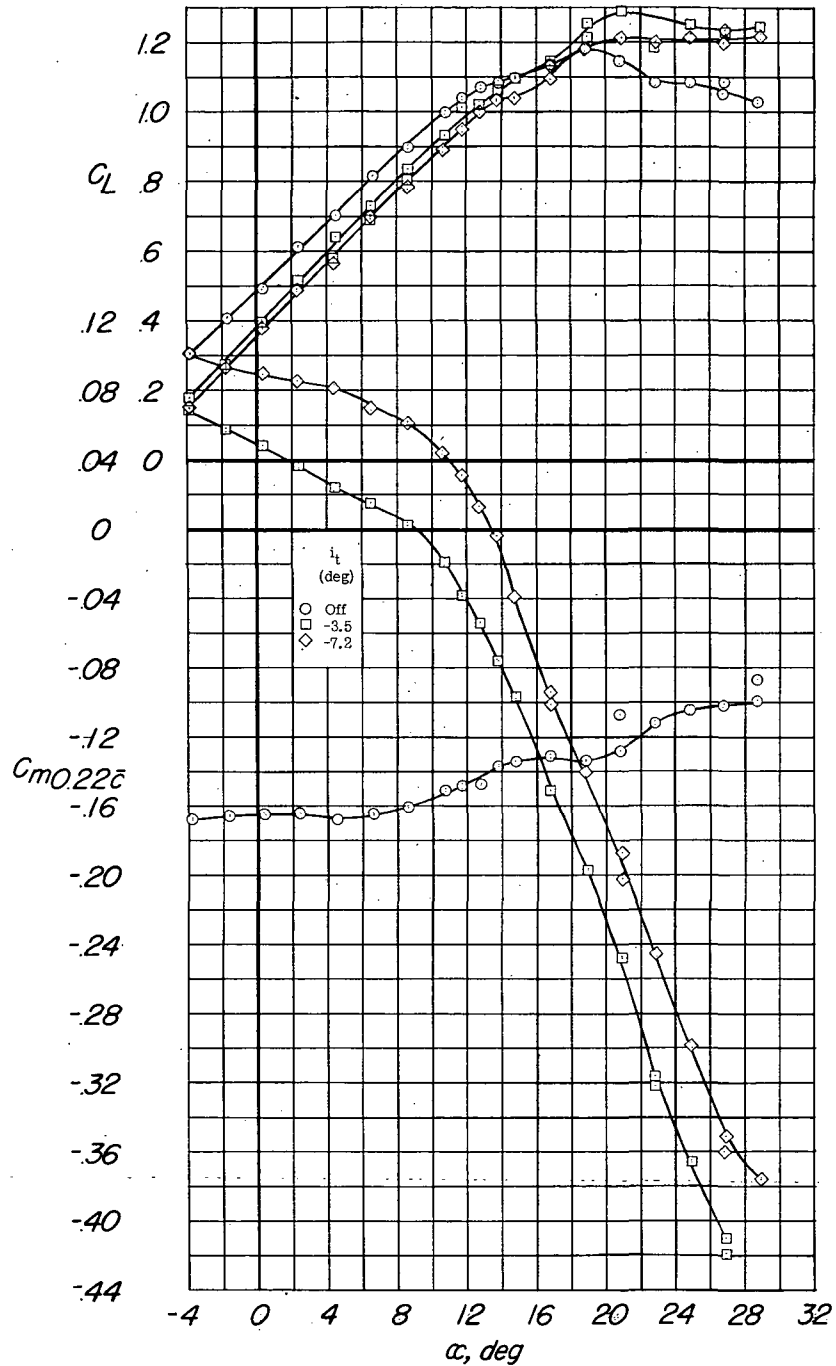
Figure 20.- Longitudinal characteristics of the model with 65-percent-span trailing-edge flaps deflected  $40^\circ$  and the leading-edge flaps drooped  $20^\circ$ . Configuration: A + V +  $I_{SE}$  +  $(-0.123)T$  +  $0.65F_{40}$  +  $N_{20}$  +  $E_{0.450}$ ; center-of-gravity location,  $0.38\bar{c}$ .



(b)  $C_D$  and  $C_{m_{0.38c}}$  against  $C_L$ .

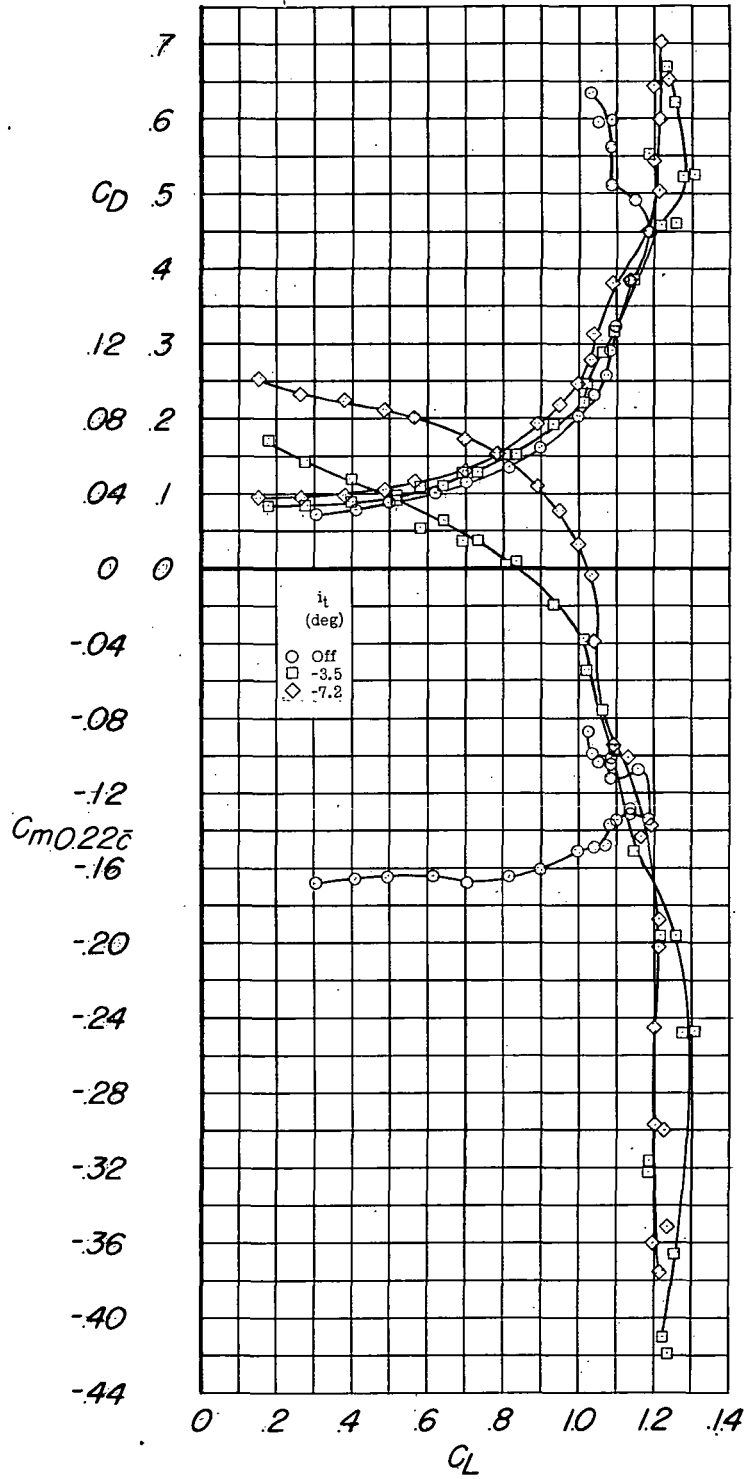
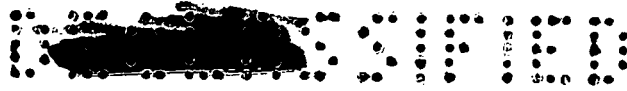
Figure 20.- Concluded.





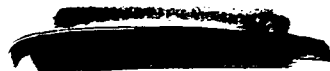
(a)  $C_L$  and  $C_{m0.22\bar{c}}$  against  $\alpha$ .

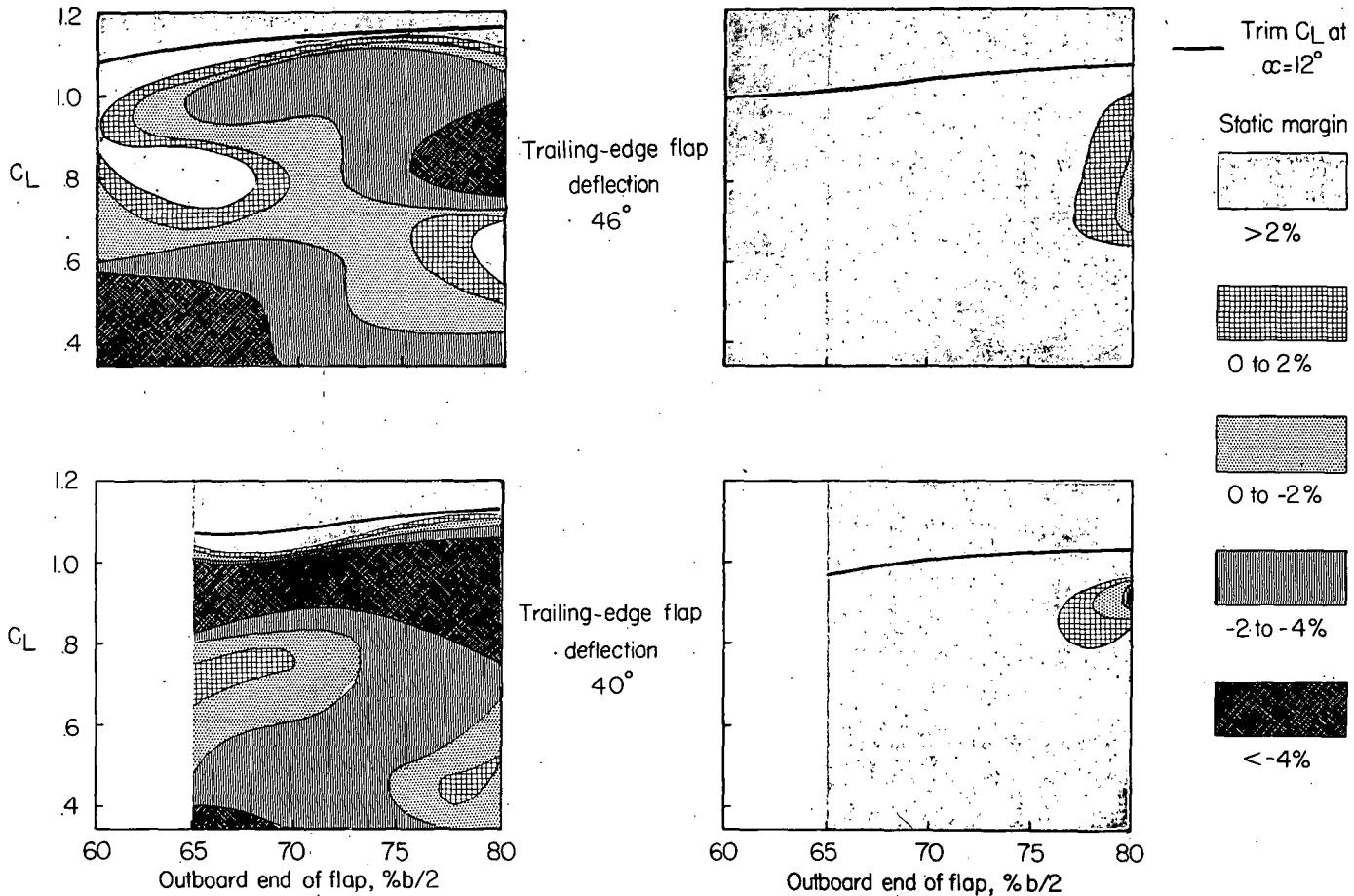
Figure 21.- Longitudinal characteristics of the model with 65-percent-span trailing-edge flaps deflected  $40^\circ$  and the leading-edge flaps drooped  $20^\circ$ . Configuration: A + V + I<sub>SE</sub> + (-0.123)T + 0.65F<sub>40</sub> + N<sub>20</sub> + E<sub>0</sub>450; center-of-gravity location, 0.22 $\bar{c}$ .



(b)  $C_D$  and  $C_{m0.22c}$  against  $C_L$ .

Figure 21.- Concluded.



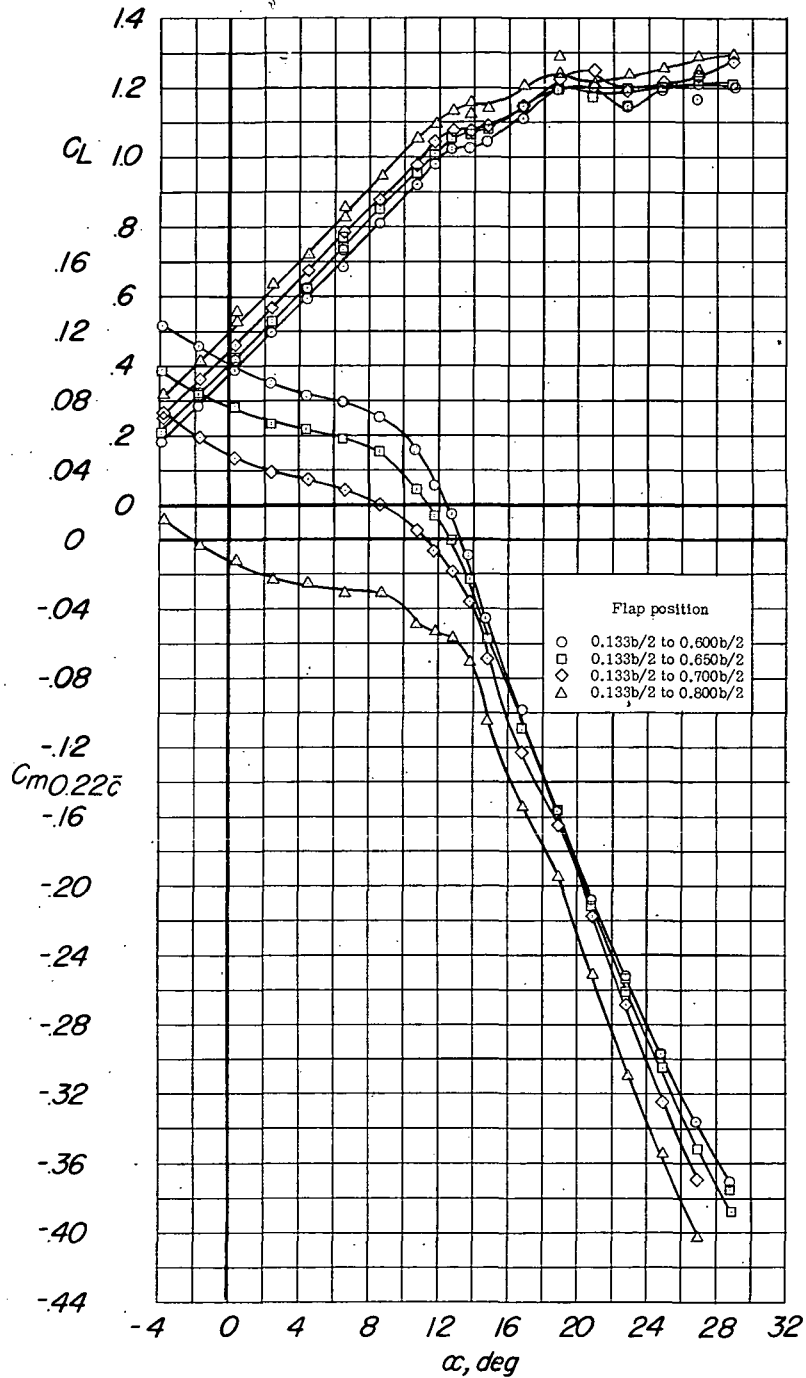


(a) Center of gravity at 38 percent  $\bar{c}$ .

(b) Center of gravity at 22 percent  $\bar{c}$ .

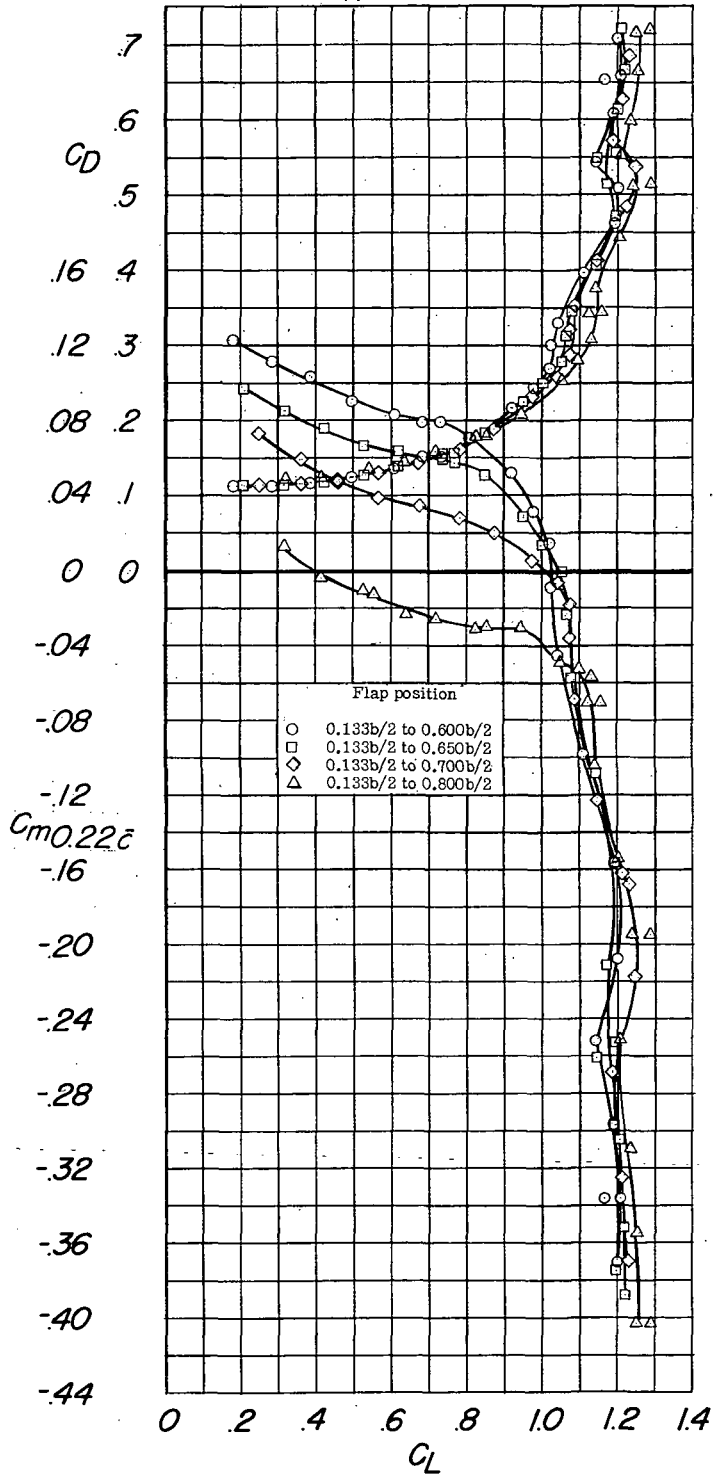
Figure 22.- A summary of the longitudinal stability characteristics of a 1/4-scale model of the F-105 airplane. Configuration: A + V + I<sub>SE</sub> + F + N + -0.123T.

NACA RM. 51.122



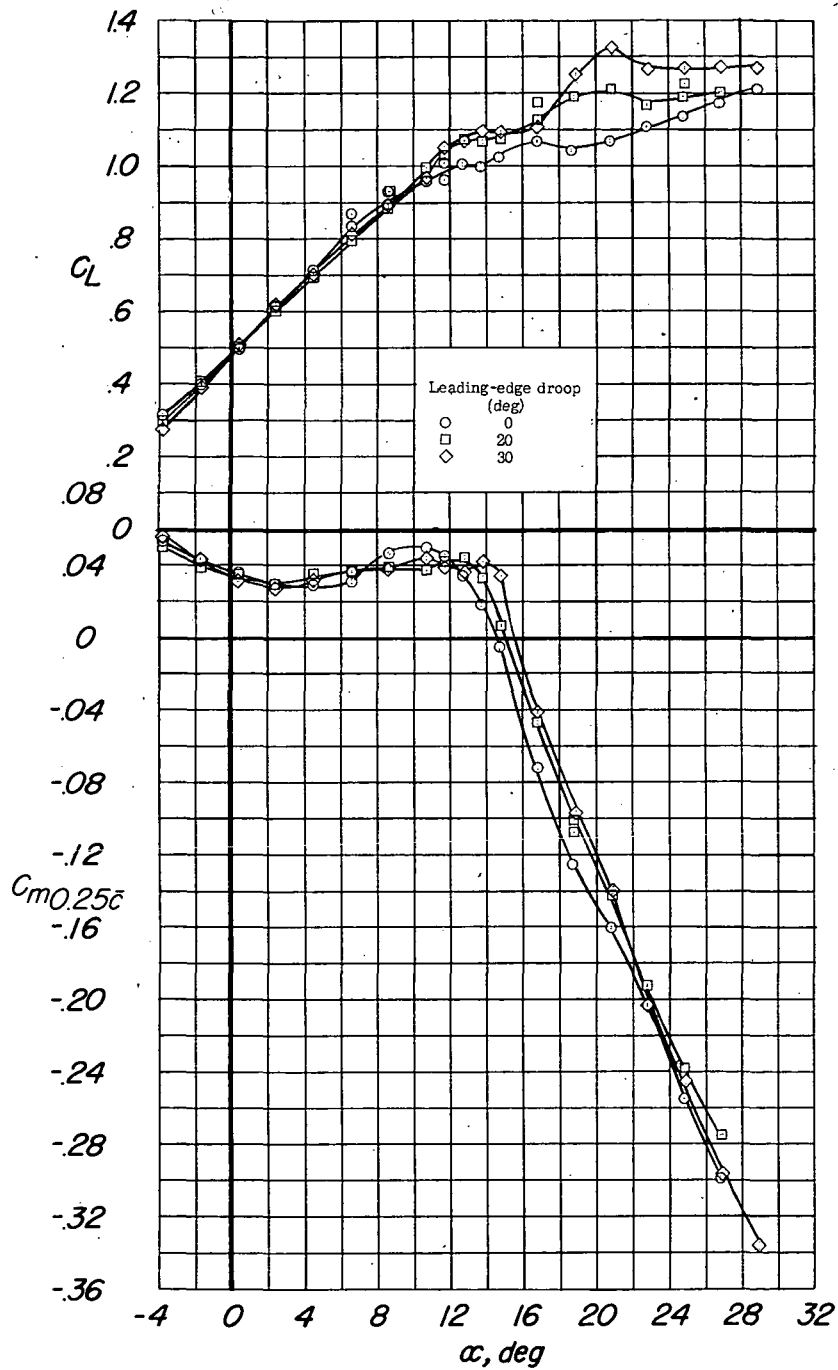
(a)  $C_L$  and  $C_{m_{0.22\bar{c}}}$  against  $\alpha$ .

Figure 23.- Longitudinal characteristics of the model with various span trailing-edge flaps deflected  $46^\circ$  and the leading-edge flaps drooped  $20^\circ$ . Configuration: A + V + I<sub>SE</sub> + (-0.123)T<sub>-7.3</sub> + F<sub>46</sub> + N<sub>20</sub> + E<sub>0</sub><sup>450</sup>; center-of-gravity location, 0.22 $\bar{c}$ .



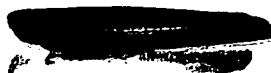
(b)  $C_D$  and  $C_{m0.22\bar{c}}$  against  $C_L$ .

Figure 23.- Concluded.

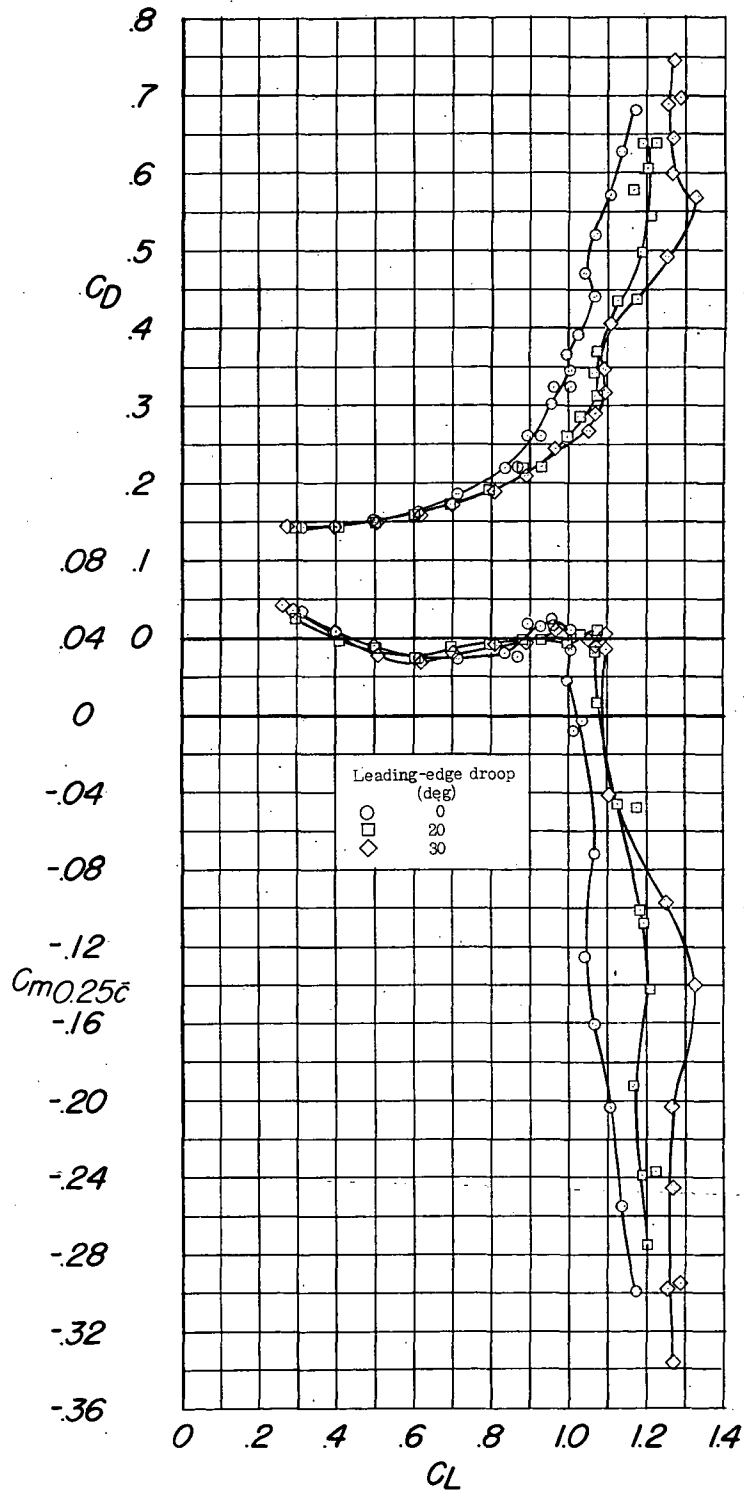


(a)  $C_L$  and  $C_{m_{0.25\bar{c}}}$  against  $\alpha$ .

Figure 24.- Longitudinal characteristics of the model with 80-percent-span trailing-edge flaps deflected  $46^\circ$  and the leading-edge flaps drooped various amounts. Configuration: A + V + I<sub>SE</sub> + (-0.123)T-14.3 + 0.80F<sub>46</sub> + N + E<sub>0</sub><sup>450</sup>; center-of-gravity location,  $0.25\bar{c}$ .

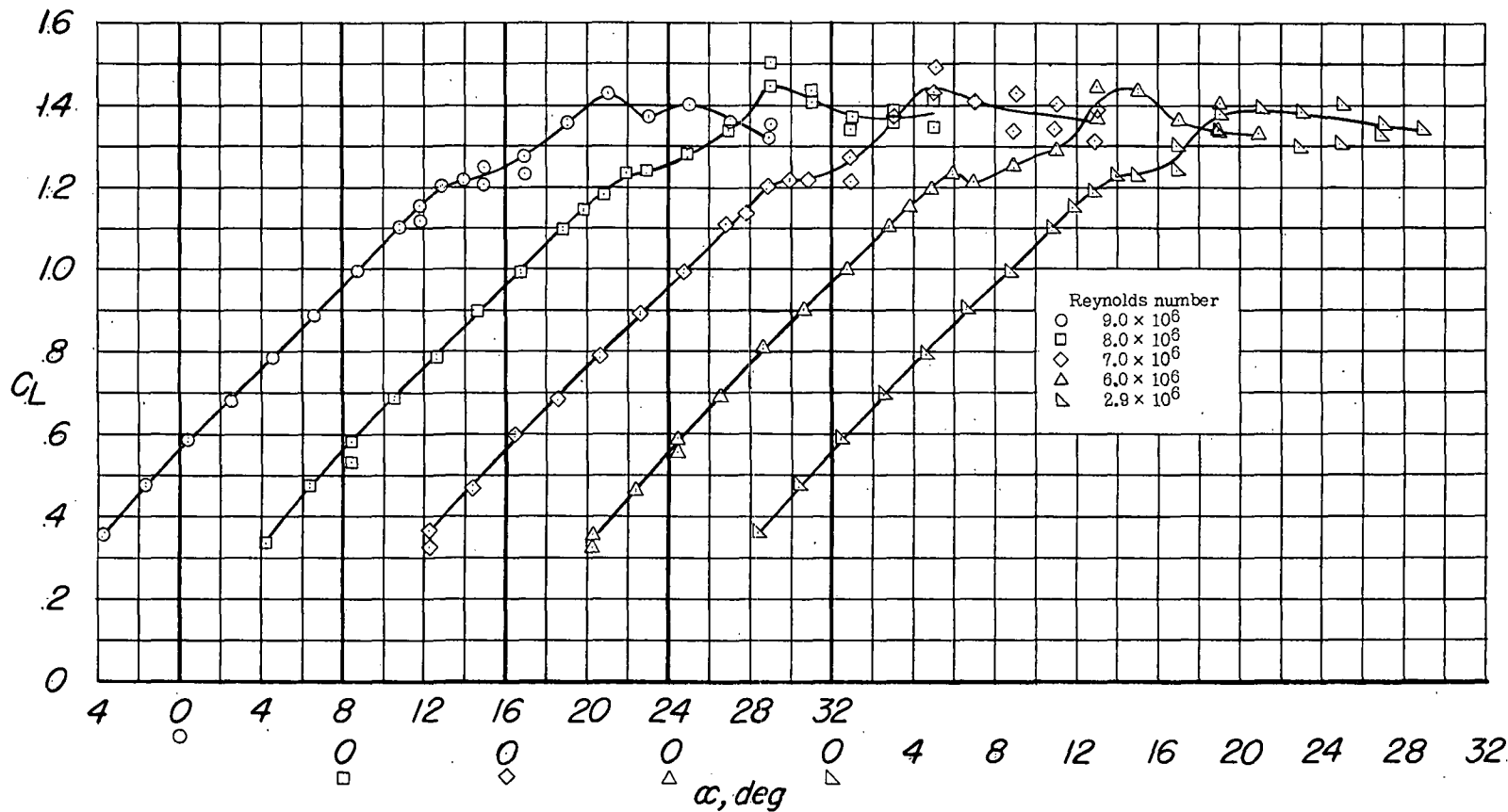






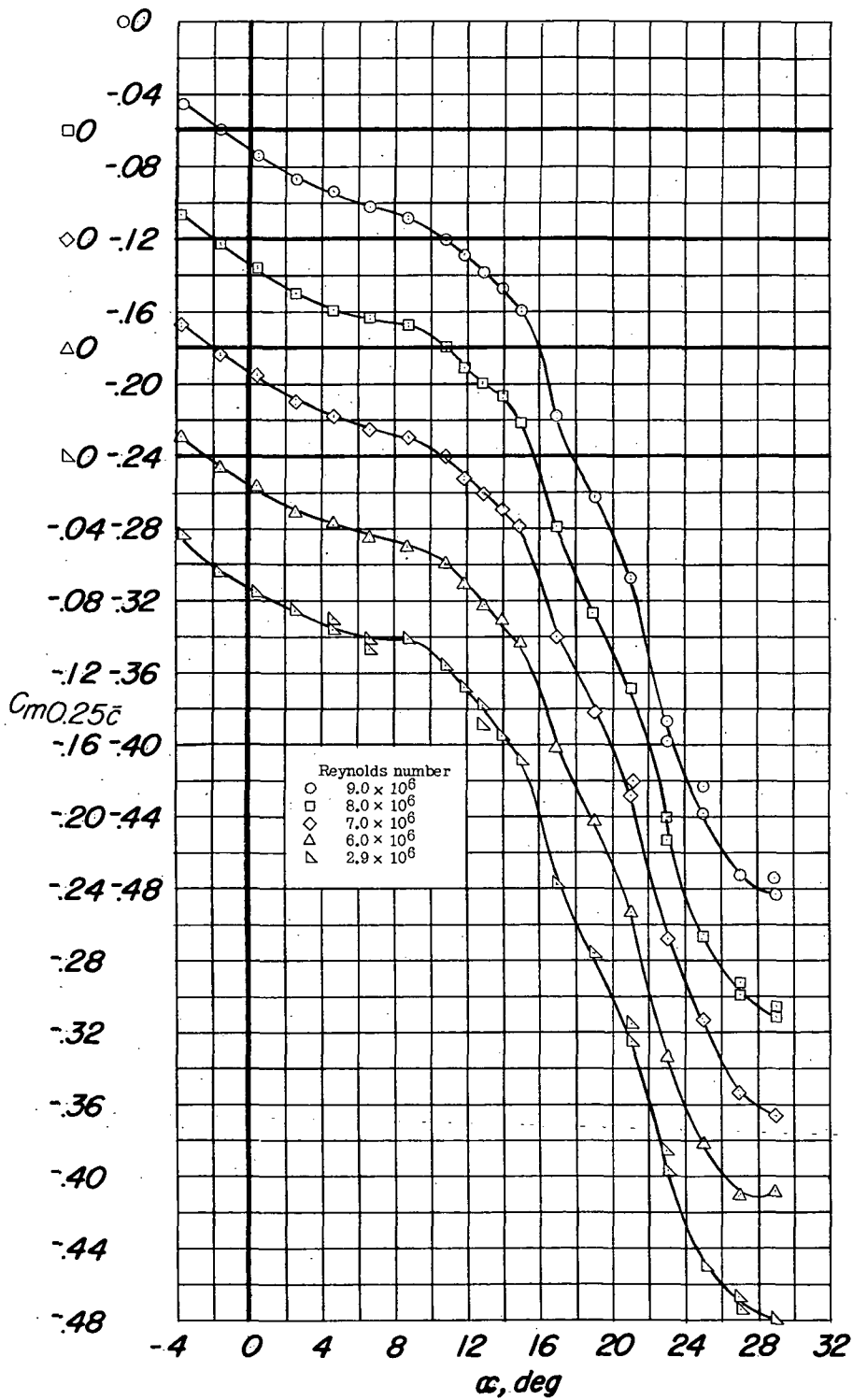
(b)  $C_D$  and  $C_{m0.25c}$  against  $C_L$ .

Figure 24.- Concluded.



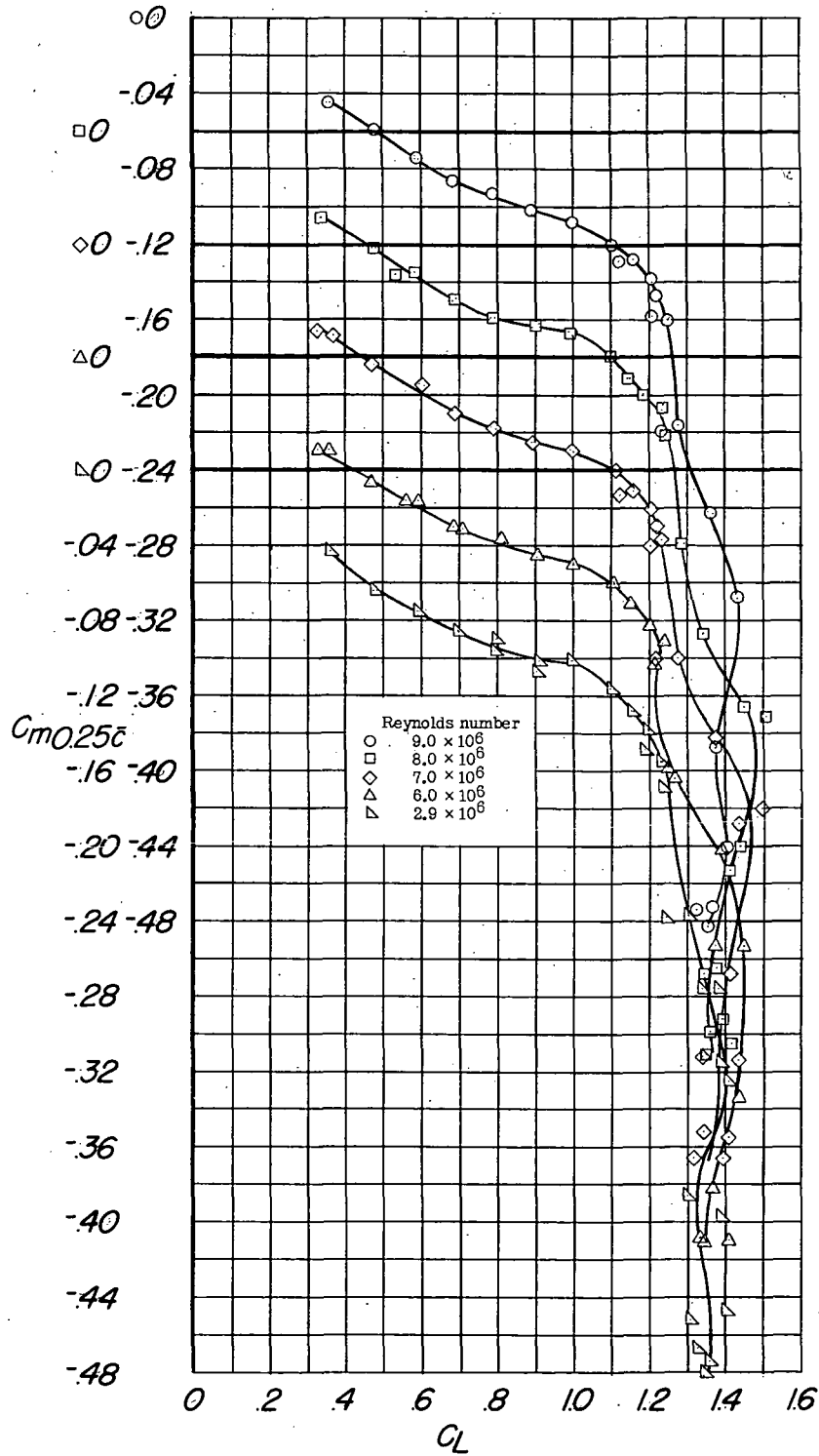
(a)  $C_L$  against  $\alpha$ .

Figure 25.- Longitudinal characteristics at various Reynolds numbers of the model with 80-percent-span trailing-edge flaps deflected  $46^\circ$  and the leading-edge flaps drooped  $30^\circ$ . Configuration: A + V +  $I_{SE}$  +  $(-0.123)T_{-0.2} + 0.80F_{46} + N_{30} + E_{0450}$ ; center-of-gravity location,  $0.25\bar{c}$ .



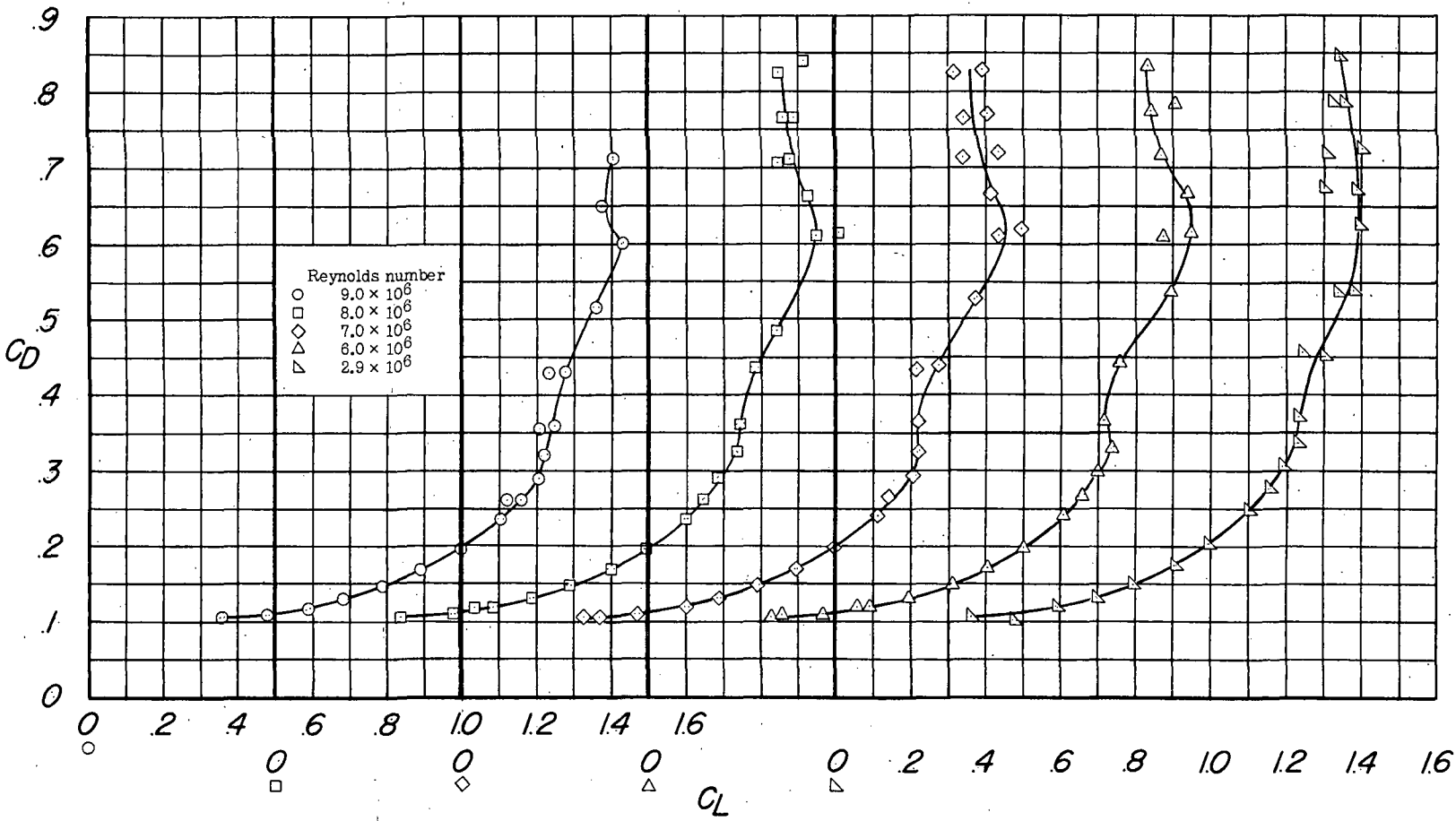
(b)  $C_{m0.25c}$  against  $\alpha$ .

Figure 25.- Continued.



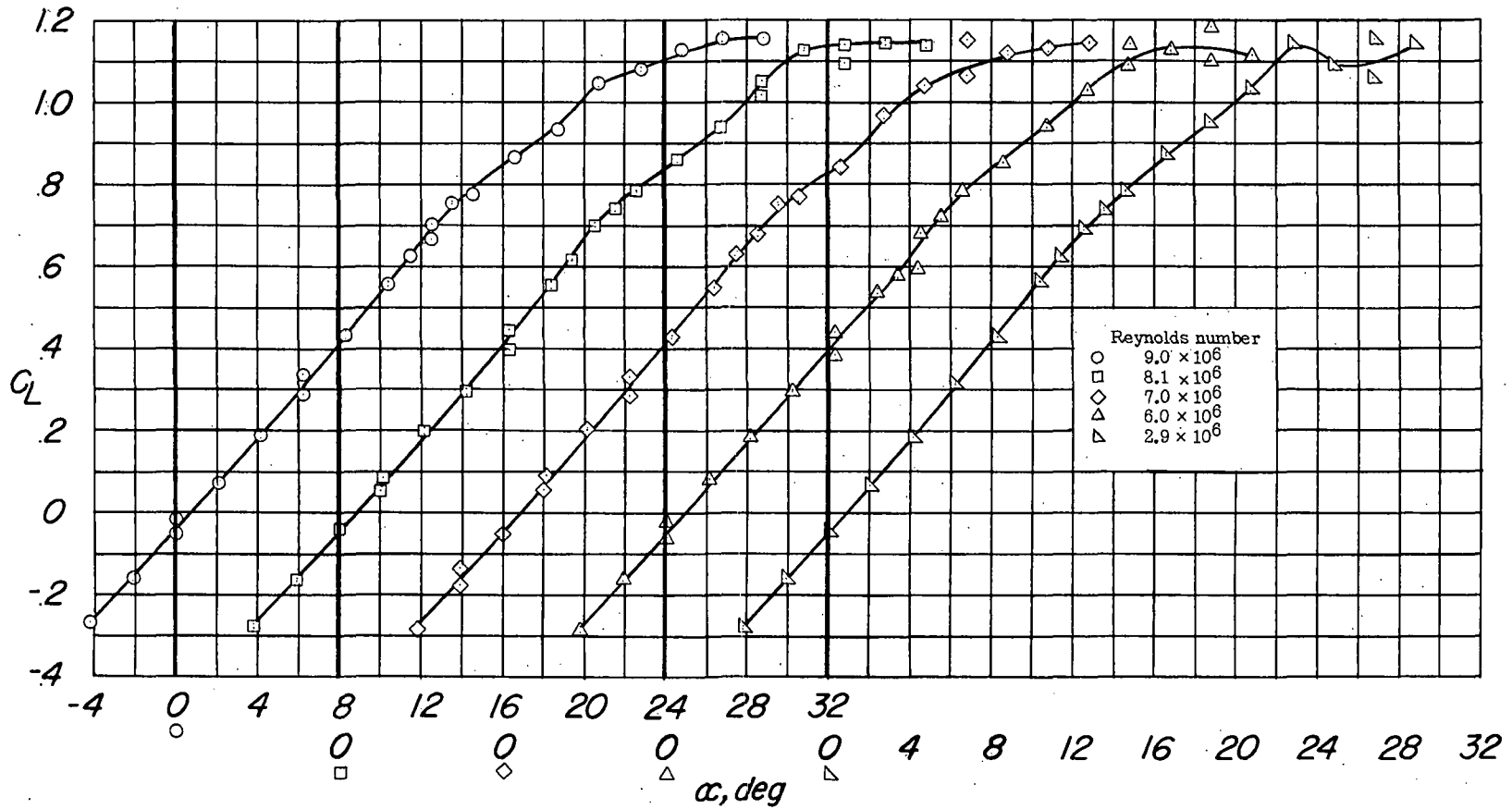
(c)  $C_{m0.25c}$  against  $C_L$ .

Figure 25.- Continued.



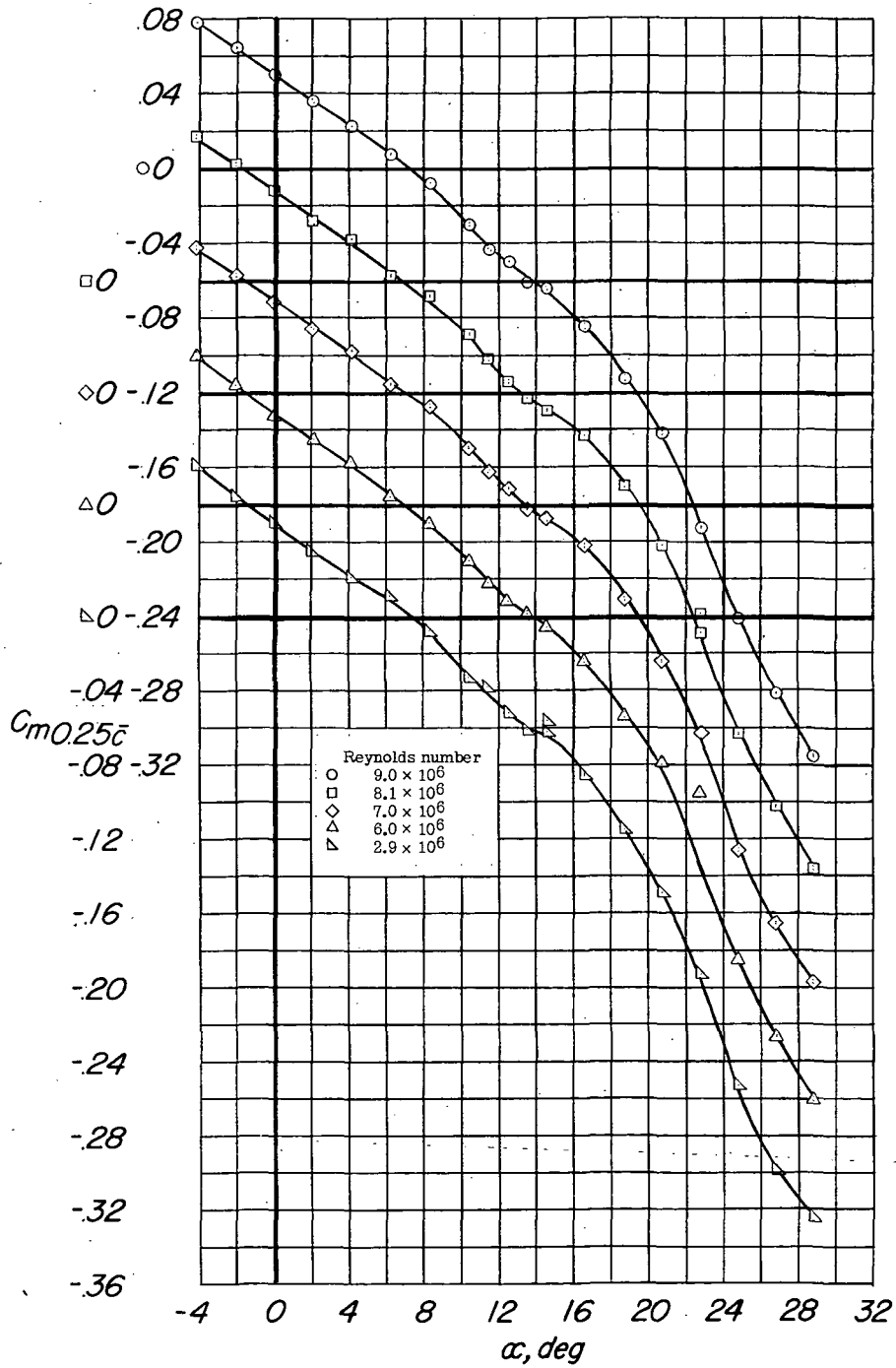
(d)  $C_D$  against  $C_L$ .

Figure 25.- Concluded.



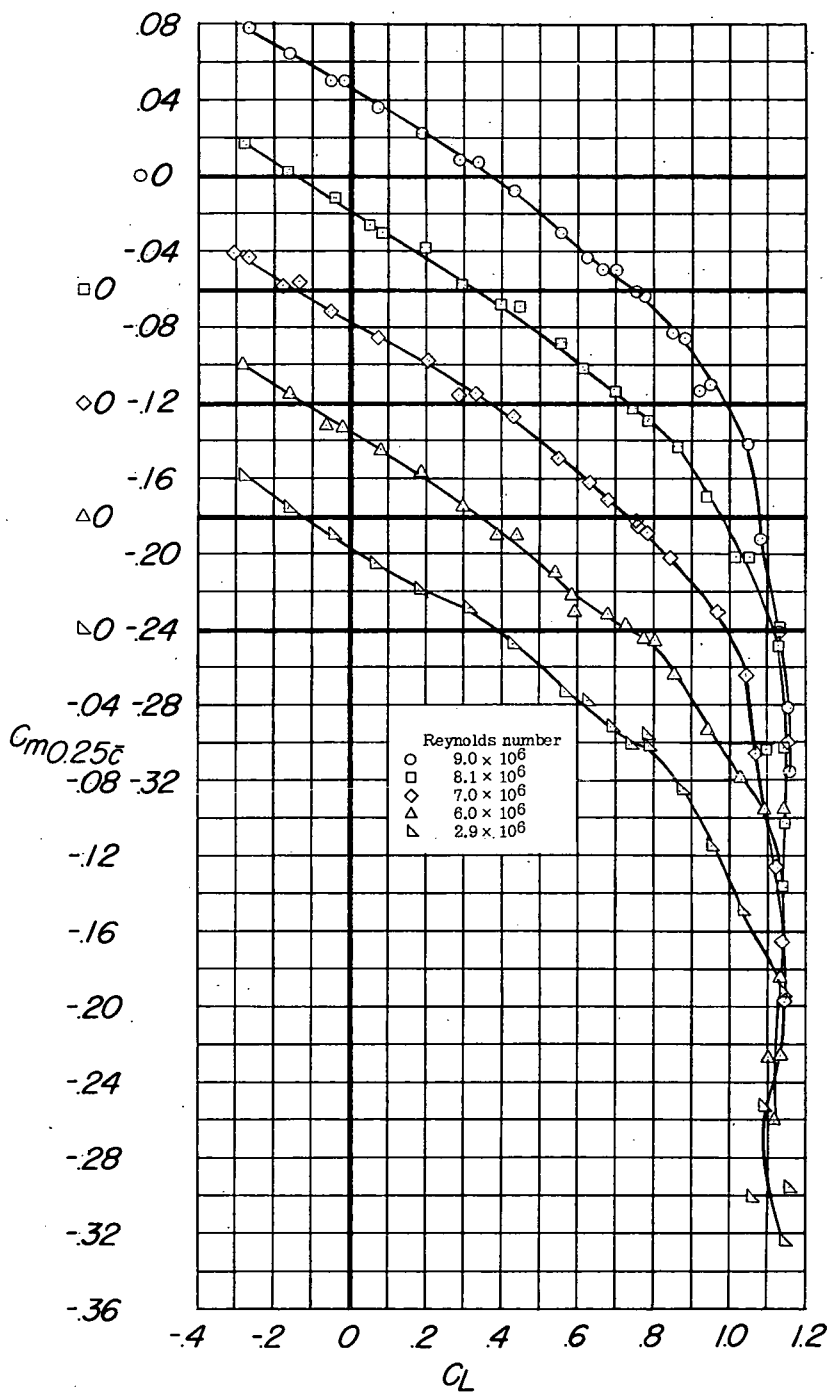
(a)  $C_L$  against  $\alpha$ .

Figure 26.- Longitudinal characteristics at various Reynolds numbers of the model with the leading-edge flaps drooped  $7.5^\circ$ . Configuration: A + V + ISE + (-0.123)T<sub>-3.5</sub> + N<sub>7.5</sub>; center-of-gravity location,  $0.25\bar{c}$ .



(b)  $C_{m0.25c}$  against  $\alpha$ .

Figure 26.- Continued.

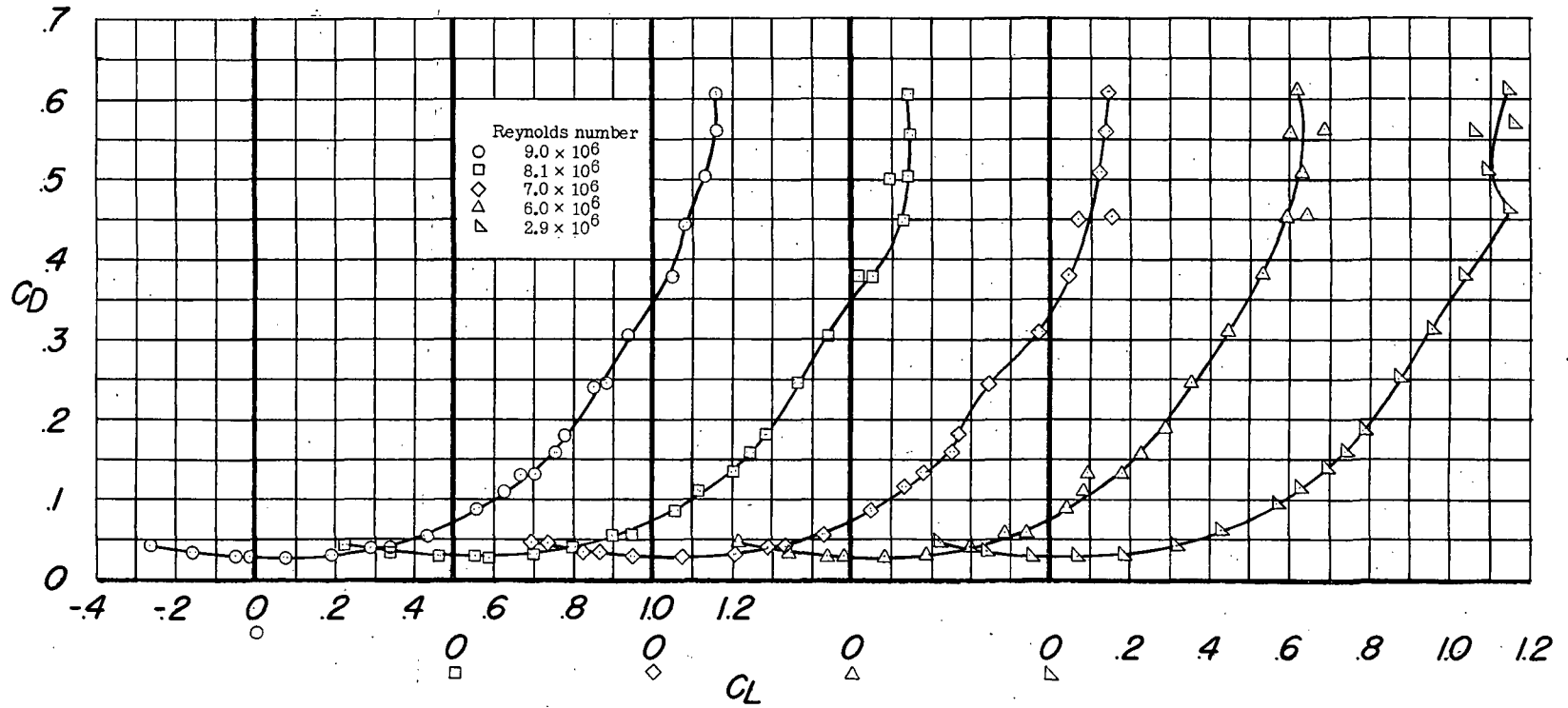


(c)  $C_{m0.25c}$  against  $C_L$ .

Figure 26.- Continued.

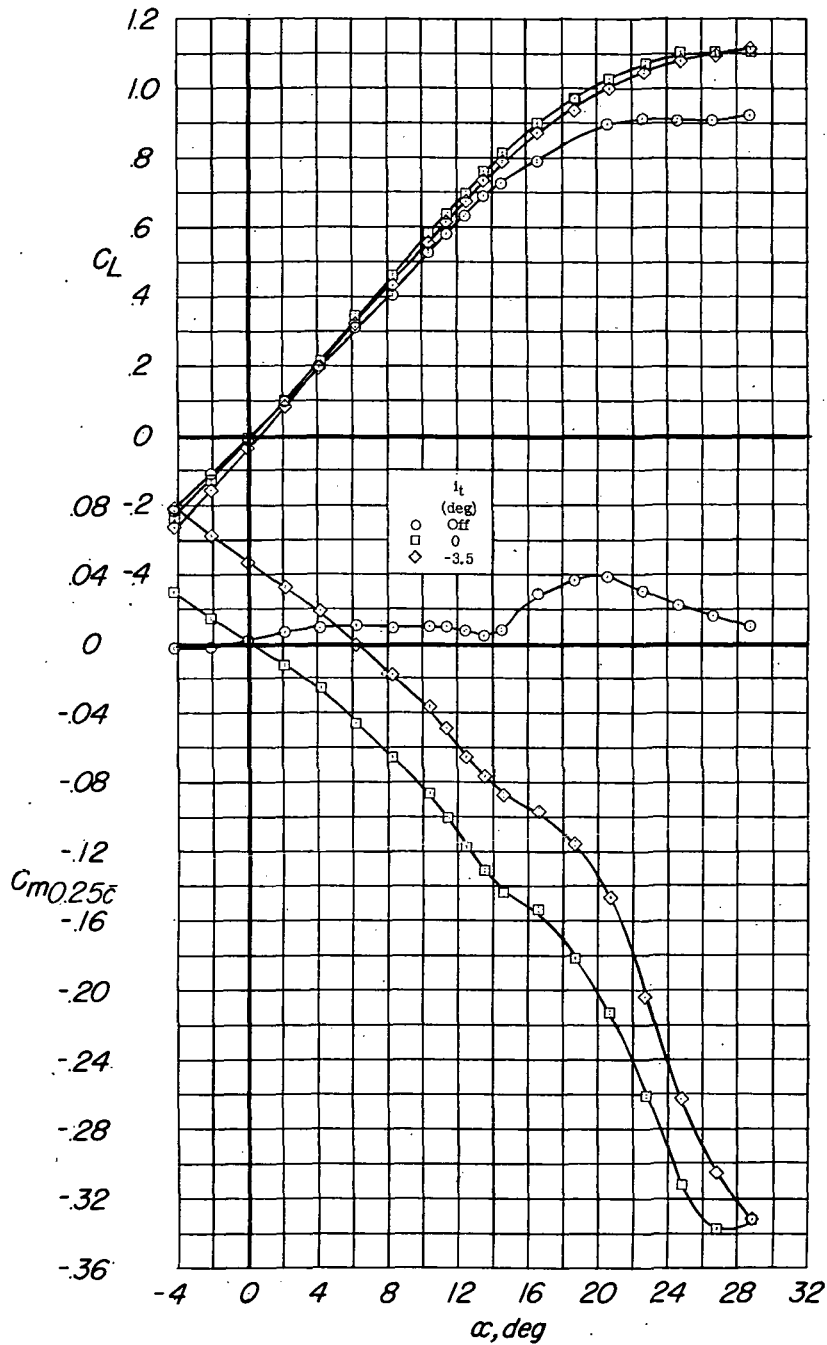






(d)  $C_D$  against  $C_L$ .

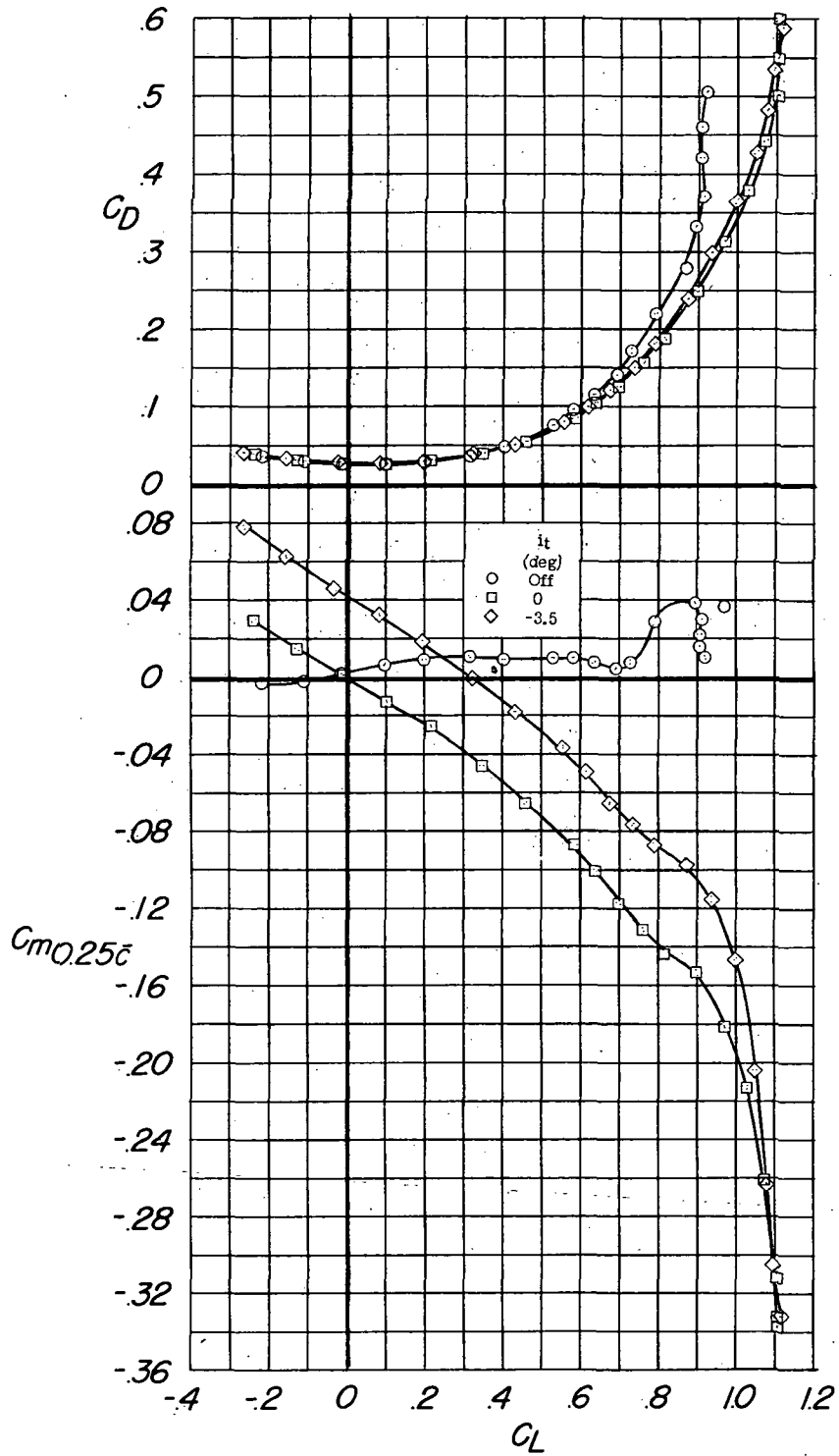
Figure 26.- Concluded.



(a)  $C_L$  and  $C_{m0.25\bar{c}}$  against  $\alpha$ .

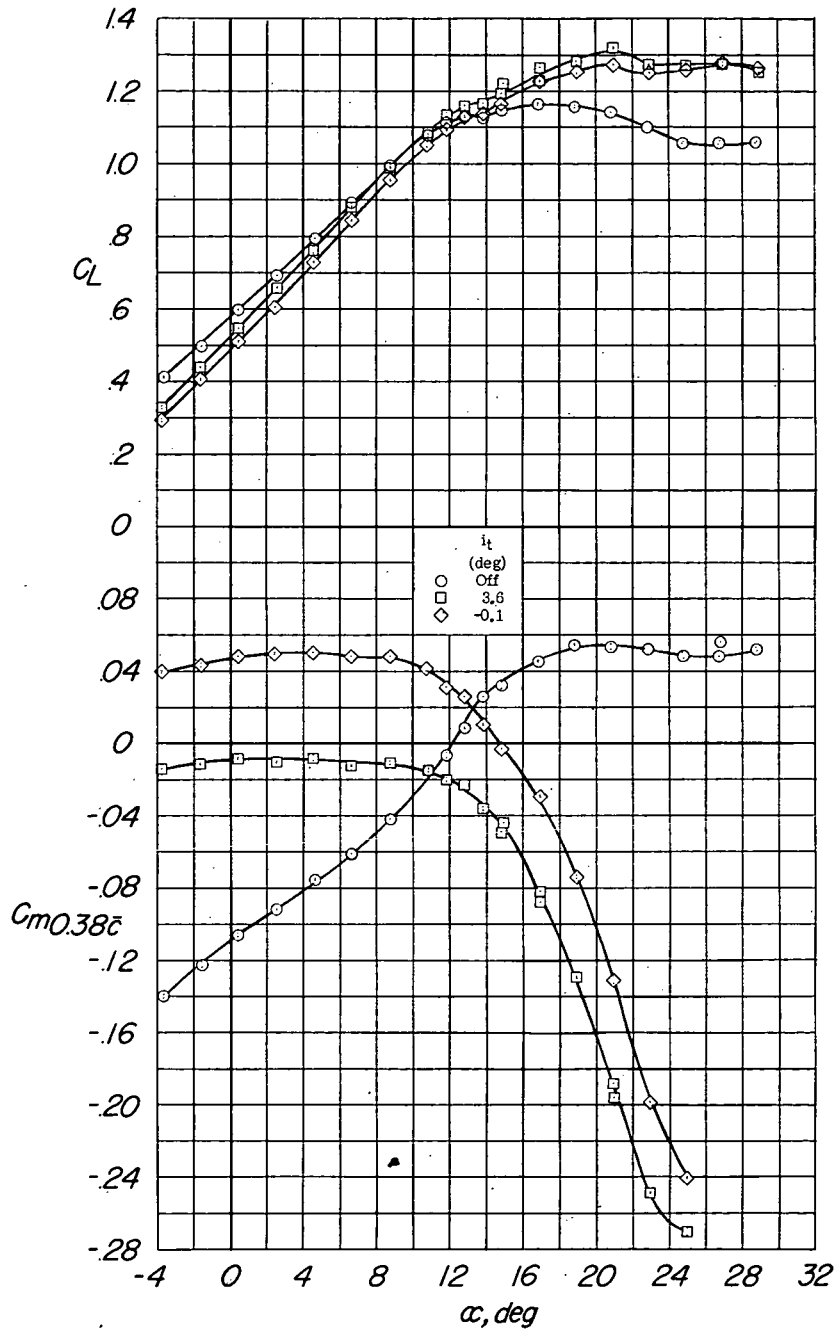
Figure 27.- Longitudinal characteristics of the model equipped with a transonic-type elliptical wing-root inlet and leading-edge flaps drooped  $7.5^\circ$ . Configuration: A + V +  $I_{TE}$  +  $(-0.123)T$  +  $N_{7.5}$ ; center-of-gravity location,  $0.25\bar{c}$ .





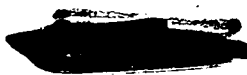
(b)  $C_D$  and  $C_{m0.25\bar{c}}$  against  $C_L$ .

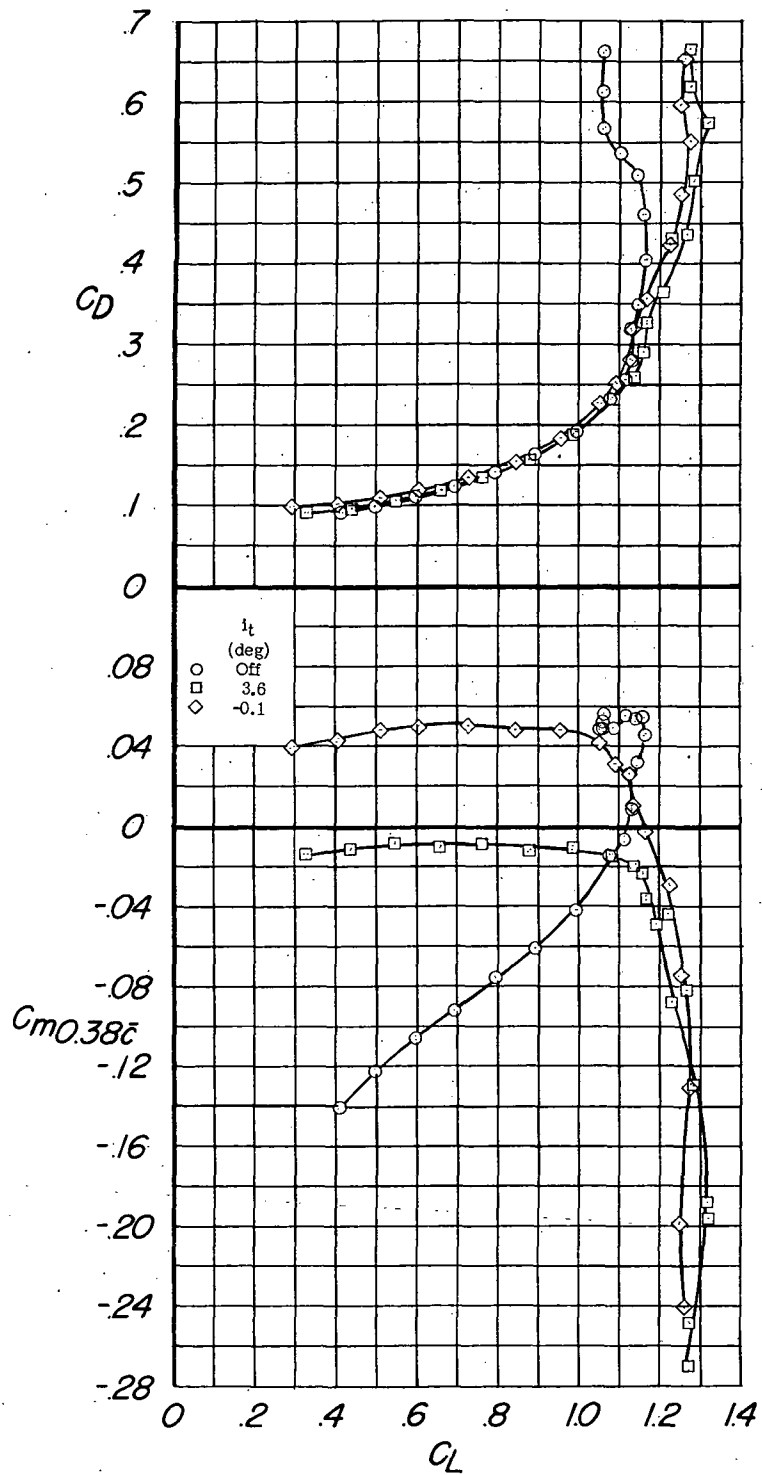
Figure 27.- Concluded.



(a)  $C_L$  and  $C_{m0.38c}$  against  $\alpha$ .

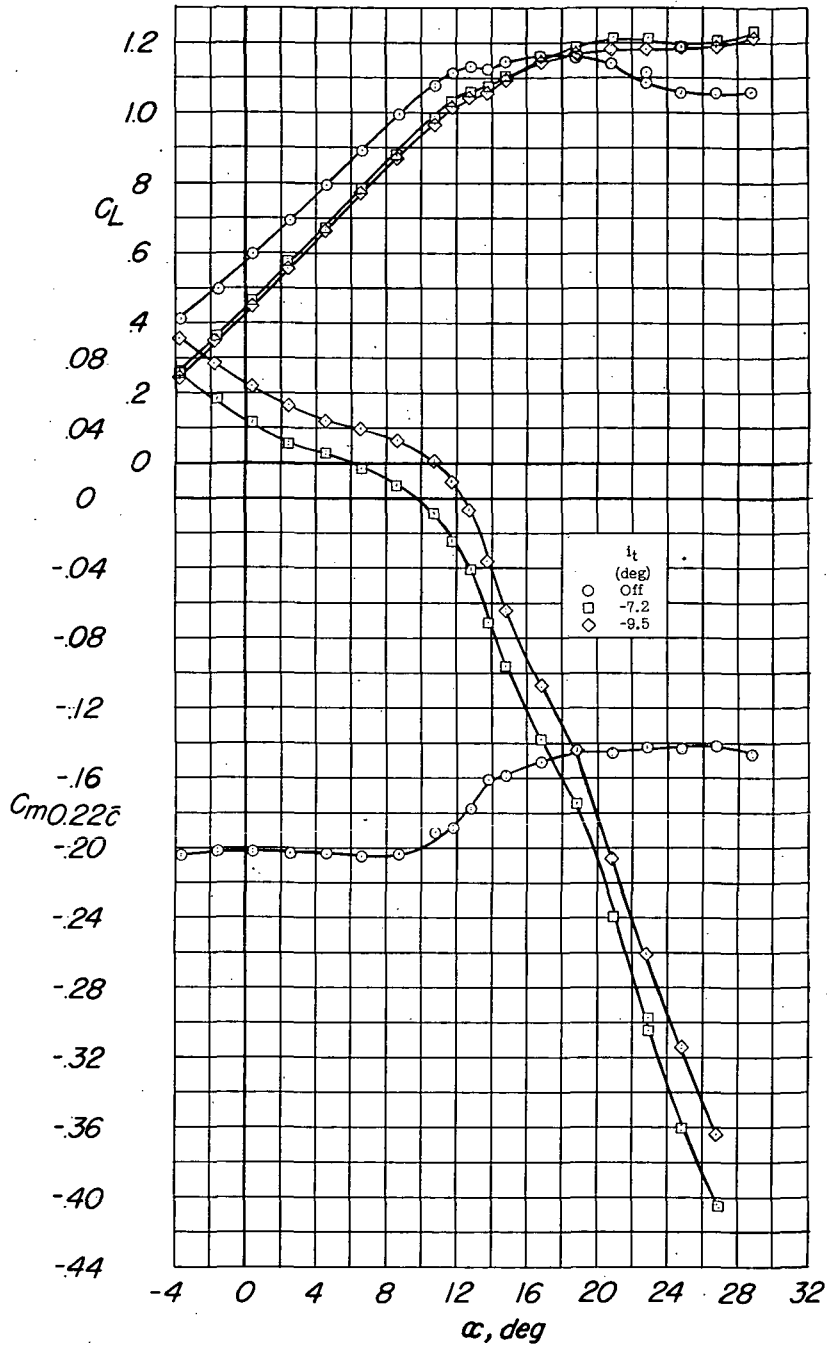
Figure 28.- Longitudinal characteristics of the model equipped with a transonic-type elliptical wing-root inlet, 70-percent-span trailing-edge flaps deflected  $46^\circ$ , and the leading-edge flaps drooped  $20^\circ$ . Configuration: A + V +  $I_{TE}$  +  $(-0.123)T$  +  $0.70F_{46}$  +  $N_{20}$  +  $E_0^{450}$ ; center-of-gravity location,  $0.38\bar{c}$ .





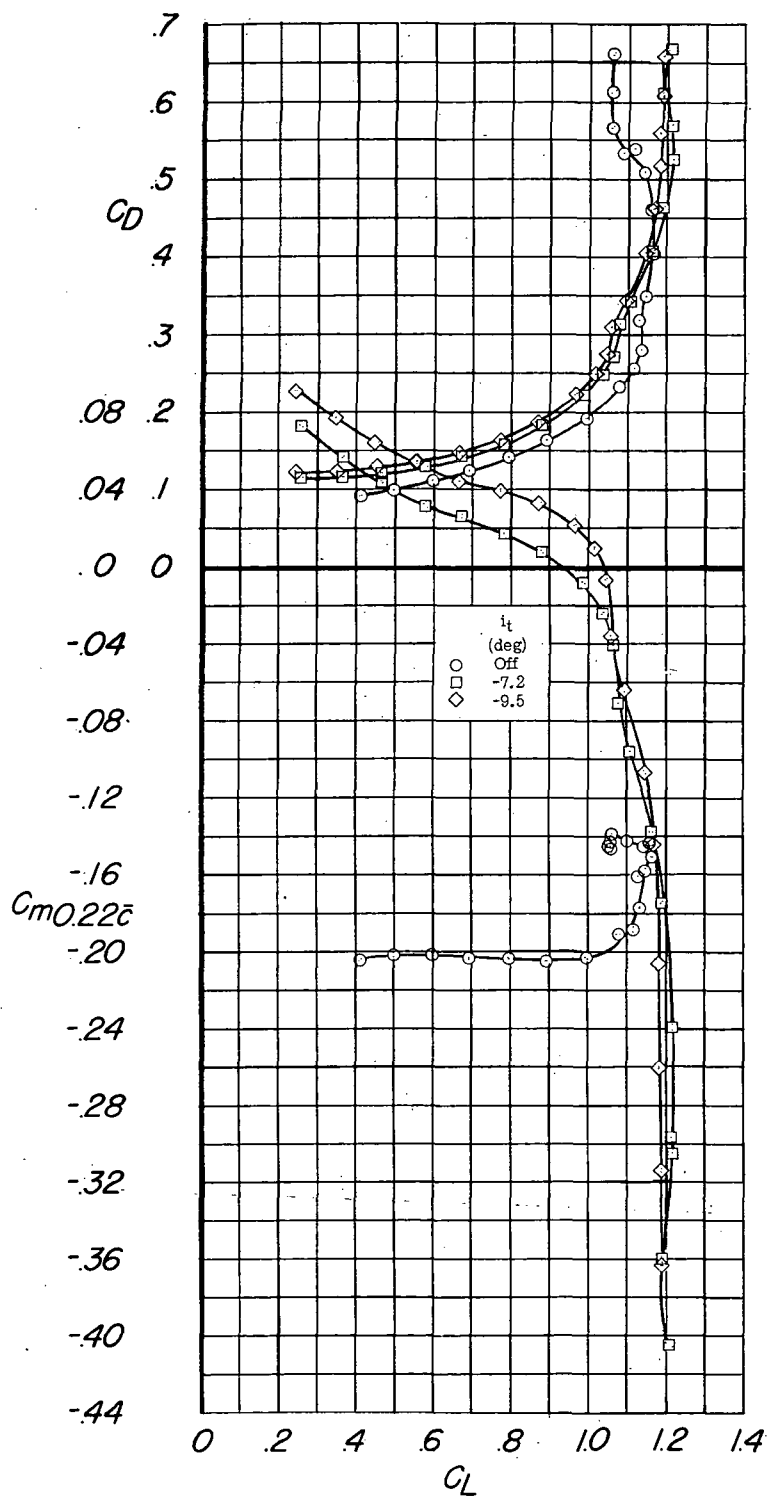
(b)  $C_D$  and  $C_{m0.38c}$  against  $C_L$ .

Figure 28.- Concluded.



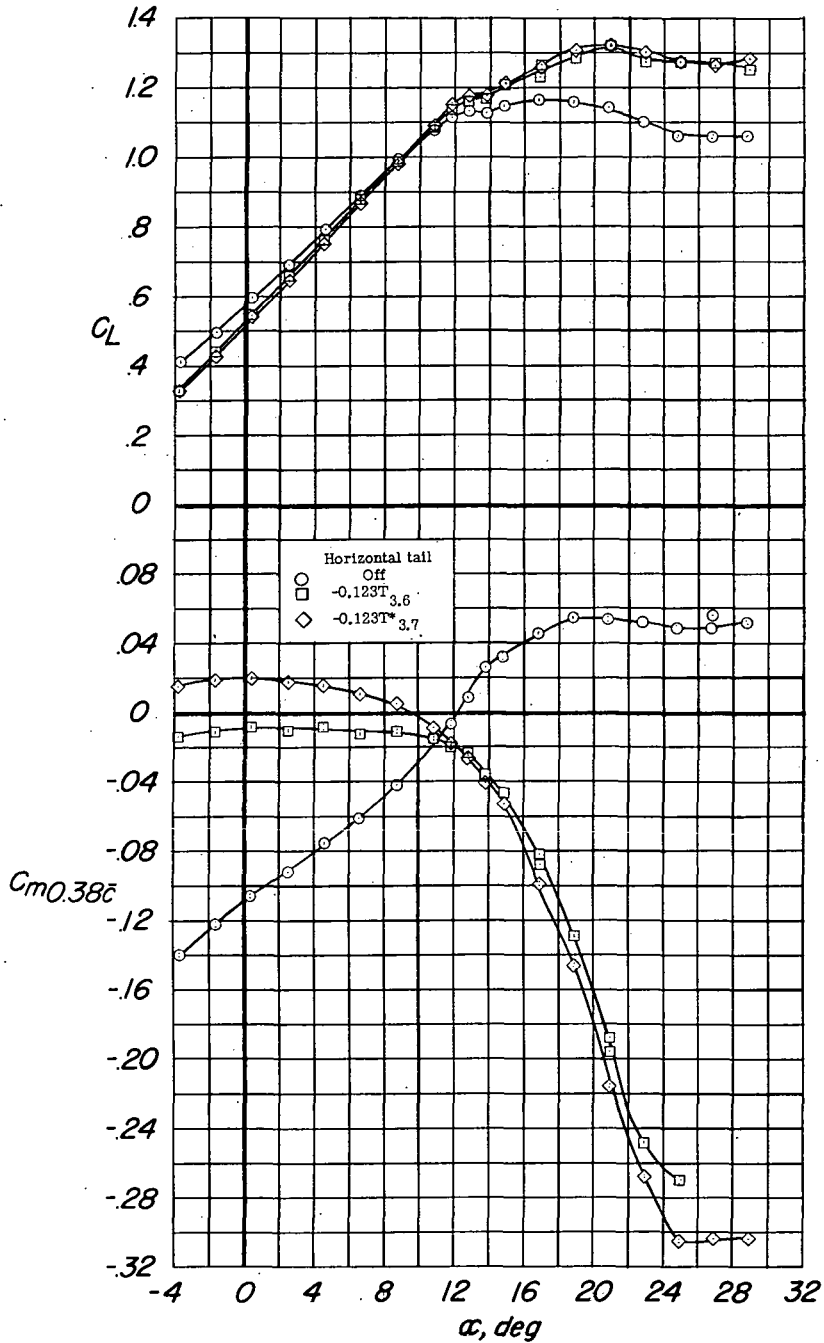
(a)  $C_L$  and  $C_{m0.22\bar{c}}$  against  $\alpha$ .

Figure 29.- Longitudinal characteristics of the model equipped with a transonic-type elliptical wing-root inlet, 70-percent-span trailing-edge flaps deflected  $46^\circ$ , and the leading-edge flaps drooped  $20^\circ$ . Configuration: A + V +  $I_{TE}$  +  $(-0.123)T$  +  $0.70F_{46}$  +  $N_{20}$  +  $E_0^{450}$ ; center-of-gravity location,  $0.22\bar{c}$ .



(b)  $C_D$  and  $C_{m_{0.22\bar{c}}}$  against  $C_L$ .

Figure 29.- Concluded.

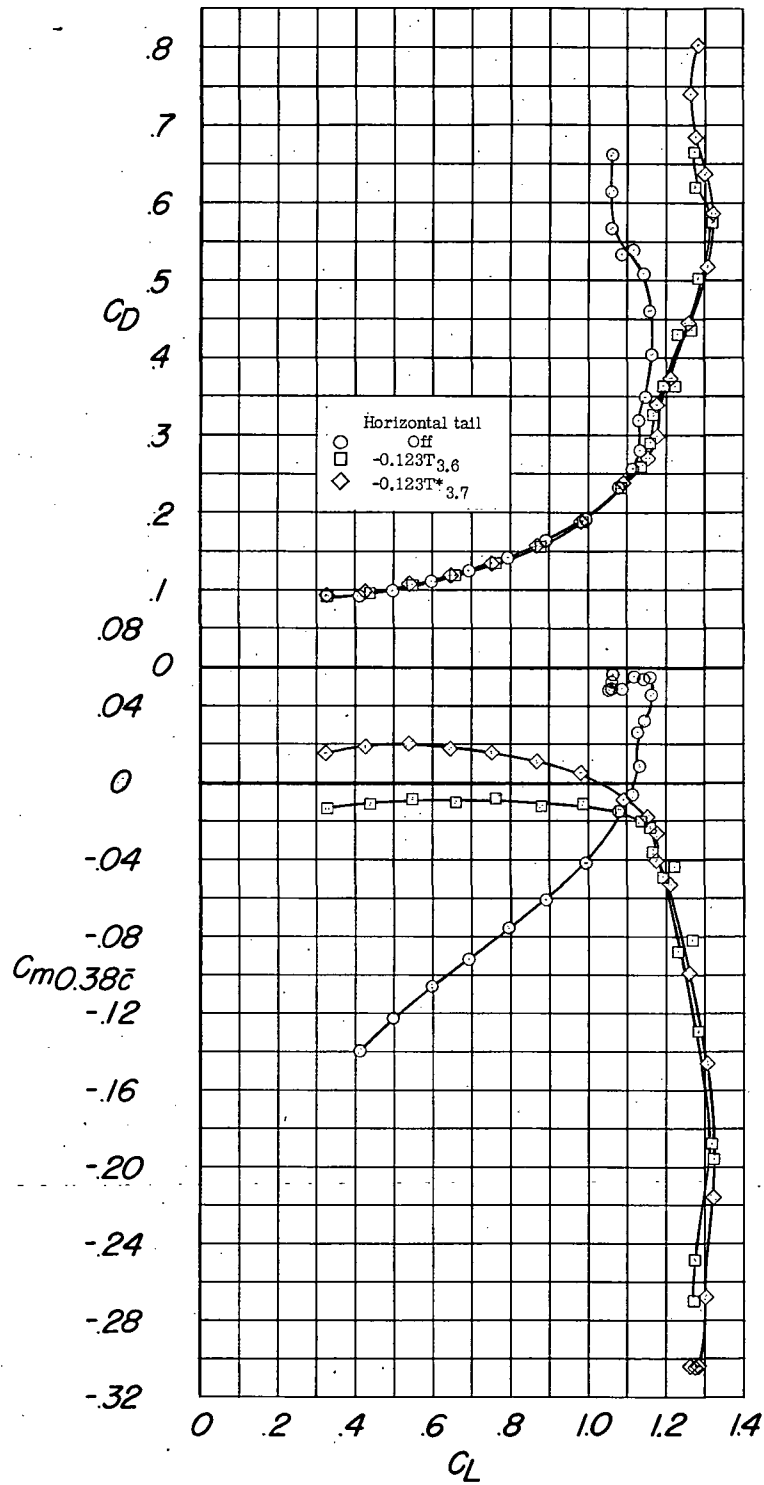


(a)  $C_L$  and  $C_{m0.38\bar{c}}$  against  $\alpha$ .

Figure 30.- Longitudinal characteristics of the model equipped with a transonic-type elliptical wing-root inlet, an increased span horizontal tail, 70-percent-span trailing-edge flaps deflected  $46^\circ$ , and the leading-edge flaps drooped  $20^\circ$ . Configuration: A + V + I<sub>TE</sub> + (-0.123)T + 0.70F<sub>46</sub> + N<sub>20</sub> + E<sub>0</sub>450; center-of-gravity location, 0.38 $\bar{c}$ .







(b)  $C_D$  and  $C_{m0.38c}$  against  $C_L$ .

Figure 30.- Concluded.